

**OPTIMIZATION OF LASER WELDING
SEAM GEOMETRY
USING RESPONSE SURFACE METHODOLOGY (RSM)**

M.Sc. THESIS

Ash BOZAN

Department of Mechanical Engineering

System Dynamics and Control

Thesis Advisor: Assist. Prof. Dr. Ayhan Kural

JANUARY 2012

ISTANBUL TECHNICAL UNIVERSITY ★ GRADUATE SCHOOL OF SCIENCE
ENGINEERING AND TECHNOLOGY

**OPTIMIZATION OF LASER WELDING
SEAM GEOMETRY
USING RESPONSE SURFACE METHODOLOGY (RSM)**

M.Sc. THESIS

**Aslı BOZAN
503071619**

Department of Mechanical Engineering

System Dynamics and Control

Thesis Advisor: Assist. Prof. Dr. Ayhan KURAL

JANUARY 2012

İSTANBUL TEKNİK ÜNİVERSİTESİ ★ FEN BİLİMLERİ ENSTİTÜSÜ

**LAZER KAYNAK DİKİŞİ
GEOMETRİSİNİN CEVAP YÜZEYİ METODU
(RSM) İLE OPTİMİZASYONU**

YÜKSEK LİSANS TEZİ

**Aslı BOZAN
503071619**

Makina Mühendisliği Anabilim Dalı

Sistem Dinamiği ve Kontrol

Tez Danışmanı: Yrd. Doç. Dr. Ayhan KURAL

OCAK 2012

Asli BOZAN, a **M.Sc.** student of ITU **Institute of Science** student ID 503071619, successfully defended the **thesis** entitled “The optimization of laser welding seam geometry by using response surface methodology”, which she prepared after fulfilling the requirements specified in the associated legislations, before the jury whose signatures are below.

Thesis Advisor : **Assist. Prof. Dr. Ayhan KURAL**
İstanbul Technical University

Jury Members : **Prof. Dr. Can OZSOY**
İstanbul Technical University

Prof. Dr. Recep KOZAN
Sakarya University

Date of Submission : 20 January 2012
Date of Defense : 30 January 2012

FOREWORD

I particularly thank to my supervisor Assist. Prof. Dr. Ayhan KURAL for his guiding and help in analysis studies, to Prof. Dr. Can ÖZSOY for their supports and giving chance to me perform my master thesis at RBTR.

I would like to express my deep appreciation and thanks for my advisor Haluk ÇANGAR at RBTR for his motivation and problem solving supports through the project and valuable advices and suggestions both in technical and personal development areas. In addition, special thanks to my section manager Mr. Nills Lippmann and a laser process engineer Çetin YILMAZER and technicians of TEF 11 Necdet MADENCİ, Gürdal İLTER and Kadir ATIK for their collaboration and technical support and to MFG department manager Mr. Mustafa Bulut for his financial supports.

Finally, I thank very much to my family for their motivation support as usual and MFG engineers for their helps and their friendship.

January 2012

Aslı BOZAN

Mechanical Engineer

TABLE OF CONTENTS

	<u>Page</u>
TABLE OF CONTENTS.....	ix
ABBREVIATIONS	xi
LIST OF TABLES	xiii
LIST OF FIGURES	xv
SUMMARY	xix
ÖZET.....	xxi
1. INTRODUCTION.....	1
1.1 Purpose of the Thesis	1
1.2 Background	2
1.3 Hypothesis	2
2. LASER INFORMATION.....	5
2.1 Laser	5
2.2 Types of Laser	8
2.3 Laser Welding	8
2.4 The Advantages of Laser welding.....	8
2.5 The Disadvantages of Laser welding	9
2.6 Laser Welding Parameters	9
2.6.1 Laser parameters	10
2.6.2 Process parameters	11
2.6.3 Material parameters.....	12
3. DESIGN OF EXPERIMENT.....	15
3.1 DOE Types	16
3.1.1 One factor design	16
3.1.2 Factorial design	17
3.1.2.1 2^k Factorial design	19
3.1.2.2 General full factorial design.....	21
3.1.2.3 Two level factorial designs.....	21
3.1.2.4 Two level fructional factorial designs	21
3.1.2.5 Plackett-Burman design	21
3.1.2.6 Taguchi's orthogonal arrays.....	21
3.1.3 Response surface method designs	21
3.1.4 Reliability DOE	22
3.2 Least Square and Regression	22
3.3 Analysis of Variance	25
3.3.1 Coefficients	28
3.3.2 Sum of squares	29
3.3.3 Degrees of freedom	30
3.3.4 Mean square	31
3.3.5 F test	31
3.3.6 p-values	31
3.3.7 R^2	32

3.3.8 Predicted R^2	32
3.3.9 Adjusted R^2	33
3.4 Response Surface Methodology Theory	33
3.4.1 Response surface methodology analysis	33
3.4.2 Response optimization	37
3.4.2.1 Response optimizer	37
3.4.2.1.1 Individual desirabilities	39
4. DETAILS OF EXPERIMENTS	43
4.1 Information of The Station	43
4.1.1 Laser unit	43
4.1.2 Focusing optic	43
4.1.3 Working station	44
4.1.4 Security system	44
4.1.5 Actuator	44
4.1.6 Fiberoptics	44
4.1.7 Collimation	45
4.1.8 Nd:YAG laser	46
4.2 General Information About Experiment	46
4.2.1 The process and product information	46
4.2.2 The differences between collimation A and Collimation B	48
5. EXPERIMENTAL RESULTS	51
5.1 Main Effects and Interaction Plots Comparison of Collimations	51
5.2 Optimization Results for Collimation A Using RSM	54
5.2.1 RSM results of depth values	54
5.2.2 RSM results of width values	57
5.2.3 RSM results of thickness values	59
5.3 Optimization Results for Collimation B Using RSM	61
5.3.1 RSM results of depth values	61
5.3.2 RSM results of width values	64
5.3.3 RSM results of thickness Values	66
5.4 Optimization Results of Experiments Within Different Steps for Collimation A Using RSM	68
6. CONCLUSIONS	73
7. RECOMMENDATIONS	79
REFERENCES	81
APPENDICES	83
CURRICULUM VITAE	85

ABBREVIATIONS

ANOVA	: Analysis Of Variance
App	: Appendix
CO₂	: carbon dioxide
DF	: Degree Of Freedom
DOE	: Design of Experiment
F	: F test in statistic
HDEV4.1	: The named of the injector
M²	: Beam quality factor
MFG	: Manufacturing Gasoline System
Nd:YAG	: Neodymium-doped yttrium- aluminium garnet
p	: Probability of obtaining statistic test
P	: Laser power
R²	: Coefficient of determination
RBTR	: Robert Bosch Turkey
RSM	: Response Surface Methodology
S	: Welding Speed
W	: Watt

LIST OF TABLES

	<u>Page</u>
Table 3.1: ANOVA Table	28
Table 3.2: The example matrix form.....	37
Table 4.1: Parameter values of experiment.....	49
Table 5.1: ANOVA table of depth values from collimation A.....	55
Table 5.2: ANOVA table of width values from collimation A.....	57
Table 5.3: ANOVA table of thickness values from collimation A.....	59
Table 5.4: ANOVA table of depth values from collimation B.....	61
Table 5.5: ANOVA table of width values from collimation B.....	64
Table 5.6: ANOVA table of thickness values from collimation B.....	66
Table 5.7: Additional experiment steps and results	68
Table 5.8: ANOVA table of depth values	69
Table 5.9: ANOVA table of width values.....	70
Table 5.10: ANOVA table of thickness values	71
Table A.1 : The experimental data for collimation A.	81
Table A.2 : The experimental data for collimation B.	82

LIST OF FIGURES

	<u>Page</u>
Figure 2.1: Laser Beam Resonator.....	6
Figure 2.2: Types of Laser	7
Figure 3.1: Create a functional design window in Minitab 16.....	17
Figure 3.2: Create a functional design window-display available in Minitab 16	18
Figure 3.3: Create a functional designs window in Minitab 16	18
Figure 3.4: Create a functional designs-factors window in Minitab 16.....	19
Figure 3.5: The concentration of reactant, the amount of the catalyst.....	20
Figure 3.6: The treatment combinations in 2^2 design	20
Figure 3.7: Response optimizer-setup.....	38
Figure 3.8: The weight values of the desirability function.....	40
Figure 3.9: The goals of the desirability function.....	41
Figure 4.1: Schematic diagram of Laser installation Components	43
Figure 4.2 : Fiber optic beam delivery (a)steps index fiber; (b)graded index.....	45
Figure 4.3 : a)1000 trdisk Laser Unit (b)Nd:YAG laser	46
Figure 4.4 : Laser welding station where the experiments have been done.....	47
Figure 4.5 : Cross section welding area and welding pool	47
Figure 4.6 : Representation of collimation.....	48
Figure 4.7 : Cross section photos of welding area samples for collimation A.	49
Figure 4.8 : Cross section photos of welding area samples for collimation B.....	50
Figure 5.1: Main effects plots of depth for collimation A and B.....	51
Figure 5.2: Interaction plots of depth for collimation A and B	52
Figure 5.3: Main effects plots of width for collimation A and B	52
Figure 5.4: Interaction plots of width for collimation A and B	53
Figure 5.5: Main effects plots of thickness for collimation A and B	53
Figure 5.6: Interaction plots of thickness for collimation A and B.....	54
Figure 5.7: The scatter plot of actual and fitted depth values for collimation A	55
Figure 5.8: 3D graph shows the effects of laser power and welding speed on the depth at collimation A.....	56
Figure 5.9: Contour graph shows the effect of laser power and welding speed on the depth values at collimation A.....	56
Figure 5.10: The scatter plot of actual and fitted width values for collimation A	58
Figure 5.11: 3D graph shows the effects of laser power and welding speed on the width at collimation A.....	58
Figure 5.12: Contour graph shows the effect of laser power and welding speed on the width values at collimation A	59
Figure 5.13: The scatter plot of actual and fitted thickness values for collimation A	60
Figure 5.14: 3D graph shows the effects of laser power and welding speed on the thickness at collimation A.....	60
Figure 5.15: Contour graph shows the effect of laser power and welding speed on the thickness values at collimation A.....	61

LIST OF FIGURES

	<u>Page</u>
Figure 5.16: The scatter plot of actual and fitted depth values for collimation B	62
Figure 5.17: 3D graph shows the effects of laser power and welding speed on the depth at collimation B	63
Figure 5.18: Contour graph shows the effect of laser power and welding speed on the depth values at collimation B	63
Figure 5.19: The scatter plot of actual and fitted width values for collimation B	65
Figure 5.20: 3D graph shows the effects of laser power and welding speed on the width at collimation B	65
Figure 5.21: Contour graph shows the effect of laser power and welding speed on the width values at collimation B	66
Figure 5.22: The scatter plot of actual and fitted thickness values for collimation B	67
Figure 5.23: 3D graph shows the effects of laser power and welding speed on the thickness at collimation B	67
Figure 5.24: Contour graph shows the effect of laser power and welding speed on the thickness values at collimation B	68
Figure 5.25: The scatter plot of actual and fitted depth values for additional test of collimation A.....	69
Figure 5.26: The scatter plot of actual and fitted width values for additional test of collimation A.....	70
Figure 5.27: The scatter plot of actual and fitted thickness values for additional test of collimation A	71
Figure 6.1: The verification results of depth.....	74
Figure 6.2: The verification results of width.....	75
Figure 6.3: The verification results of thickness.....	75
Figure 6.4: Contour graph shows the effect of laser power and welding speed on depth,width and thickness values and optimum feasible area at collimation A.....	76
Figure 6.5 : Contour graph shows the effect of laser power and welding speed on depth,width and thickness values and optimum feasible area at collimation B	76

THE OPTIMIZATION OF LASER WELDING SEAM GEOMETRY BY USING RESPONSE SURFACE METHODOLOGY (RSM)

SUMMARY

In last two decades, laser welding is employed as an important industrial production process for jointing a variety of metallic and also nonmetallic materials. Laser welding thechnology is capable of jointing dissimilar materials, generating narrow welding area and controlling deepness with sensitive temperatures.

Statistical based experimental analysis techniques are particularly useful in engineering studies for improving the understanding of the production processes and the development of new process conditions. Nowadays, application of design of experiment (DOE), regression and RSM (response surface methodology) are widely used to develop mathematical model from the welding process input parameters to the output variables of the welding pool regarding the desired weld quality.

Response surface methodology (RSM) is defined as a collection of mathematical and statistical methods that are used to develop, to improve, or to optimize a product or process. It comprises of statistical experimental designs, regression modeling techniques, and optimization methods.

This study focuses on the development of mathematical models for selection of process parameters and the prediction of weld seam geometry in Nd:YAG laser welding. Factorial design can be employed as a guide for optimization of process parameters. Welding input parameters play a significant role in determining the quality of weld seam geometry.

Two factors for two different collimations were incorporated into the factorial model; laser power and welding speed. The RSM results shows that developed mathematical models can be applied to estimate the effectiveness of process parameters for a given seem geometry (width,depth, thickness) and indicate optimum inputs values for a good welding quality.

At the end of this study, response surface optimizer was used for finding the best conformity of the input (laser welding and welding speed) parameters that were found from the output tolerances which means the suitable laser welding seam geometry. The values, which were occured from the response surface optimizer, were tried on the laser welding process bench and all output parameters (width,depth, thickness) were conform. The conformation of the this study indicates that the study is real-like and achieved it's objective.

LAZER KAYNAK DİKİŞİ GEOMETRİSİNİN CEVAP YÜZEYİ METODU (RSM) İLE OPTİMİZASYONU

ÖZET

Son yıllarda, endüstride lazerle kaynak, üretimde büyük önem kazanmıştır. Özellikle dar kaynak bölgesi, hassas sıcaklıkla derinlik kontrolü ile ısıtma ve farklı tip metallerin birbirine kaynak işlemlerinde kullanabilirliği sayesinde lazer kaynak pek çok yerde büyük imkanlara sahiptir.

Günümüzde, mühendislik alanlarında, proses parametrelerinin geliştirilmesinde ve parametrelerin birbirleriyle etkileşimlerini anlamada istatistiksel deney analiz teknikleri büyük kolaylıklar sağlamaktadır. Bunlara örnek olarak, deney analiz teknikleri (DOE), regresyon ve yüzey cevap metodu (RSM), üretimdeki problemleri çözmede ve anlamada yaygın olarak kullanılmaktadırlar.

Design of Experiment adı verilen deney tasarımı metodu, ileri düzey istatistiksel araçları içeren bir yöntem olup, özellikle üretim amaçlı olarak proses girdileri ile çıktıları arasındaki ilişkileri matematiksel modeller ile ortaya koymaktadır. Bu sayede üretim prosesinin çıktısı olan kriterleri en iyi seviyelere ayarlamak için deneme yanılma veya her seferinde bir faktör çalışmaları yerine bilimsel bir yöntem kullanmamıza olanak sağlamaktadır. Bu çalışmalara dayanarak prosesin kritik parametrelerini olması gereken en optimum seviyeye ayarlama olanağına ulaşılabilmektedir.

RSM (yüzey cevap metodu); İki veya daha fazla değişken yardımıyla tanımlanan yüzeylerin matematiksel ve istatistiksel tekniklerin yardımı ile modellenmesidir. Kalitenin iyileştirilmesi, değişkenliğin azaltılarak ürün performansının ve sürecin iyileştirilmesi için, genellikle doğrudan RSM kullanılarak başarılabilmektedir. Yöntem ilk kez G.E.P Box ve K. B. Wilson tarafından 1951'de ortaya atılmıştır.

Yüzey cevap metodu, süreç açısından en iyi yanıtın bulunması için faktörlerin belirlenmesini, süreçte etkin olan faktör seviyelerinin bulunmasını, mevcut koşullarda elde edilen bir kalite düzeyinin üzerinde bir ürün kalitesi sağlanabilmesi için yeni üretim koşullarını belirlemeyi, yanıt ve nicel faktörler arasındaki ilişkiyi bir modelle tanımlamayı sağlar.

Bu çalışma, lazer kaynak prosesinin matematiksel modellenmesi ve bu modellerden girdi değerlerinin değiştirilmesiyle elde edilebilecek olan çıktı (derinlik, kalınlık ve genişlik) değerlerinin nasıl değişeceğini gözlemleyebilmek ve istenilen toleranslarda kaynak bölgesi sağlayabilmek için girdilerin aralarındaki ilişkiyi görmek amaçlı yapılmıştır.

Farklı iki girdi parametresi, farklı iki kolimasyon cihazı için, ayrı ayrı değiştirilerek denemeler yapılmıştır. Lazer kaynak prosesini etkileyen birçok önemli parametreler (vakum, lazer ışın kalitesi, lazer ışın iz düşümü, ortamın steril olması... vs.) bulunmaktadır. Bunların arasından kaynak kalitesine en çok etken olduğu bilinen-tecrübe ve önceki çalışmalar sonucunda- lazer gücü ve kaynak hızı girdi parametreleri olarak belirlenmiştir.

Her iki kolimasyon için, kolimasyon özelliklerinden farklılığından dolayı farklı lazer gücü ve kaynak hızı değerleri belirlenmiştir. Diğer proses şartlarının da bu seçime etkileri bulunmaktadır.

Her bir kolimasyon cihazı için girdilerin çıktılara olan etkileri teker teker incelenmiştir. Ayrıca, her iki girdinin birbirleriyle etkileşiminin kaynak geometrisindeki değişkenlikleri gözlenmiştir.

Bu çalışmalar sonucunda proses şartları göz önünde bulundurularak; en iyi kalitede kaynak geometrisi sağlayacak olan kolimasyon laboratuvar sonuçlarıyla hem görsel hem de değer bazında belli olmuştur.

RSM (yüzey cevap) metodu kullanılarak, matematiksel modeli çıkarılan prosesin ayrıca düzgün kaynak kalitesi için, deney sonuçlarından optimum girdi değerleri de kullanılarak çıkarılmıştır. Matematiksel modelleme için gerçek proses değerlerinden faydalanılmıştır. Bu değerler belirlenen lazer gücü ve kaynak hızı kombinasyonları denenerek elde edilmişlerdir. Bu kombinasyonlar oluşturulurken DOE (deney tasarımı) metodlarından yararlanılmıştır.

Bu kombinasyonlardan oluşturulan deneme gruplarından, her bir çıktı için ayrı matematiksel modeller oluşturulmuştur. Oluşturulan kombinasyonlardan onar tane örnek alınıp, bu grupların stabilliğine bakılmıştır. Matematiksel modellerde farklı girdi değerleri denenerek; prosesten elde edilen gerçek verilerle, matematiksel modellemekten çıkan veriler birbirleriyle kıyaslanmıştır.

Bu kıyaslamada hem matematiksel modelde hem de gerçek proseste aynı girdi değerleri denenmiştir. Bu kıyaslama sonucunda, gerçek proses değerleri ile matematiksel modellerden elde ettiğimiz değerler arasındaki varyasyon (hata) oranının düşük çıkması, matematiksel modellerimizin gerçek sonuca yakınsadığını bize gösterebilmiştir.

Son olarak, yüzey cevap optimizasyon kullanılarak, tek bir kolimasyon cihazı için, çıktı (derinlik, kalınlık ve genişlik) toleranslarının birbiriyle çakıştığı bölgedeki en uygun girdi verileri bulunmuş olup; bu girdi değerleri gerçek olarak lazer kaynak proses hattında denenmiştir.

Çıkan değerler, toleranslar içinde uygun değerlerde çıkmıştır. Bu sonuçlar, matematiksel modellerden çıkan değerlerle kıyas edilmiştir. Bu da yapmış olduğumuz çalışmalarının doğruluğunu bize ispatlamıştır.

Ayrıca, bu çıkan değerler için , yüzey cevap optimizasyonda ön görülmüş kalınlık, genişlik ve derinlik değerleri de prosesten elde edilen gerçek datalarla kıyaslanmıştır. Bu kıyaslama, yüzey cevap metodunun bu proses için seçilmiş bir yöntem olduğunu göstermiş olup; değerler birbirine hemen hemen yakın gelmiştir.

Lazer kaynak prosesini ortam şartları etkileyebilmektedir. Buna rağmen, yapmış olduğumuz ve yüzey cevap metodunda kullanmış olduğumuz datalardan elde ettiğimiz optimum girdi parametre değerlerinden oluşan çıktılar ile çalışmanın son aşamasında yapmış olduğumuz denemelerden elde ettiğimiz çıktılar arasında önemsenmeyecek boyutta varyasyonlar bulunmaktadır. Yani iki çıktı arasındaki hata oranı düşük bulunmuştur.

Yüzey cevap optimizasyon sayesinde bulunan girdi değerlerinin, optimum çalışma değerleri olarak alınması, en uygun kaynak dikiş kalitesinin oluşmasını sağlayacaktır. Buradan çıkan girdi değerleri sayesinde, optimum lazer gücü ve kaynak hızı değerleri, en uygun kalitedeki çıktı değerleri için belirlenmiştir.

Bu çalışmada Robert BOSCH firmasının yeni devreye alınan lazer kaynak istasyonundan faydalanılmış olup, çalışma daha sonra bu istasyon çalışmalarında faydalı bir kaynak olmuştur.

1. INTRODUCTION

In recent years, laser technology is commonly used for medical, fashion, surveying, communication, military, aircraft and space sections as its feasibility and ductility. In industries; drilling, cutting, welding, measuring, bonding and writing are such a kind of examples of laser processes most particularly.

Laser welding is a process which is occurred by high energy density beam that used for jointing similar and also dissimilar materials together at the necessary case. That enables assembling on the products by automation.

Production of gasoline injectors contains for basic stages; cleaning, grinding, assembly and required tests. At the assembly lines, there are several welding stations which play important roles for manufacturing of the injector.

Laser welding is used for critical jointing areas on the injector, for this reason, quality of welded cross-section occurs significantly life treat at a car. Therefore, controlling of welding parameters and analyzing defects of welded cross-section are required more serious experiences.

The factors which effected welding quality, are represented is in three stages mainly; laser-related, process-related and material-related. The interactions of these factors can also affect the quality of welding area. Some serious problems such as fuel leakage can be seen during injector continuous working due to defects and quality of the welding area.

This study has been performed at the assembly line on one of the welding stations at RBTR Gasoline production.

1.1. Purpose of thesis:

At that thesis, the most two important parameters which effect the quality of laser welding area, were chosen and both parameters were tried for two different collimation devices at the welding station. These chosen parameters are laser power and laser speed that influence the welding pool geometry more effectively. The

general full factorial design which is a part of design of experiments (DOE) tool at Minitab 16, were used for defining parameter combinations as experiment steps and the mathematical models were determined by RSM analysis. For every combination, some experiments were done and the welding pool geometry was analyzed.

1.2. Background:

Laser technology has approximately 30 years history at BOSCH Group and it has been used for welding processes for 20 years with its ability of fastening and sensitivity. Laser welding determines with weld width, high penetration and parallel sided fusion zone. It has advantages on bonding process over the other widely used joining techniques through high power density.

K.Y.Benyounis, A.G.Olabi, M.S.J.Hoshmi were used RSM in their assignment which is called effect of laser welding parameters on the heat input and weld-bead profile. In this study, laser power, welding speed and focal position were the input parameters. Penetration, welded zone width and heat affected zone width were investigated using response surface methodology by these input parameters. The second order polynomial regression equations were developed to find optimum welding conditions for desired criteria. It was published in Journal of Materials Processing Technology in 2005. Our study was originated at this article. [1]

Several experiments have been done with different effected parameter combinations and observed the interaction between each other. The most important parameters due to these experiments were chosen and these were tried at different every two collimation devices. Minitab 16 program was used for experimental designing, regressing, optimizing and evaluating actual data statically.

1.3. Hypothesis:

On this thesis; for both collimation devices, some designed experiments have been done with changing laser power and speed in combination by using full factorial design and all output values(width, depth, thickness) were measured. Output values were written on design table, main effects and interaction diagrams for every output were drawn by using Minitab 16 tools. The mathematical models which show the

behavior of our welding outputs were determined using response surface methodology (RSM) for illustrating optimum inputs values.

This thesis proves how laser welding parameters and their combinations affect the welding pool (seam) geometry and obtains optimum laser power and welding speed values at the different collimation device.

2. LASER INFORMATION

2.1. Laser

A laser is a device that emits electromagnetic radiation (lights), is based on the stimulated emission of photons. It has 10 nm to 1mm wavelength tolerances. It is an abbreviation and it stands for Light Amplification by Stimulated Emission of Radiation.

A laser was invented by Charles H. Townes and Arthur Schawlow in 1958. Laser technology has been investigated day by day that is used in industrial area widely.

Laser produces light that has unique qualities: monochromatic, coherent, collimated and uniformly polarized. Energy source (pump), lasing medium (solid, liquid, gas) and optical resonator are necessary to produce laser light. Laser light has high power density compared to other kinds of light and it diminishes very little on the way from the source. According to this, laser beam is a controllable, clean, high intensity heat source that can heat, melt and evaporate all materials so it is used as a welding heat source. You can see the figure 2.1, which is a resonating device. A beam input which is generated by laser pump is fed to resonator where it is reflected on the lasing medium (crystalline disk). This crystalline disk produces laser beam that we need.

The wavelength of the laser beam is of high importance regarding processed work piece(s). Each material has different reflection behavior. The less laser beam is reflected, the more heat energy is absorbed by the material. Energy absorption is essential for laser welding. For energy absorption in alloyed steel, laser beam at a wavelength of 1064nm is an optimal solution. In our case, Nd:YAG crystal is an industrial solution which can produce laser beam at a wavelength of 1064nm.

Figure 2.1 shows kind of laser beam resonator called crystalline disk.

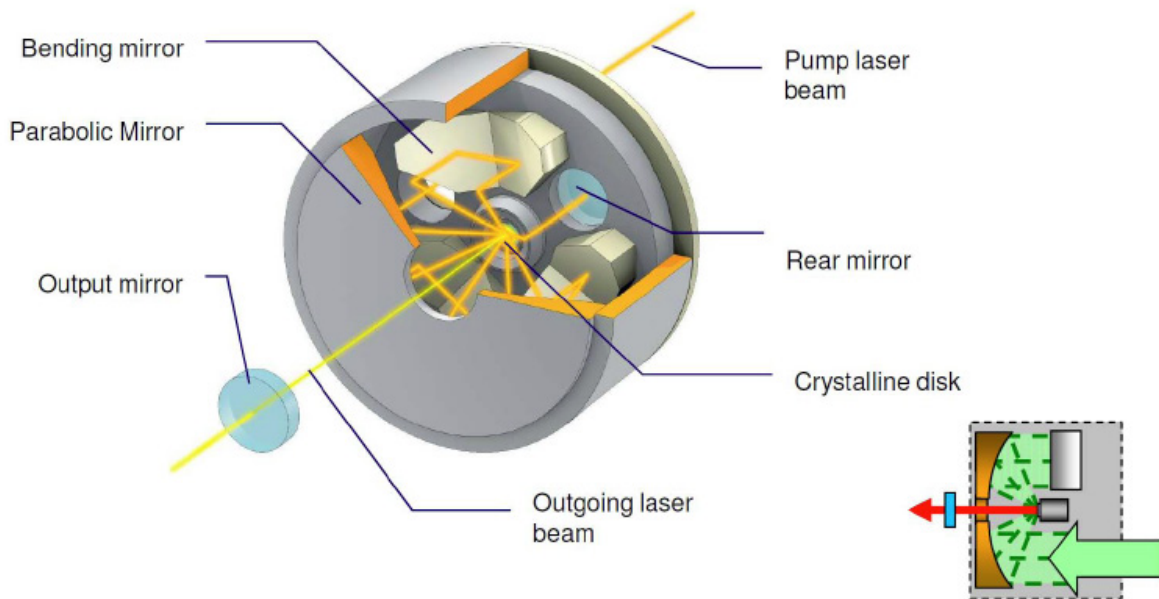


Figure 2.1: Laser Beam Resonator (Dr. Ramsayer Reiner, 2010)

2.2. Types of Lasers

There are generally 4 types of laser;

Solid-state lasers have lasing material distributed in a solid matrix

Gas lasers; have a primary output of visible red light. It is commonly used for cutting hard materials.

Dye lasers use complex organic dyes, in liquid solution or suspension as lasing media. They are tunable over a broad range of wavelengths

Semiconductor lasers are not solid-state lasers. They are known as diode lasers mostly. Those kind of devices have small sizes and use lower power. Some laser printers and CD drives have semiconductor lasers.

Figure 2.2 shows the types of lasers and the corresponding wavelengths.

According to type of use, laser beams are also characterized by the duration of laser emission – continuous wave or pulsed laser. A Q-Switched laser is a pulsed laser which contains a shutter-like device that does not allow emission of laser light until opened. Energy is built-up in a Q-Switched laser and released by opening the device to produce a single, intense laser pulse.

Types of Lasers

Gas Lasers

•Atom Lasers

Helium-Neon Laser (632.8nm)
(0.5-100mW)

•Molecule Lasers

CO₂ Laser (10.6μm)
(1-10000 W)

Nitrogen Laser (337nm)
(250 kW-1MW)

Far-infrared Laser (99-373 μm)
(1kW ve 100mW)

Excimer Laser (KrF, XeF, ArF)

•Ion Lasers

Argon Ion Laser (488nm)
(50mW-50W)

Krypton Ion Laser

•Metal Steam Lasers

Copper Steam Laser (510.5nm)
(1MW)

Gold Steam Laser

Dye Lasers

•Dye Laser

Solid-state Lasers

Ruby Laser

Nd-YAG Laser

Ti-Sapphire Laser

Semiconductor Lasers

Diode Laser

Other Lasers

•**X-Ray Laser**
(40-400Å)

•**Free-Electron Laser**
(248nm-8mm) (1GW ve 10 W)

•**Fiber Laser**

Figure 2.2: Types of Laser (Dr. Ramsayer Reiner, 2010)

Continuous Wave (CW) lasers operate at an average power. In higher power systems, one is able to adjust the power. In low power gas lasers, such as HeNe, which has fixed power level whose performance decreases usually with long term use.

Single Pulsed (normal mode) lasers generally have pulse durations of a few hundred microseconds to a few milliseconds. This operation is sometimes called as long pulse or normal mode.

Single Pulsed Q-switched lasers are the result of an intracavity delay (Q switch cell) which allows the laser media to store a maximum of potential energy. These pulses will have high peak powers often in the range from 10^6 to 10^9 watts peak. Under optimum gain conditions, emission occurs in single pulses; typically of 10^{-8} second time domain Repetitively Pulsed or scanning lasers generally involve the operation of pulsed laser performance operating at a fixed (or variable) pulse rate which may range from a few pulses per second to as high as 20,000 pulses per second.

Mode Locked lasers operate as a result of the resonant modes of the optical cavity which can affect the characteristics of the output beam. The result is a laser output which is observed as regularly spaced pulsations. Lasers operating in this mode-locked fashion usually produce a train of regularly spaced pulses, each having a duration of 10^{-15} (femto-) to 10^{-12} (pico-) seconds. A mode-locked laser can deliver

much higher peak powers than the same laser operating in the Q-switched mode. These pulses will have enormous peak powers often in the range from 10^{12} watts peak (Benypounis, Olabi, Hashmi, 2005).

2.3. Laser Welding Process

Welding is the process of joining metals by melting an using a filler to form a joint. Laser welding transfers high energy by beam; that melts and joints materials by heating. Focusing and directing of the laser beam is done by optics, it increases the concentration of light waves and achieves high power densities. Generated light energy can be converted to heat energy into materials which causes good welding area.

Welding is not the optimum solution for all types of metals, such as stainless steel, showing tendency to cracking and distortion when overheated. Alloys are particularly problematic, since it's hard to know the exact chemical composition of the metal. Welding has become highly automated over the last decade. Laser beam welding is one of the most modern techniques used.

2.4. The Advantages of Laser Welding

- High welding speed according to materials and laser power
- Very low heat input (non or rarely deformation and distortion can be seen)
- Very good manufacturing speed, strong and reliable welding seam
- Very good weld view. Grinding process is not needed after welding.
- Narrow weld seam has high depth/width ratio
- Welded materials are not affected due to sudden cooling
- Achieve welding on places which can not be welded by other types of welding processes.
- Possible to weld dissimilar and hardly weldable materials
- Laser output is not electrical, so it has not magnetic effects on welding materials.

- Transparent materials can be welded
- High stability at laser beam quality
- Easily adjustable laser beam parameters e.g. power, duration.
- Enables welding seam at even very complex geometrical forms on the parts (Celen Serap, 2006)

2.5. The Disadvantages of Laser Welding

- Forms extreme hard welding seam onto hardenable materials. Independent from sudden cooling and heating, cold and warm cracks can be seen.
- Needs high investment costs
- Not applicable on thick sheets. Suitable for 0,1-8 mm thickness of sheets.
- Damage skin and eye directly and indirectly. Therefore, it is essential to use warning sign against laser radiation danger and warning lamp to indicate that laser is on. Operators must be trained before working at laser welding section and be aware of its danger.
- Laser equipments must be kept in clean and safe areas.
- Optical part of laser device to be cleaned frequently due to nature of the process. (spatters)
- Physical mechanisms at the welding station such as work piece holder, turn table, running line should be kept clean.
- System is very sensitive to mechanical deviations as well, so that optimum mechanical adjustments should be kept well.
- More care should be taken during welding onto non-reflecting materials. (black surfaces, graphite, manganese covered surface ... etc.) (Celen Serap, 2006)

2.6. Laser Welding Parameters

Laser welding parameters regarding keyhole welding and the relationship between material and laser process have effects on welding quality. Depending on the laser parameters, material aspects and process specifications, laser welding as an output

can be changed accordingly. These parameters can be summarized under three main groups as shown below (Tabak Derya, 2010).

2.6.1. Laser parameters

Power: Laser power is related to power density which is a crucial parameter to have keyhole welding and to control welding performance. When the power density is too low, energy transfer from laser beam to work piece and penetration can be weak. If the power density is too high, this can cause welding defects such as spatter, undercut, underfill. Power should be adjusted according to material and its thickness. Each application regarding material thickness and specifications has a different implementation which is driven by experience.

Wavelength: Depending on the reflectivity level, each material requires different wavelength in order to enable maximum energy absorption in to the material. Unless the optimum wavelength is chosen, most of the energy to be transferred is lost due to highly reflected laser beam from the surface of the workpiece. The lasing material whether it is solid or nonsolid generates laser beam at different wavelengths due to its nature. For this reason, selection of the right lasing material and corresponding laser beam wavelength are very important to the application.

Beam Quality: Laser beam quality is an important factor with its beam profile distribution. The ideal form is Gaussian distribution. A perfect Gaussian beam profile is the best case where the focusability reaches its high level for laser welding. M^2 is called the beam quality factor to be measured and calculated as a parameter; in its ideal case it reaches up to 1 with a perfect Gaussian beam profile. Laser beam quality has high impact on welding results; with high beam quality narrow weld seams at high welding speeds can be achieved.

Spot Size: It is the diameter of the laser beam projected on the work piece. The main purpose of optical devices is to focus the laser beam onto the work piece where the welding seam to be performed. Due to focusing, it has a conical shape and peak of the cone is directed to work piece. In order to obtain narrow welding seams, smaller spot sizes are advantageous with its higher power density without any change at the power level. As the power density increases, deeper penetration into the material becomes possible providing narrower width. Depending on the requirements, spot size can be adjusted to achieve necessary depth and width. In general, spot size can

be adjusted by changing optic systems settings and/or the fiber optic cable diameter. However it should be kept in mind that unless the power is changed, if the spot size exceeds a certain diameter the energy coupling can not be established. The reason behind that very low power density projected onto workpiece doesn't transfer enough heat energy into the material; hence welding doesn't occur only the temperature of the material increases a bit. The spot size should be well decided, otherwise unnecessarily smaller spot size may cause undesired welding results such as other cut all underfill defects. In industrial use its range varies from 0.1 to 1.0 mm.

Pulse Energy and Duration: In order to weld, necessary amount of energy should be coupled to target material. The laser beam generated is directly proportional to necessary energy. Level of power and duration of it are the main parameters for a stable system. If two parts to be jointed are thick, due to necessity of deep penetration, power and duration of it should be chosen high enough. Depending on the welding speed, duration should be at least equal to movement period. If the welding speed increases, the power level should be increased as well in order to have equal energy intensity. Pulse energy is the main parameter of penetration and secondary parameter for weld diameter or welding seam width.

2.6.2. Process parameters

Focusing: The focusing means the placement of the laser beam spot or minimum waist diameter on the work piece. Focusing can be done mechanically by adjusting physical distance between workpiece and the optic device. The quality of laser beam coupling to material and weld pool is affected by the placement of focusing on or above the workpiece. The laser beam should be focused well, where the best penetration and weld pool geometry tolerances are achieved.

Shielding Gas: It is used to protect weld zone from oxidation and optic lenses from weld spatter, to control the convection in weld pool and the plasma formation. Shield gas is chosen in respect of process parameters and cost. Shielding gas is not necessarily used for every case. If for example, outer appearances of the welding seam is not important and weld pool geometry and weld pool strength are within specific tolerances, it is not necessary to have shielding gas.

For CO₂ lasers pure helium or helium-argon mixture is used. Helium has high ionization potential, thus it withstands plasma formation provides better penetration

and weld seam. Argon is cheaper than helium and heavier than air but its ionization degree is very low so there is remarkable laser energy absorption.

In general, nitrogen is the most suitable shielding gas for butt and overlapping welds. The welds done with nitrogen as shielding gas enables lowest porosity and better penetration values than that with helium and argon.

Weld Speed: Depending on the application whether optic device or workpiece(s) are moved, in general rotated or linearly moved. This changes the energy density on the workpiece; the lower the welding speed the more energy density. The lower welding speed causes loss of alloying material and excessive melting while higher welding speeds are the reason of fine microstructure and the decrease in alloying elements evaporation. If the rest of parameters are kept the same, penetration is inversely proportional to the welding speed. The tolerances of the welding speed depend on the laser type and material properties.

2.6.3 Material parameters

Composition: Depending on the materials to be welded, different laser beam characteristics should be chosen. Contents of the material define some main parameters such as wavelength and power. Physical properties of materials and alloys such as absorption coefficient, thermal conductivity coefficient, specific heat are effective parameters on weld quality. For example, if absorption coefficient of the workpiece is low, higher laser power has to be used for good welding performance. For example, volatile elements in alloys play important role during the laser beam welding because of their high vaporization pressure and low vaporization temperature that make the keyhole more stable. Thus, threshold power density required for energy transfer (coupling) is decreased by the increase of these elements.

Thickness: As the thickness of the materials to be welded increases, penetration depth increases as well. For this reason, thicker materials require higher power density and/or lower welding speed. The problem of the welding of thicker materials is plasma formation above the keyhole for CO₂ lasers and similarly power which is available for Nd: YAG lasers.

Surface condition: Independent from the composition of material, surface condition itself plays important role. For this reason, final processes on the surface of the workpiece such as turning, grinding, polishing, cleaning, drying and coating are of

vital importance. All these factors and also environmental factors such as transportation and storage conditions, contamination, oxidation and corrosion have negative effects on energy absorption and uniformity of it. Welding characteristics and the defect rates vary depending on the changing surface conditions from one part to another; for example spatter and porosity rates change due to different reflectivity, absorption and vaporization level of the each surface (Tabak Derya, 2010).

3. DESIGN OF EXPERIMENT

An experiment is a series of test systematically to understand the process behaviors and to research a new product or process requirements. DOE is a shortening of design of experiments, a tool for using to understand widely engineering and scientific approaches. The design and analysis of experiments relates to understand of the effects of different inputs on outputs. Mathematically, the DOE aim is to generate a cause-and-effect relationship between a number of parameters (independent variables) and response (dependent variables). Experiment step involves a combination of the different values of the investigated parameters.

Design of experiment method can be used to find answers in situations such as defining the main contributing factor to a problem, understanding the system/process performance with noise effect, finding the best configuration of factor values to minimize variation in a response etc. This method can be used problem solving, parameter design and robustness studies.

Using this tool starts with identifying the input variables and the response (output) that will be measured. For each input variable, a number of levels are defined which represent the combination of input variables and will show the effects of inputs on outputs. Analysis after measuring is to look for differences between outputs for different groups of the input variations. These differences can show the input variables single effects or an interaction with another input variable. It does only not offer one change at a time, also allows getting results from the output of input behaviors alone. One factor designs, factorial designs, response surface method designs and reliability DOE are some of the most common DOE types.

In factorial design, which was used on our thesis research, multiple parameters are investigated simultaneously during the test. The aim of this design is to specify the parameters that have significant effects on the responses, as well as view the effect of interactions. This design contains all possible combinations of the experiment levels that characterize the different alternatives of parameters. In general full factorial

design, each parameters can have a different number of levels and the parameters can be quantitative, qualitative or both (Shukor Sivarao, Anand&Ammar).

Response surface method designs (RSM) are used to identify settings of the response to obtain an optimum value of the parameters. RSM is widely used to predict the welding seam geometry and mechanical properties in many welding processes. RSM can analyze the process factors and define the results using regression and presents in ANOVA table. The analysis of variances, the coefficient dimension and coefficients which occur the regression model are calculated through working on RSM tool in Minitab 16. In this work RSM is used to find optimum input values at an optimum welding geometry. RSM includes Response Optimizer to define optimum solutions of the parameters. Response optimizer uses the limitations of outputs to find optimum combination of input parameters in between these limitation values and gives desirability values for understanding the validation of the system.

In this study; DOE is used for designing experiment steps due to full factorial design that is used to combine laser power and welding speed levels and is based to be drawn main effect and interaction diagrams of inputs. RSM generates regression model which shows the developed models of outputs one by one which can be applied to estimate the effectiveness of process parameters for a given weld seam geometry. RSM is based on determining response optimization that indicates optimum solutions of weld seam geometry dimensions (Benypounis, Olabi, Hasmi, 2005).

3.1 DOE Types

3.1.1 One factor designs

These are the designs where only one factor is under investigation, and the objective is to determine whether the response is significantly different at different factor levels. The factor can be *qualitative* or *quantitative*. In the case of qualitative factors (*e.g.* different suppliers, different materials, etc.), no extrapolations (*i.e.* predictions) can be performed outside the tested levels, and only the effect of the factor on the response can be determined. On the other hand, data from tests where the factor is quantitative (*e.g.* temperature, voltage, load, etc.) can be used for both effect investigation and prediction, provided that sufficient data are available.

3.1.2. Factorial designs

In factorial designs, multiple factors are investigated simultaneously during the test. As in one factor designs, qualitative and/or quantitative factors can be considered. The objective of these designs is to identify the factors that have a significant effect on the response, as well as investigate the effect of interactions (depending on the experiment design used). Predictions can also be performed when quantitative factors are present, but care must be taken since certain designs are very limited in the choice of the predictive model. For example, in two level designs only a linear relationship between the response and the factors can be used, which may not be realistic (Mathews Paul, 2004).

In Minitab, there is a tool of Design of experiment for factorial design. Figure 3.1 indicates the start page of this tool which is used for creating factorial design window in Minitab 16.

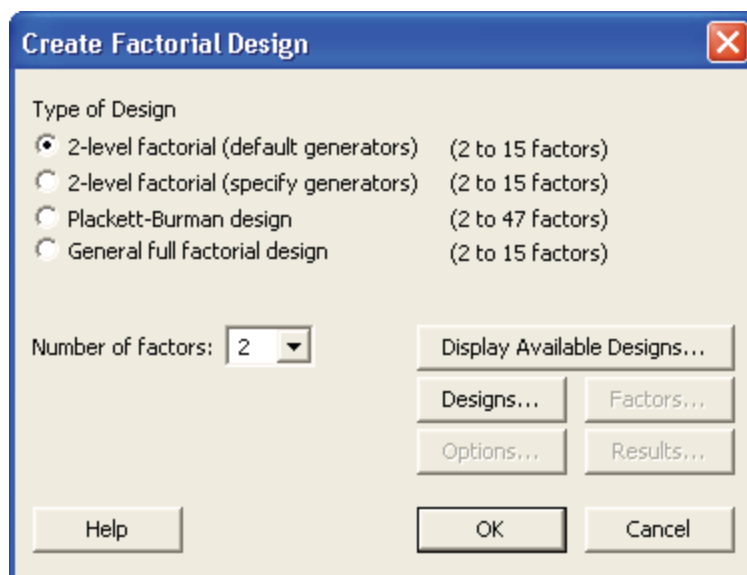


Figure 3.1: Create factorial design window in Minitab 16 (Mathews Paul, 2004)

When you create a design in Minitab, initially only two buttons are enabled, Display Available Designs and Designs. The other buttons are enabled after you complete the Designs subdialog box. (See figure 3.2)

For most design types, Minitab displays all the possible designs and number of required runs in the Display Available Designs dialog box.(see figure 3.3)

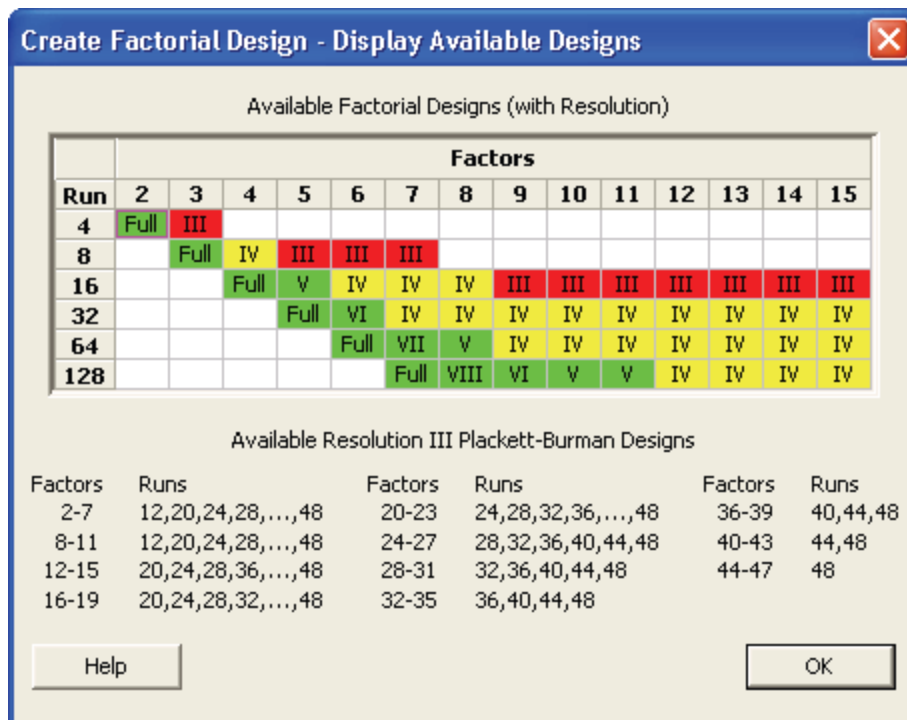


Figure 3.2: Create factorial design window-Display available designs in Minitab 16 (Mathews Paul, 2004).

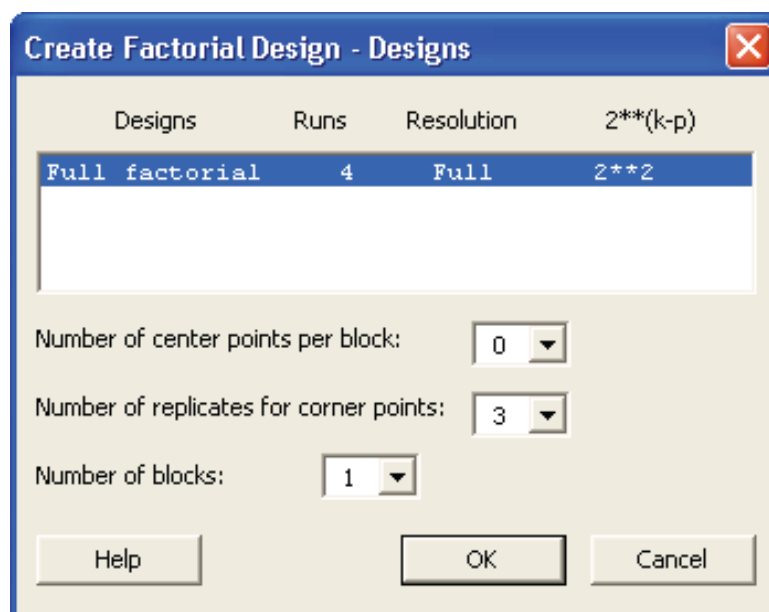


Figure 3.3: Create factorial design-designs window in Minitab 16 (Mathews Paul, 2004)

At the design bottom, The box at the top shows all available designs for the design type and the number of factors you chose. In this example, because you are conducting a factorial design with two factors, you have only one option: a full

factorial design with four runs. A two-level design with two factors has 2^2 (or four) possible factor combinations. In Number of replicates for corner points, choose 3. Minitab enters the names and levels you enter for each factor into the worksheet and uses the names as the labels for the factors on the analysis output and graphs. If you do not enter factor levels, Minitab sets the low level at -1 and the high level at 1 . (See figure 3.4)

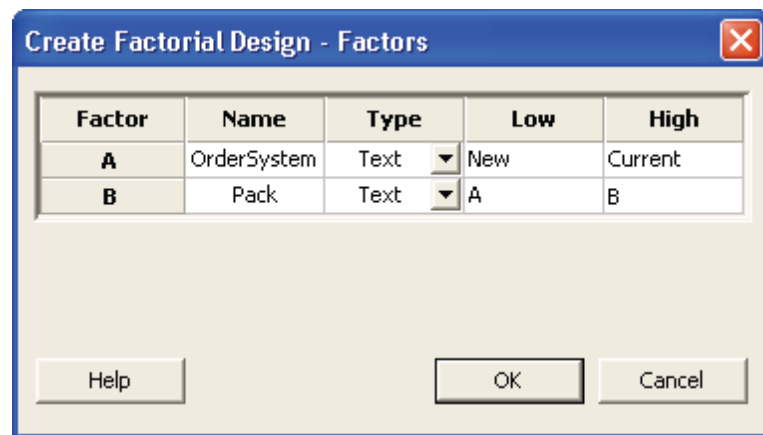


Figure 3.4: Create factorial design-factors window in Minitab 16 (Mathews Paul, 2004).

Factor A, type *OrderSystem* in **Name**, *New* in **Low**, and *Current* in **High**.

Factor B, type *Pack* in **Name**, *A* in **Low**, and *B* in **High**. Under **Type**,

In each complete replication of an experiment, all possible combinations of the levels of the factors are explored. If factor A has a levels and factor B has b levels, each replicate has $a*b$ treatment combinations. Subjects are randomly assigned to different ab combinations.

3.1.2.1. 2^k Factorial design

2^k Factorial Design is the special cases of the general factorial design that has k factors and each factor has only two levels; quantitative (temperature, pressure,...), or qualitative (machine, operator,...); high and low; each replicate has $2 \times \dots \times 2 = 2^k$ observations. Example in figure 3.5; two factors are A and B, and each factor has two levels, low and high (Menasce Daniel, 2001)

Factor		Treatment Combination	Replicate			Total
A	B		I	II	III	
-	-	A low, B low	28	25	27	80
+	-	A high, B low	36	32	32	100
-	+	A low, B high	18	19	23	60
+	+	A high, B high	31	30	29	90

Figure 3.5 : The concentration of reactant, The amount of the catalyst (Menasce Daniel,2001)

“-” And “+” denote the low and high levels of a factor, respectively. Low and high are arbitrary terms. Geometrically, the four runs form the corners of a square. Factors can be quantitative or qualitative, although their treatment in the final model will be different (see figure 3.6) .

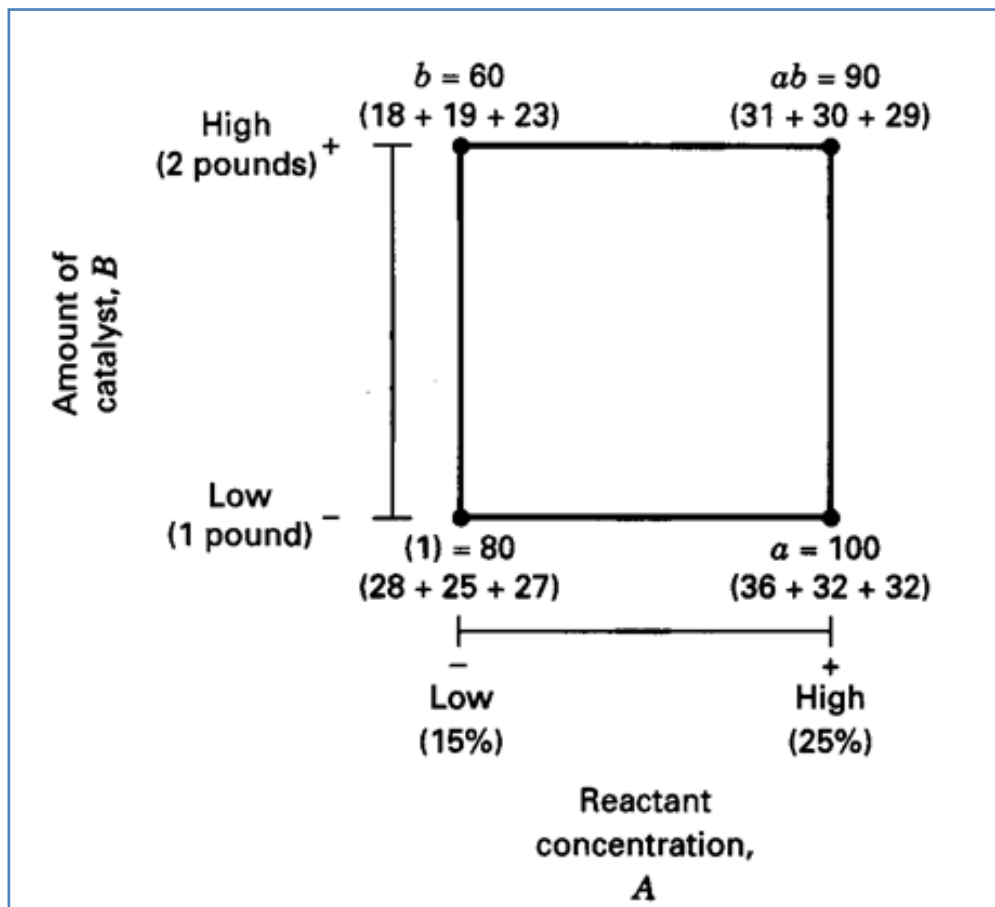


Figure 3.6: The treatment combinations in 2^2 design (Menasce Daniel,2001)

3.1.2.2. General full factorial design

In general full factorial designs, each factor can have a different number of levels, and the factors can be quantitative, qualitative or both (Minitab 16 helpdesk).

3.1.2.3. Two level full factorial designs

These are factorial designs where the number of levels for each factor is restricted to two. Restricting the levels to two and running a full factorial experiment reduces the number of treatments (compared to a general full factorial experiment) and allows for the investigation of all the factors and all their interactions. If all factors are quantitative, then the data from such experiments can be used for predictive purposes, provided a linear model is appropriate for modelling the response (since only two levels are used, curvature cannot be modelled) (Minitab 16 helpdesk).

3.1.2.4. Two level fractional factorial designs

This is a special category of two level designs where not all factor level combinations are considered and the experimenter can choose which combinations are to be excluded. Based on the excluded combinations, certain interactions cannot be determined (Minitab 16 helpdesk)..

3.1.2.5. Plackett-Burman designs

This is a special category of two level fractional factorial designs, proposed by R. L. Plackett and J. P. Burman, where only a few specifically chosen runs are performed to investigate just the main effects (*i.e.* no interactions) (Minitab 16 helpdesk)..

3.1.2.6. Taguchi's orthogonal arrays

Taguchi's orthogonal arrays are highly fractional designs, used to estimate main effects using only a few experimental runs. These designs are not only applicable to two level factorial experiments, but also can investigate main effects when factors have more than two levels. Designs are also available to investigate main effects for certain mixed level experiments where the factors included do not have the same number of levels (Anawa, Olabi, 2007).

3.1.3. Response surface method designs

These are special designs that are used to determine the settings of the factors to achieve an optimum value of the response.

3.1.4. Reliability DOE

This is a special category of DOE where traditional designs, such as the two level designs, are combined with reliability methods to investigate effects of different factors on the life of a unit. In Reliability DOE, the response is a life metric (*e.g.* age, miles, cycles, etc.), and the data may contain censored observations (suspensions, interval data).

3.2. Least square and regression

Y_x is the output variables and x is the inputs; thus $E(Y_x)=g(x)$, where $g(x)$ is increasing function. A linear increase of the function is assumed then $g(x)=a+bx$ is general linear function. When a and b are unknown constants that $E(Y_x)=a+bx$ is assumed. The variance of the outputs can be assumed that $V[Y_x]=\sigma^2$ is a constant for all values of input (x). x values can be picked like x_1, x_2, \dots, x_n for each of these we select one (or more) value(s) at random from corresponding groups of y values; y_1, y_2, \dots, y_n . Assuming selecting values at random from output groups of y values, it follows that Y_1, Y_2, \dots, Y_n are independent random variables and $E(Y_i)=a+bx_i$, $i=1, 2, \dots, n$. We certainly would not expect the observed value selected from the population of y values with inputs x_i to be equal to $a+bx_i$, the mean of the population; e_i represents the deviation between the value selected, Y_i , and the population mean $a+bx_i$, that is (Devor, Tsong-how, 1992),

$$e_i = Y_i - (a + bx_i) \quad (3.1)$$

from which it is written;

$$Y_i = a + bx_i + e_i, \quad i = 1, 2, \dots, n \quad (3.2)$$

These quantities e_1, e_2, \dots, e_n are sometimes are called measurement errors or errors of observation; they are unobservable random variables, denoted by lowercase letters to be consistent with the notation the is used for this model.

$$E[e_i] = E[Y_i - (a + bx_i)] = 0 \quad (3.3)$$

and

$$Var[e_i] = Var[Y_i] = \sigma^2 \quad (3.4)$$

The model which is named as a simple linear regression model can be summarized;

$$Var[e_i] = Var[Y_i] = \sigma^2 \quad (3.5)$$

1. We have population of y values for each x ; the population random variable corresponding to x_i is Y_i .
2. $E[Y_i] = a + bx_i$ for each x_i .
3. $Var[Y_i] = \sigma^2$ for each x_i .
4. The errors of observation $e_i = Y_i - a - bx_i$ are uncorrelated (as we have described the model. They are actually independent, but we do not really need such a strong assumption)

The simple linear regression model has three unknown parameters, a, b, and σ^2 . The most frequently used method for estimating unknown parameters is called least squares (Devor, Tsong-how, 1992).

Y_1, Y_2, \dots, Y_n is uncorrelated, $E(Y_x) = g(x_i)$, $Var[Y_i] = \sigma^2$, $i=1, 2, \dots, n$, where the x_i 's are constants and the function $g(x_i)$ involves unknown parameters. The least squares estimators of the unknown parameters in $g(x)$ are those values that minimize,

$$Q = \sum_{i=1}^n (Y_i - g(x_i))^2 = \sum_{i=1}^n e_i^2 \quad (3.6)$$

The estimator for σ^2 is

$$S^2 = \frac{1}{n-2} \sum (Y_i - \hat{g}(x_i))^2 \quad (3.7)$$

Where $\hat{g}(x_i)$ is the least square estimator for $E(Y_x) = g(x_i)$ and k is chosen to make S^2 unbiased [2].

It is quite straightforward to find the values that minimize

$$Q = \sum (Y_i - g(x_i))^2 = \sum (Y_i - a - bx_i)^2 \quad (3.8)$$

Q is a quadratic function of a and b, it is a differentiable function of both and the minimizing values are those that satisfy $\frac{\partial Q}{\partial a} = \frac{\partial Q}{\partial b} = 0$. Thus;

$$\frac{\partial Q}{\partial a} = -2 \sum (y_i - a - bx_i) = -2 \sum y_i + 2na + 2b \sum x_i \quad (3.9)$$

$$\frac{\partial Q}{\partial b} = -2 \sum x_i (y_i - a - bx_i) = -2 \sum x_i y_i + 2a \sum x_i + 2b \sum x_i^2 \quad (3.10)$$

The least squares estimates for a and b must satisfy

$$-2 \sum y_i + 2n\hat{a} + 2\hat{b} \sum x_i = 0 \quad (3.11)$$

$$-2 \sum x_i y_i + 2\hat{a} \sum x_i + 2\hat{b} \sum x_i^2 = 0 \quad (3.12)$$

Which is equivalent to

$$n\hat{a} + \hat{b} \sum x_i = \sum y_i \quad (3.13)$$

$$\hat{a} \sum x_i + \hat{b} \sum x_i^2 = \sum x_i y_i \quad (3.14)$$

These latter equations are called normal equations, the equations whose solutions determine the least square estimates. From the first normal equation [2];

$$\hat{a} = \bar{y} - \hat{b}\bar{x} \quad (3.15)$$

Where

$$\bar{y} = \frac{1}{n} \sum y_i \quad \bar{x} = \frac{1}{n} \sum x_i \quad (3.16)$$

and substituting this in the second gives

$$(\bar{y} - \hat{b}\bar{x}) \sum x_i + \hat{b} \sum x_i^2 = \sum x_i y_i \quad (3.17)$$

From which we find

$$\hat{b} = \frac{\sum x_i y_i - \bar{y} \sum x_i}{\sum x_i^2 - \bar{x} \sum x_i} \quad (3.18)$$

There are many ways to write this equation for \hat{b} ;

$$\sum (x_i - \bar{x})^2 = \sum x_i^2 - \frac{(\sum x_i)^2}{n} = \sum x_i^2 - \bar{x} \sum x_i \quad (3.19)$$

So the n-denominator can be written $\sum (x_i - \bar{x})^2$. Similarly;

$$\begin{aligned} \sum (x_i - \bar{x})(y_i - \bar{y}) &= \sum (x_i y_i - x_i \bar{y} - \bar{x} y_i + \bar{x} \bar{y}) \\ &= \sum x_i y_i - \bar{y} \sum x_i - \bar{x} \sum y_i + n \bar{x} \bar{y} \\ &= \sum x_i y_i - \bar{y} \sum x_i \\ &= \sum (x_i - \bar{x}) y_i \end{aligned} \quad (3.20)$$

Since $n\bar{y} = \sum y_i$. Thus the least squares estimate for b can be written

$$\hat{b} = \frac{\sum (x_i - \bar{x})(y_i - \bar{y})}{\sum (x_i - \bar{x})^2} \quad (3.21)$$

Which is most used formula for \hat{b} . The ratio of

$$\sum x_i y_i - \frac{(\sum x_i)(\sum y_i)}{n} \quad (3.22)$$

to

$$\sum x_i^2 - \frac{(\sum x_i)^2}{n} \quad (3.23)$$

provides the most accuracy. The least squares estimators are $\hat{A} = \bar{Y} - \hat{B}\bar{x}$,

$$\hat{B} = \frac{\sum (x_i - \bar{x})(y_i - \bar{y})}{\sum (x_i - \bar{x})^2} \quad (3.24)$$

The estimator for the scatter graphic line is $\hat{Y} = \hat{A} + \hat{B}x$. [2] The unbiased estimator for σ^2 is

$$\begin{aligned} S^2 &= \frac{1}{n-2} \sum (Y_i - \hat{Y}_i)^2 = \frac{1}{n-2} \sum (Y_i - \hat{A} - \hat{B}x_i)^2 \\ &= \frac{1}{n-2} [\sum (Y_i - \bar{Y})^2 - \hat{B}^2 \sum (x_i - \bar{x})^2] \end{aligned} \quad (3.25)$$

3.3 Analysis of Variance

Suppose independent samples are taken from each of k different populations or groups of experiments. The sample from population i is of size $n_i = 1, 2, \dots, k$. The sample random variables are Y_{ij} ; $i = 1, 2, \dots, k$, $j = 1, 2, \dots, n_i$. Assumed that Y_{ij} 's are independent, normal, $E[Y_{ij}] = \mu_i$, $\text{Var}[Y_{ij}] = \sigma^2$ and want to test $H_0: \mu_1 = \mu_2 = \dots = \mu_k$ (null hypothesis) versus $H_1: H_0$ is false. We have samples of size n_i from populations μ_i , $i = 1, 2, \dots, k$. the sum of all expected values of the sample random variables;

$$\sum_i \sum_j E[Y_{ij}] = \sum_i \sum_j \mu_i = \sum_i n_i \mu_i \quad (3.26)$$

And the average expected value is this total divided by the complete sample size

$$\mu = \frac{\sum n_i \mu_i}{\sum n_i} \quad (3.27)$$

τ_i represents the deviation of the i th population mean from this average, $\tau_i = \mu_i - \mu$, and

$$\sum n_i \tau_i = \sum n_i (\mu_i - \mu) = \sum n_i \mu_i - \mu \sum n_i = 0 \quad (3.28)$$

The weighted sum of these deviations equal zero. Through the original hypothesis that $\mu_1 = \mu_2 = \dots = \mu_k$ is equivalent to $\mu_1 - \mu = \mu_2 - \mu = \dots = \mu_k - \mu$, that is $\tau_1 = \tau_2 = \dots = \tau_k$, which, together with $\sum n_i \tau_i = 0$ actually implies that hypothesis of equal population means becomes $H_0: \tau_1 = \tau_2 = \dots = \tau_k = 0$, and $E[Y_{ij}] = \mu + \tau_i$, $\text{Var}[Y_{ij}] = \sigma^2$. It is also convenient to introduce errors of observation e_{ij} , deviations between the sample random variables and their expected values,

$$e_{ij} = Y_{ij} - (\mu + \tau_i) \quad (3.29)$$

as section 3.2. We observe $\sum n_i$ random variables, Y_{ij} , where

$$Y_{ij} = \mu + \tau_i + e_{ij} \quad i=1,2,\dots,k \quad j = 1,2, \dots, n_i \quad (3.30)$$

$\mu, \tau_1, \tau_2, \dots, \tau_k$ are unknown constants, the e_{ij} 's are normal and independent, with means 0 and variance σ^2 .

The model is called the completely randomized model in the literature of design of experiments. Independent samples are selected completely at random from each of k , different normal populations. With the explicit introduction of the observation errors, a natural method of estimation of μ and τ_i is given by least squares (Devor, Tsonghow, 1992). We want the values for $\mu, \tau_1, \tau_2, \dots, \tau_k$ such that

$$Q = \sum_i \sum_j e_{ij}^2 = \sum_i \sum_j (Y_{ij} - \mu - \tau_i)^2 \quad (3.31)$$

is minimized (and recall that $\sum n_i \tau_i = 0$, which simplifies things). We have

$$\frac{\partial Q}{\partial \mu} = -2 \sum_i \sum_j (Y_{ij} - \mu - \tau_i) \quad (3.32)$$

$$\begin{aligned}
&= -2Y_{..} + 2n_{..}\mu + 2 \sum n_i \tau_i = -2Y_{..} + 2n_{..}\mu \\
\frac{\partial Q}{\partial \tau_i} &= -2 \sum_j (Y_{ij} - \mu - \tau_i) \\
&= -2Y_{i.} + 2n_i\mu + 2n_i\tau_i \quad i = 1, 2, \dots, k
\end{aligned} \tag{3.33}$$

Summary of subscript;

$$Y_{i.} = \sum_j Y_{ij} \quad Y_{..} = \sum_i Y_{i.} = \sum_i \sum_j Y_{ij} \quad n_{..} = \sum_i n_i. \tag{3.34}$$

The equations to be solved for the estimators are,

And the solutions are easily found to be

$$\hat{\mu} = \bar{Y}_{..} \quad \hat{\tau}_i = \bar{Y}_{i.} - \bar{Y}_{..} \quad i=1, 2, \dots, k \tag{3.35}$$

Where super bars indicate averaging:

$$\bar{Y}_{..} = \frac{1}{n_{..}} Y_{..} \quad \bar{Y}_{i.} = \frac{1}{n_i} Y_{i.} \tag{3.36}$$

The least square estimator μ is $\bar{Y}_{..}$, the overall mean, and the estimator for τ_i is $\bar{Y}_{i.} - \bar{Y}_{..}$, the deviation between i th sample and the overall mean (Devor, Tsong-how, 1992).

The unbiased estimator for σ^2 is

$$\begin{aligned}
S^2 &= \frac{1}{n-k} \sum \sum (Y_{ij} - \hat{\mu} - \hat{\tau}_i)^2 \\
&= \frac{1}{n-k} \sum \sum (Y_{ij} - \bar{Y}_{i.})^2
\end{aligned} \tag{3.37}$$

Where the divisor is $n_{..} - k$, the total sample size ($n_{..} = \sum_i n_i$) less the number of independent parameters specifying the population means (k). the estimators $\bar{Y}_{..}$ (for μ) and $\bar{Y}_{i.} - \bar{Y}_{..}$ (for τ_i) are both linear functions of normal random variables and thus are themselves normal. The total sum of squares of all the observations about the overall observed mean is

$$\sum_i \sum_j (Y_{ij} - \bar{Y}_{..})^2 \tag{3.38}$$

The quantity can be partitioned as follows;

$$\begin{aligned}
\sum_i \sum_j (Y_{ij} - \bar{Y}_{i.} - \bar{Y}_{..})^2 &= \sum_i \sum_j \{ (Y_{ij} - \bar{Y}_{i.})^2 + (\bar{Y}_{i.} - \bar{Y}_{..})^2 + 2(Y_{ij} - \bar{Y}_{i.})(\bar{Y}_{i.} - \bar{Y}_{..}) \} \\
&= \sum_i \sum_j \{ (Y_{ij} - \bar{Y}_{i.})^2 + (\bar{Y}_{i.} - \bar{Y}_{..})^2 + 2(Y_{ij} - \bar{Y}_{i.})(\bar{Y}_{i.} - \bar{Y}_{..}) \} \\
&= \sum_i \sum_j (Y_{ij} - \bar{Y}_{i.})^2 + \sum_i \sum_j (\bar{Y}_{i.} - \bar{Y}_{..})^2
\end{aligned} \tag{3.39}$$

Since

$$\begin{aligned}
2 \sum_i \sum_j (Y_{ij} - \bar{Y}_{i.})(\bar{Y}_{i.} - \bar{Y}_{..}) &= 2 \sum_i (\bar{Y}_{i.} - \bar{Y}_{..}) \sum_j (Y_{ij} - \bar{Y}_{i.}) \\
&= 2 \sum_i (\bar{Y}_{i.} - \bar{Y}_{..}) \cdot 0 = 0
\end{aligned} \tag{3.40}$$

Also,

$$\sum_i \sum_j (\bar{Y}_{i.} - \bar{Y}_{..})^2 = \sum_i n_i (\bar{Y}_{i.} - \bar{Y}_{..})^2 \tag{3.41}$$

Because the summand does not depend on j . This gives us basic identification.

$$\sum_i \sum_j (Y_{ij} - \bar{Y}_{..})^2 = \sum_i \sum_j (Y_{ij} - \bar{Y}_{i.})^2 + \sum_i n_i (\bar{Y}_{i.} - \bar{Y}_{..})^2 \quad (3.42)$$

The first quantity is the sum of squares of the residuals.

$$\widehat{e}_{ij} = Y_{ij} - \hat{\mu} - \hat{\tau}_i \quad (3.43)$$

The numerator of S^2 , used to estimate σ^2 regardless of whether the populations means are equal; divided by σ^2 it is in fact a χ^2 random variable with $\sum_i (n_i - k) = n - k$ degrees of freedom. The second quantity (right side) is actually $\sum_i n_i \widehat{\tau}_i^2$ and is independent of S^2 of all τ_i 's are equal to 0, it is showed that

$$\frac{1}{\sigma^2} \sum_i n_i (\bar{Y}_{i.} - \bar{Y}_{..})^2 \quad (3.44)$$

is a χ^2 random variable with $k - 1$ degrees of freedom. If all τ_i 's are equal to 0, it is expected that the τ_i 's to be small because of the least square estimators unbiased, and thus $\sum_i n_i \widehat{\tau}_i^2$

Should be relatively small; when τ_i 's are unequal, $\sum_i n_i \widehat{\tau}_i^2$ tend to get a larger.

$$\frac{\sum \sum (Y_{ij} - \bar{Y}_{i.})^2}{\sigma^2} \quad (3.45)$$

and

$$\frac{\sum n_i (\bar{Y}_{i.} - \bar{Y}_{..})^2}{\sigma^2} \quad (3.46)$$

Are independent χ^2 random variables so the ratio

$$\frac{\sum n_i (\bar{Y}_{i.} - \bar{Y}_{..})^2}{k-1} / \frac{\sum \sum (Y_{ij} - \bar{Y}_{i.})^2}{n_i-1} \quad (3.47)$$

Has an F-distribution with $k - 1, n - 1$ degrees of freedom if $\tau_1 = \tau_2 = \dots = \tau_k = 0$, we reject $H_0: \tau_1 = \tau_2 = \dots = \tau_k = 0$ if this ratio exceeds $F_{1-\alpha}$, the $100(1-\alpha)$ th of F-distribution with $k - 1, n - 1$ degrees of freedom, to have P (type error) $= \alpha$, this is in fact the generalized likelihood ratio test for H_0 (Devor, Tsong-how, 1992)..

The quantities used in testing $H_0: \tau_1 = \tau_2 = \dots = \tau_k = 0$ are represented in an analysis of variance. Table 3.1 presents the analysis of variance (ANOVA) table for the randomized model, based on sample of size n_1, n_2, \dots, n_k from k population. The first column identifies the source of the variation, the second column gives the degrees of freedom for the different sources (sum of total degrees of freedom), the third column indicates the sums of the squares for the sources and the final column gives the mean squares (ratio of sums of squares over degrees of freedom) (Wonnacott, 1981). The ratio of the between populations mean square to the residual mean square is the F statistic whose value is compared with the appropriate F value

in deciding whether to reject $H_0: \tau_1 = \tau_2 = \dots = \tau_k = 0$. Formulas are showed below;

Total sum of squares

$$\sum \sum (Y_{ij} - \bar{Y}_{..})^2 = \sum \sum Y_{ij}^2 - \frac{(Y_{..})^2}{n} = SS_T \quad (3.48)$$

Among populations sum of squares

$$\sum n_i (\bar{Y}_{i.} - \bar{Y}_{..})^2 = \sum \frac{Y_{i.}^2}{n_i} - \frac{(Y_{..})^2}{n} = SS_A \quad (3.49)$$

Residual sum of squares

$$\sum \sum \hat{e}_{ij}^2 = \sum \sum (Y_{ij} - \bar{Y}_{i.})^2 = \sum \sum Y_{ij}^2 - \sum \frac{(Y_{i.})^2}{n_i} = SS_R \quad (3.50)$$

Table 3.1 represents the analysis of variance table[2].

Source	Degrees of Freedom	Sums of Squares	MeanSquares
Among Population	k - 1	$SS_A = \sum n_i (\bar{Y}_{i.} - \bar{Y}_{..})^2$	$MSR = SS_A / (k - 1)$
Residual	n - k	$SS_R = \sum \sum (\bar{Y}_{ij} - \bar{Y}_{i.})^2$	$MSE = SS_R / (n - k)$
Total	n - 1	$SS_T = \sum \sum (\bar{Y}_{ij} - \bar{Y}_{..})^2$	

Table 3.1 : ANOVA Table (Khurillandre, Mukhopadhyay,2006)

3.3.1 Coefficients (Coeff)

It means the estimates of the population regression coefficients in a regression equation. For each factor, Minitab calculates k-1 coefficients, where k is the number of levels in the factor. The formulas for coefficients for the factors and interactions are:

$$\text{Coeff A} = \bar{y}_A - \bar{y}_{..} \quad (3.51)$$

$$\text{Coeff B} = \bar{y}_B - \bar{y}_{..} \quad (3.52)$$

$$\text{Coeff AB} = \bar{y}_{AB} - \bar{y}_A - \bar{y}_B + \bar{y}_{..} \quad (3.53)$$

The Standard error of the coefficient for a design is;

$$e = \sqrt{\frac{MS_E}{n}} \quad (3.54)$$

\bar{y}_A = mean of y at the high level of factor A

$\bar{y}_{..}$ = overall mean of all observations

\bar{y}_B =mean of y at the high level of factor B

\bar{y}_{AB} = mean of y at the levels of A and B

MS_E =mean square error

n=number of the estimated term

3.3.2 Sum of squares (SS)

SS means the sum of squared deviations. The formulas presented are for a balanced two-factor model with factors A and B. These formulas can be extended to models with more than two factors.

SS Total is the total variation in the model. SS (A) and SS (B) is the deviation of the estimated factor level mean around the overall mean. They are also known as the sum of squares between treatments. SS Error is the deviation of an observation from its corresponding factor level mean. It is also known as error within treatments (Khurillandre, Mukhopadhyay,2006). The calculations are

$$SS(A) = nb \sum_i (\bar{y}_{i..} - \bar{y} \dots)^2 \quad (3.55)$$

$$SS(B) = na \sum_j (\bar{y}_{.j.} - \bar{y} \dots)^2 \quad (3.56)$$

$$SS \text{ main effects} = SS(A) + SS(B) \quad (3.57)$$

$$SS(AB) = SS \text{ Total} - SS \text{ Error} - SS(A) - SS(B) \quad (3.58)$$

$$SS \text{ Error} = SS \text{ Total} - SS(A) - SS(B) - SS(AB) \quad (3.59)$$

$$SS \text{ Total} = \sum_i \sum_j \sum_k (y_{ijk} - \bar{y} \dots)^2 \quad (3.60)$$

If the model includes replicates, SS Pure Error is displayed

$$SS \text{ Pure error} = \sum_i \sum_j \sum_k (y_{ijk} - \bar{y}_{ij.} \dots)^2 \quad (3.61)$$

If you fit a reduced model, SS Lack of Fit displayed

$$SS \text{ Lack of fit} = \sum_{i=1}^n n_i (\bar{y}_i - \hat{y}_i)^2 \quad (3.62)$$

If the model includes center points, SS Curvature is displayed:

n split-plot designs, two additional sum of squares are displayed for whole plot and subplot error variation.

SS WP Error= sum of the squared whole plot residuals

SS SP Error= sum of the squared residuals

Notation

a= number of levels in factor A

b= number of levels in factor B

n= total number of replicates

$\bar{y}_{i..}$ = mean of the i^{th} level of factor A

$\bar{y} \dots$ = Overall mean of all observations

$\bar{y}_{j..}$ = mean of the j^{th} level of factor B

y_{ijk} = *observation at the i^{th} level of factor A, j^{th} level of factor B, and k^{th} replicate*

$\bar{y}_{ij.}$ = mean of the i^{th} level of factor A and j^{th} level of factor B

\bar{y}_C = mean of response for factorial points

n_F = number of factorial points

3.3.3 Degrees of freedom (df)

For a full factorial design with factors A and B, and a blocking variable, the number of degrees of freedom associated with each sum of squares is:

$$\text{DF Block} = c-1 \quad (3.63)$$

$$\text{DF (A)} = a-1 \quad (3.64)$$

$$\text{DF (B)} = b-1 \quad (3.65)$$

$$\text{DF main Effect} = \text{DF (A)} + \text{DF (B)} \quad (3.66)$$

$$\text{DF(AB)} = (a-1)(b-1) \quad (3.67)$$

$$\text{DF Error} = n-p \quad (3.68)$$

$$\text{DF Pure Error} = \sum_i (n_i-1) \quad (3.69)$$

$$\text{DF Lack of fit} = m-p \quad (3.70)$$

$$\text{Total} = n-1 \quad (3.71)$$

Notation

a = number of levels in factor A

b = number of levels in factor B

c = number of blocks

n = total number of observations

n_i = total number of observations for i^{th} factor level combination

m = number of factor level combinations

p = number of parameters

The degrees of freedom for the test are:

- Numerator = degrees of freedom for term
- Denominator = degrees of freedom for error

3.3.4 Mean square (MS)

The calculation for the mean square for the model terms is;

$$MS \text{ Term} = \frac{\text{Adj SS Term}}{\text{DF Term}} \quad (3.72)$$

3.3.5 F Test

F is a test to determine whether the interaction and main effects are significant. The formula for the model terms is;

$$F = \frac{MS \text{ Term(Regression)}}{MS \text{ (Error)}} = \frac{MSR}{MSE} \quad (3.73)$$

Larger values of F support rejecting the null hypothesis that there is not a significant effect. ANOVA table can be used to test the null hypothesis that $\mu_1 = \mu_2 = \dots = \mu_n$ when looking at the means of several groups, it can also be used in regression. In the case of means, the null hypothesis means that knowing the group membership provides no extra information about y . In the case of regression, the corresponding null hypothesis would be that knowing x provides no extra information about y . If we were to guess the same y value for every x , that would mean that the regression line was flat, that it had no slope. Therefore, the null hypothesis for the ANOVA table in regression is $H_0: \beta_1 = 0$ and the alternate hypothesis is $H_1: \beta_1 \neq 0$.

For balanced split-plot designs, the F statistic for hard-to-change factors uses the MS for whole plot error in the denominator. If the F-statistic is large, it seems unlikely that the population means of each level of inputs are truly equal. Mathematical theory proves that if the appropriate assumptions hold, the F-statistic follows an F distribution with degrees of freedom (df) (Khurillandre, Mukhopadhyay, 2006).

3.3.6 p-values

Used in hypothesis tests to help you decide whether to reject or fail to reject a null hypothesis. The p-value is the probability of obtaining a test statistic that is at least as extreme as the actual calculated value, if the null hypothesis is true. A commonly used cut-off value for the p-value is 0.05. For example, if the calculated p-value of a test statistic is less than 0.05, you reject the null hypothesis. The p-value is looked up

in an F table and gives the likelihood of observing an F statistic at least this extreme (at least this large) assuming that the true population factor has equal level means. Thus, when the p-value is small (i.e. less than 0.05 or 0.1) the effect size of that factor is statistically significant (Pana,Wang,Hsiao, Ho,2006).

3.3.7 R^2 (R-sq)

R^2 means that the coefficient of determination; indicates how much variation in the response is explained by the model. The higher the R^2 , the better the model fits your data (Minitab 16 Helpdesk). The formula is:

$$R^2 = 1 - \frac{SS \text{ Error}}{SS \text{ Total}} \quad (3.74)$$

Another presentation of the formula is normally used analysis of variance as regression:

$$R^2 = \frac{SS \text{ Regression}}{SS \text{ Total}} \quad (3.75)$$

R^2 can also be calculated as the Correlation $(Y, \hat{Y})^2$. For more information see table 3.1.

3.3.8 Predicted R^2

Indicates how well the model predicts responses for new observations. Larger values of predicted R^2 suggest models of greater predictive ability(Minitab 16 Hepdesk).. The formula is:

$$R^2(\text{pred}) = 1 - \frac{PRESS}{SSTotal} =: - \frac{\sum_1^n (\frac{e_i}{1-h_i})^2}{\sum (y_i - \bar{y})^2} \quad (3.76)$$

PRESS = predicted ability

$y_i = i^{\text{th}}$ observed response value

\bar{y} = mean response

n = number of observations

$e_i = i^{\text{th}}$ residual

$h_i = i^{\text{th}}$ diagonal element of $X(X^T X)^{-1} X^T$

X = predictor matrix

3.3.9 Adjusted R² (R-sq adj)

Adjusted R² accounts for the number of factors in your model (Minitab 16 Hepdesk).. The formula is:

$$\text{Adj } R^2 = 1 - \frac{\text{MS (Error)}}{\text{SSTotal/DF Total}} \quad (3.77)$$

3.4 Response Surface Methodology Theory

3.4.1 Response surface methodology analysis

RSM is based on a group of mathematical and statistical techniques that can be used to define the relationships between the response and input parameters (independent variables). RSM shows the effects of the independent variables on the processes, alone or with combinations. In addition to analyzing the effects of the independent variables, this experimental methodology also generates a mathematical model which shows the relationship between input and output parameters. The graphical perspective of the mathematical model has led to the term Response Surface Methodology. The relationship between the output and the input is given in Eq. :

$$y = f(x_1, x_2, x_3, \dots, x_n) + \epsilon \quad (3.78)$$

$$y = f'(x)\beta + \epsilon \quad (3.79)$$

where y is the response, f is the unknown function of response, $x_1, x_2, x_3, \dots, x_n$ indicate the independent variables (input parameters), also called natural variables, n is the number of the independent variables and finally ϵ is the statistical error which represents other sources of unaccounted variability from f. These sources include the effects such as the measurement error. It is generally assumed that ϵ has a normal distribution with mean zero and variance (Khurillandre, Mukhopadhyay, 2006)..

Two important models are commonly used in RSM. These are special cases of model and include the first-degree model ($d = 1$),

$$y = \beta_0 + \sum_{i=1}^k \beta_i x_i + \epsilon \quad (3.80)$$

In some situations, approximating polynomials of order higher than two are used. The general motivation for a polynomial approximation for the true response function f is based on the Taylor series expansion around the point $x_{10}, x_{20}, \dots, x_{k0}$. For example, the first-order model is developed from the first-order Taylor series expansion

$$f \cong f(x_{10}, x_{20}, \dots, x_{k0}) + \frac{\partial f}{\partial x_1} \big|_{x=x_0} (x_1 - x_{10}) + \frac{\partial f}{\partial x_2} \big|_{x=x_0} (x_2 - x_{20}) + \dots + \frac{\partial f}{\partial x_k} \big|_{x=x_0} (x_k - x_{k0}) \quad (3.81)$$

where x refers to the vector of independent variables and x_0 is the vector of independent variables at the specific point $x_{10}, x_{20}, \dots, x_{k0}$.

The model used in RSM is generally a full quadratic equation or the diminished form of this equation. The second order model can be written as follows:

$$y = \beta_0 + \sum_{j=1}^k \beta_j X_j + \sum_{j=1}^k \beta_{jj} X_j^2 + \sum \sum_{i < j} \beta_{ij} X_i X_j \quad (3.82)$$

where b_0 , b_i , b_{ii} and b_{ij} are regression coefficients for intercept, linear, quadratic and interaction coefficients respectively and X_i and X_j are coded independent variables.

The purpose of considering a model such as followings;

1. To establish a relationship, albeit approximate, between y and x_1, x_2, \dots, x_k that can be used to predict response values for given settings of the control variables.
2. To determine, through hypothesis testing, significance of the factors whose levels are represented by x_1, x_2, \dots, x_k .
3. To determine the optimum settings of x_1, x_2, \dots, x_k that result in the maximum (or minimum) response over a certain region of interest. (Bas Deniz, Boyaci Ismail, 2006)

It is easy to estimate parameters in second-order model. The method of least squares can be used for this purpose. There is considerable practical experience indicating that second-order models work well in solving real response surface problems.

There is a close connection between RSM and linear regression analysis. The β 's are a set of unknown parameters. To estimate the values of these parameters, we must collect data on the system we are studying. Regression analysis is a branch of statistical model building that uses these data to estimate the β 's. Because, in general, polynomial models are linear functions of the unknown β 's, linear regression analysis is referred as a technique.[4] The design matrix notation of the model is given in Eq. (3.83)

$$y = X\beta + \varepsilon \quad (3.83)$$

$$\underbrace{\begin{bmatrix} y_1 \\ y_2 \\ \vdots \\ y_n \end{bmatrix}}_y = \underbrace{\begin{bmatrix} 1 & x_{11} & x_{12} & \cdot & \cdot & x_{1k} \\ 1 & x_{21} & x_{22} & \cdot & \cdot & x_{2k} \\ \cdot & \cdot & \cdot & \cdot & \cdot & \cdot \\ \cdot & \cdot & \cdot & \cdot & \cdot & \cdot \\ \cdot & \cdot & \cdot & \cdot & \cdot & \cdot \\ 1 & x_{n1} & x_{n2} & \cdot & \cdot & x_{nk} \end{bmatrix}}_X \underbrace{\begin{bmatrix} \beta_0 \\ \beta_1 \\ \cdot \\ \cdot \\ \cdot \\ \beta_k \end{bmatrix}}_\beta + \underbrace{\begin{bmatrix} \varepsilon_1 \\ \varepsilon_2 \\ \cdot \\ \cdot \\ \cdot \\ \varepsilon_n \end{bmatrix}}_\varepsilon \quad (3.84)$$

The system of equations given above is solved using the least squares method. Least squares method is a multiple linear regression technique which is assumed that random errors are identically distributed with a zero mean and a number average unknown variance and they are independent of each other. The difference between the observed and the fitted value (\hat{y}) for the i^{th} observation $\varepsilon_i = y_i - \hat{y}_i$ is called the residual and is an estimate of the corresponding ε_i . Our criterion for choosing the b_i estimates is that they should minimize the sum of the squares of the residuals, which is often called the sum of squares of the errors and is denoted by SSE . (Bas Deniz, Boyaci Ismail, 2006). Thus,

$$SSE = \sum_{i=1}^n \varepsilon_i^2 = \sum (y_i - \hat{y}_i)^2 \quad (3.85)$$

$$\varepsilon = y - X\beta \quad (3.86)$$

And the SSE is

$$SSE = \varepsilon^T \varepsilon = (y - X\beta)^T (y - X\beta) \quad (3.87)$$

Differentiating the SSE with respect to β , we get a vector of partial derivatives, as follows:

$$\frac{\partial}{\partial \beta} (SSE) = -2X^T (y - X\beta) \quad (3.88)$$

Equating this derivative to zero we have $X\beta = y$ and this over-determined system of equations could be solved directly to obtain the coefficients of β by the following:

$$X^T X \beta = X^T y \quad (3.89)$$

The formal solution of these equations is then

$$\beta = (X^T X)^{-1} X^T y = C X^T y \quad (3.90)$$

Where

$$C = (X^T X)^{-1} \quad (3.91)$$

C is a square matrix. The regression coefficients were obtained which denote mathematical model of process, that the estimated response could be easily calculated using model equation. Usually the behavior of the system is unknown so one must check whether the model fits well to the experimental data. For verification of the model adequacy, some of these techniques are used such as residual analysis, scaling residuals, prediction error sum of squares (PRESS) residuals, and testing of the lack of fit. The overall predictive capability of the model is commonly explained by the coefficient of determination (R^2), which is calculated from PRESS. R^2 is a measure of the amount of the reduction in the variability of response obtained by using the repressor variables in the model. However, a large value of R^2 does not necessarily imply that the regression model is a good one. Adding a variable to the model will always increase R^2 , regardless of whether the additional variable is statistically significant or not. Thus, it is possible for models that have large values of R^2 to yield poor predictions of new observations or estimates of the mean response. If you plot experimental results versus model results, you should obtain a straight line passing the origin with the angle of 45° [$y = x$]. But in some cases you might obtain such a line [$y = a + bx$]. This line would also have a regression analysis with $R^2 = 1.000$ however it is totally insignificant. (Bradly Nuran,2007)

In DOE tool, Minitab creates a design matrix, called X, are the terms in the model. It is created from the specified factors and covariates. This description of the matrix applies primarily to general full factorial design.

The design matrix has n rows, where n = number of observations and several blocks of columns, corresponding to the terms in the model. The first block is for the constant and contains just one column, a column of all ones. The block for a covariate also contains just one column, the covariate column itself. The block of columns for a factor contains r columns, where r = degrees of freedom for the factor, and they are coded as shown in the example below.

Suppose A is a factor with 4 levels. Then it has 3 degrees of freedom and its block contains 3 columns, call them A1, A2, A3. Each row is coded as one of the following, see table 3.2.

Level of A	A1	A2	A3
1	1	0	0
2	0	1	0
3	0	0	1
4	1	1	1

Table 3.2: The example matrix form (Minitab 16 Helpdesk)

To calculate the columns for an interaction term, just multiply all the corresponding columns for the factors and/or covariates in the interaction. For example, suppose factor A has 6 levels, C has 3 levels, D has 4 levels, and Z and W are covariates. Then the term $A * C * D * Z * W * W$ has $5 \times 2 \times 3 \times 1 \times 1 \times 1 = 30$ columns. To obtain them, multiply each column for A by each for C, by each for D, by the covariates Z once and W twice.

3.4.2 Response optimization

Response optimization means to predict the response values for all possible combinations of inputs within the experimental region, and to identify an optimal experimental point. However, when several responses are treated at the same time, it is usually difficult to identify a single experimental point at which the goals for all responses are fulfilled, and therefore the final result often reflects a compromise between partially conflicting goals (Durman,Pakdil,2009) .

3.4.2.1 Response optimizer

Response optimizer helps to identify the combination of input variables that jointly optimize a single response or a set of responses. The overall desirability (D) is a measure of how well the combined goals for all the responses are achieved. It has a range of zero or one; 1 represents the ideal case; 0 indicates that one or more responses are outside their acceptable limits. Response optimizer searches for a combination of input variable levels that optimize a set of responses by satisfying the requirements for each response in the set.

In order to calculate the numerical optimal solution, you need to specify a target and lower and/ or upper bounds for each response. The boundaries needed depend on your goal: n If your goal is to *minimize* (smaller is better) the response, you need to determine a target value and the upper bound. You may want to set the target value at

the point of diminishing returns, that is, although you want to minimize the response, going below a certain value makes little or no difference. If there is no point of diminishing returns, use a very small number, one that is probably not achievable, for the target value. If your goal is to *target* the response, you probably have upper and lower specification limits for the response that can be used as lower and upper bounds. If your goal is to *maximize* (larger is better) the response, you need to determine a target value and the lower bound. Again, you may want to set the target value at the point of diminishing returns, although now you need a value on the upper end instead of the lower end of the range (Minitab 16 Helpdesk).

The response optimizer achieves to find an optimal solution for the input variable combinations and an optimization plot.

MINITAB's Response Optimizer is used to help identify the combination of input variable settings that jointly optimize a single response or a set of responses. Joint optimization must satisfy the requirements for all the responses in the set. The overall desirability (D) is a measure of how well you have satisfied the combined goals for all the responses. Overall desirability has a range of zero to one. One represents the ideal case; zero indicates that one or more responses are outside their acceptable limits. MINITAB calculates an optimal solution and draws a plot. The optimal solution serves as the starting point for the plot. This optimization plot allows you to interactively change the input variable settings to perform sensitivity analyses and possibly improve the initial solution in figure 3.7. (Menasce Daniel, 2001).

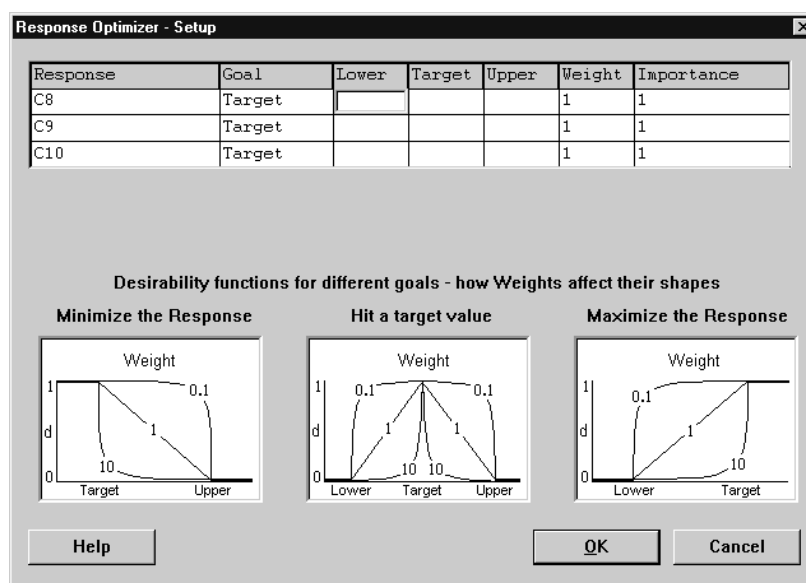


Figure 3.7: Response Optimizer-Setup (Menasce Daniel, 2001)

For each response, complete the table as Under Goal, choose Minimize, Target, or Maximize from the drop-down list., Under Lower, Target, and Upper, enter numeric values for the target and necessary bounds.

MINITAB's Response Optimizer searches for a combination of input variable levels that jointly optimize a set of responses by satisfying the requirements for each response in the set. The optimization is accomplished by obtaining the individual desirability (d) for each response, combining the individual desirabilities to obtain the combined or composite desirability (D), maximizing the composite desirability and identifying the optimal input variable settings

3.4.2.1.1 Individual desirabilities

MINITAB obtains an individual desirability (d) for each response using the goals and boundaries that you provide in the Setup subdialog box. There are three goals to choose from minimizing the response (smaller is better), target the response (target is best), maximize the response (larger is better). The boundaries needed depend on your goal:

- If your goal is to *minimize* (smaller is better) the response, you need to determine a target value and the upper bound. You may want to set the target value at the point of diminishing returns, that is, although you want to minimize the response, going below a certain value makes little or no difference. If there is no point of diminishing returns, use a very small number, one that is probably not achievable, for the target value.
- If your goal is to *target* the response, you probably have upper and lower specification limits for the response that can be used as lower and upper bounds.
- If your goal is to *maximize* (larger is better) the response, you need to determine a target value and the lower bound. Again, you may want to set the target value at the point of diminishing returns, although now you need a value on the upper end instead of the lower end of the range.

The weight defines the shape of the desirability function for each response. For each response, you can select a weight (from 0.1 to 10) to emphasize or de-emphasize the target.

A weight;

- less than 1 (minimum is 0.1) places less emphasis on the target
- equal to 1 places equal importance on the target and the bounds
- greater than 1 (maximum is 10) places more emphasis on the target

The illustrations below show how the shape of the desirability function changes when the goal is to maximize the response changes depending on the weight (Khrillandre, Mukhapadhyay,2006): Figure 3.8 indicates the weight values of the desirability function.

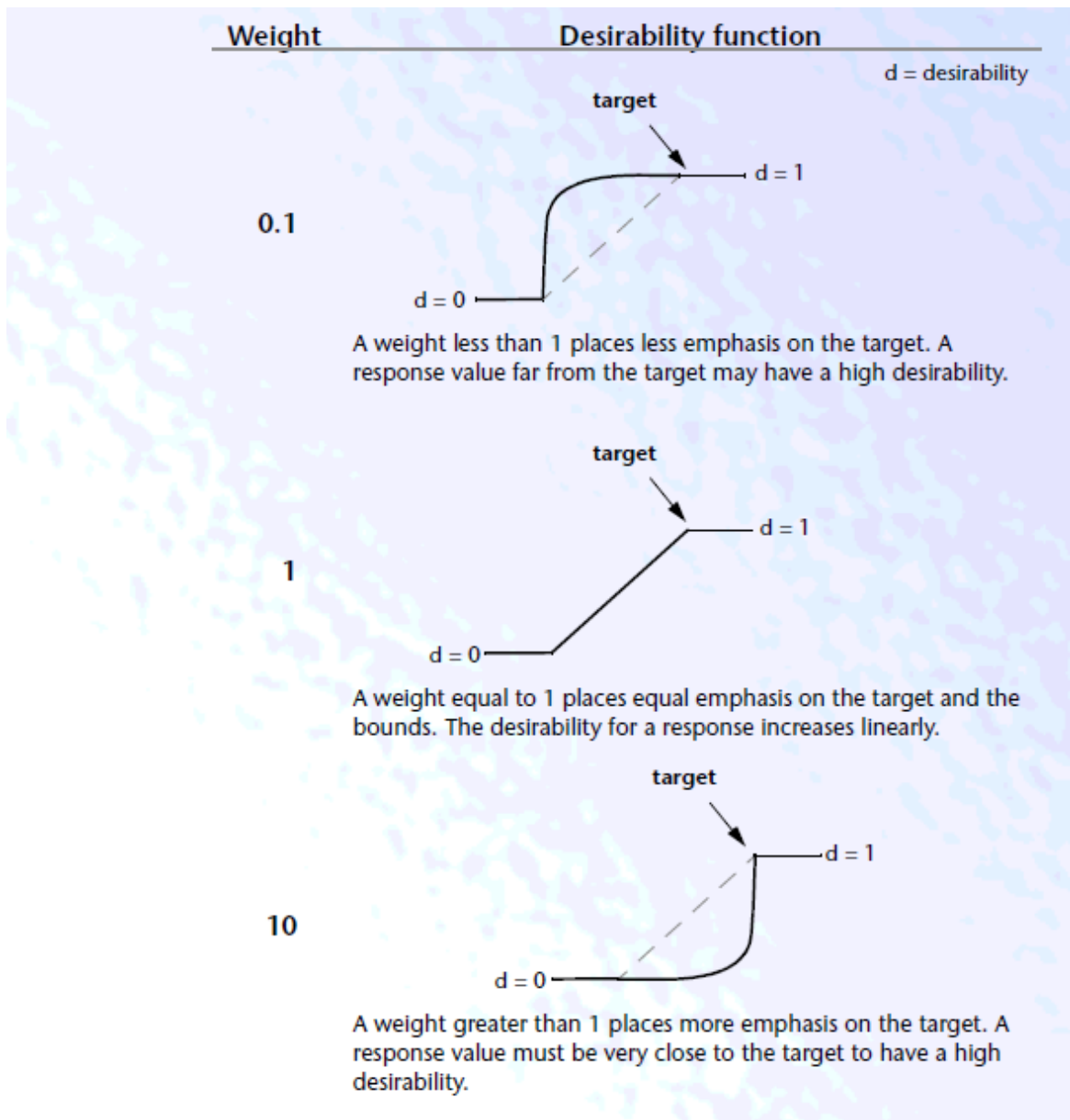


Figure 3.8: The weight values of the desirability function (Khrillandre, Mukhapadhyay,2006):

The illustrations below in figure 3.9 summarize the desirability functions:

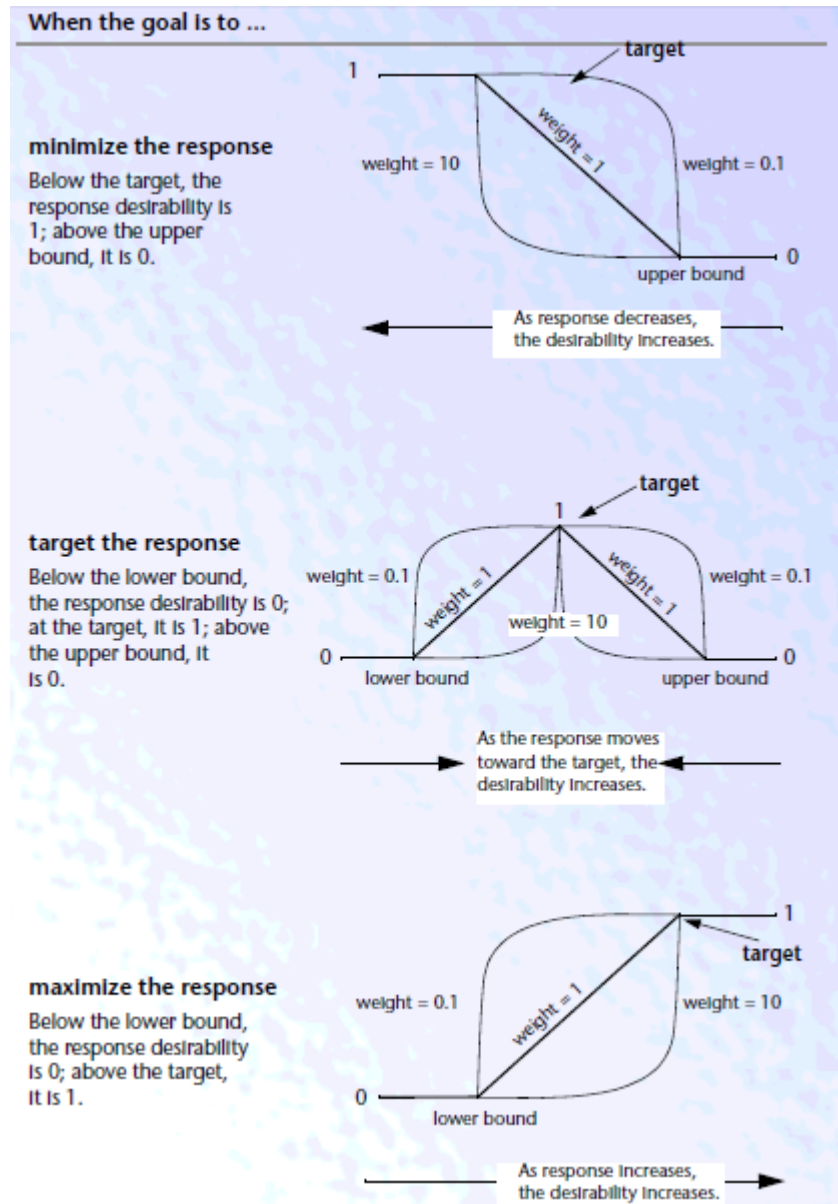


Figure 3.9: The goals of the desirability function(Khrillandre, Mukhapadhyay,2006)

Calculated the responses by using notation below in the formula(Minitab 16 Helpdesk):

\hat{y}_i = predicted value of i^{th} response

T_i = target value of i^{th} response

L_i = lowest acceptable value for i^{th} response

U_i = highest acceptable value for i^{th} response

d_i = desirability of i^{th} response

D = composite desirability

r_i = weight of desirability function of i^{th} response

w_i = importance of i^{th} response

$$W = \sum w_i \quad (3.93)$$

If you want to maximize output variables, the desirability is calculated as:

$$d_i = 0 \quad \hat{y}_i < L_i \quad (3.94)$$

$$d_i = ((\hat{y}_i - L_i)/(T_i - L_i))^{r_i} \quad L_i \leq \hat{y}_i \leq T_i \quad (3.95)$$

$$d_i = 1 \quad \hat{y}_i > T_i \quad (3.96)$$

If you want to minimize output variables, the desirability is calculated as:

$$d_i = 0 \quad \hat{y}_i > U_i \quad (3.97)$$

$$d_i = ((U_i - \hat{y}_i)/(U_i - T_i))^{r_i} \quad T_i \leq \hat{y}_i \leq U_i \quad (3.98)$$

$$d_i = 1 \quad \hat{y}_i < T_i \quad (3.99)$$

If you want to target output variables, the desirability is calculated as:

$$d_i = ((\hat{y}_i - L_i)/(T_i - L_i))^{r_i} \quad L_i \leq \hat{y}_i \leq T_i \quad (3.100)$$

$$d_i = ((U_i - \hat{y}_i)/(U_i - T_i))^{r_i} \quad T_i \leq \hat{y}_i \leq U_i \quad (3.101)$$

$$d_i = 0 \quad \hat{y}_i < L_i \quad (3.102)$$

$$d_i = 0 \quad \hat{y}_i > U_i \quad (3.103)$$

4. DETAILS OF EXPERIMENT

4.1 Information of The Station

Figure 4.1 indicates the system of the laser welding process.

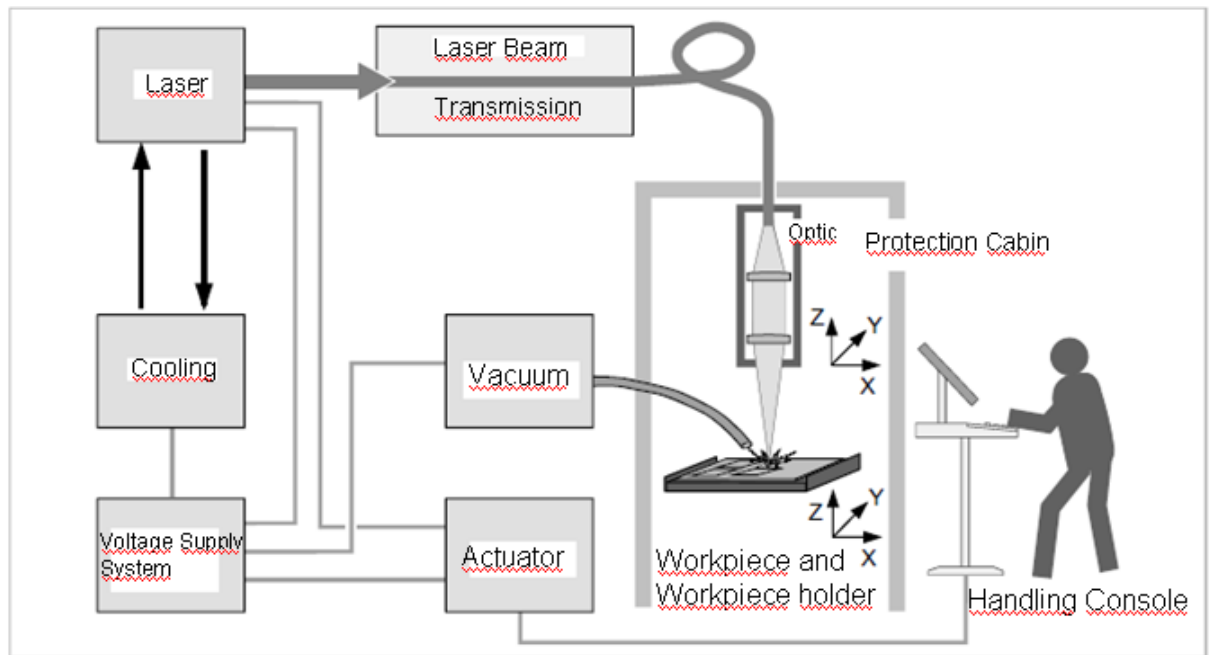


Figure 4.1: Schematic diagram of Laser installation Components (Trumpfh Technische Buch)

4.1.1. Laser unit

Laser unit is a one of the parts of the laser installation. It assures laser beam by means of cooling and voltage supply system. Thus, laser beam can be consisted, laser beam transmission components, for example; laser beam cable can transmit laser beam to the working cabins.

4.1.2 Focusing optic

Focusing optic is used for focusing laser beam to the welding surface. Measurement and adjustment systems control the welding process and if necessary, they can be interfered for process activities.

4.1.3. Working station

During welding process, workpiece must be hold and quickly moved or turned. For this activity, workpiece holders are used. Except of this activity, focus optic can be adjusted for a good welding position.

4.1.4 Security system

The function of security units is preventing from laser beam and welding smut damages during and after the process activity. Therefore, the protection caps and cabins are more important of the security.

4.1.5. Actuator

Laser system actuator controls laser activities and machine Components during welding process. In addition of those functions, it prevents connection to external units and handling console.

4.1.6. Fibreoptics

Fiber optics beam delivery is used with Nd:YAG lasers since the near infrared beam is transmitted efficiently by silica glass. It is currently unique to Nd:YAG lasers in a production environment, and round 80% of Nd:YAG lasers use this method of beam transmission in material processing applications. Many mirror-based beam delivery systems require elaborate beam alignment procedures, are susceptible to contamination and power absorption, and require complex motion of the systems when large multi-axis work envelope stations are used. Once the laser beam is focused into the fiber, it is the fiber diameter that determines the output beam diameter. The cone angle of the output beam matches that of the input beam. Therefore the beam is focused to a size that most closely matches the fiber diameter using a long a focal length lens as possible to give as small a focus cone angle as possible.

There are two main types of fiber suitable for Nd:YAG laser beam transmission, illustrated in Figure 4.2. A step index fiber comprises a low refractive index core, usually made from silica glass, clad with a high refractive index sleeve to evenly redistribute bending stresses, surrounded with jackets for protection and continuity detection. Beam transmission occurs through total internal reflection at the boundary

between the core and the cladding. Figure 4.2 shows that beam delivery at two different fiber types.

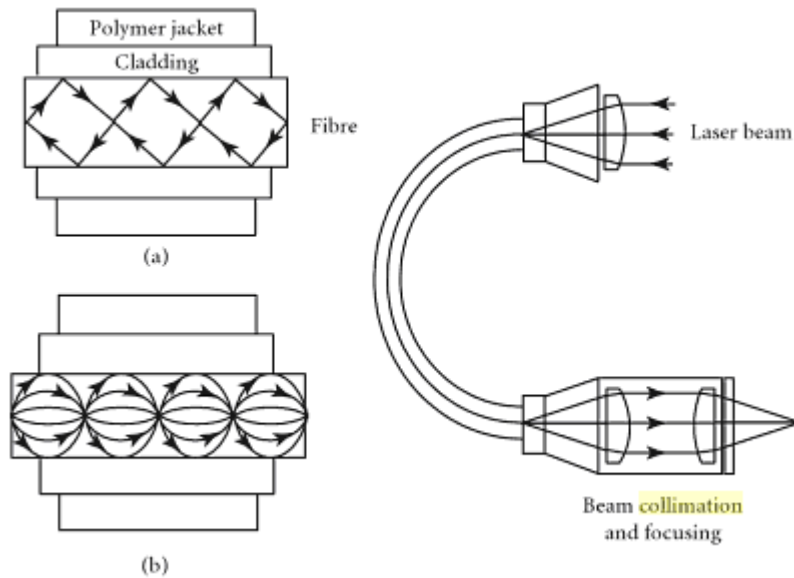


Figure 4.2 : Fiber optic Beam Delivery (a)steps index fiber; (b)graded index fibre(Norenda,Sondip,2008)

The beam is periodically focused down the the fiber. The fiber is thus able to retain some of the input beam mode structure. Graded index fibers are more expensive, but are able to produce a more intense beam, giving, for example, greater penetration in welding. (Beno B, 2002)

4.1.7 Collimation

Collimation of the laser radiation is related with the directional nature of the beam. Highly directional beams are said be highly collimated beams, which can be focused on a very small area without much loss in the beam density (Norenda,Sondip,2008).

In order to ensure consistent performance, a constant power density must be maintained at the workpiece, irrespective of the location of the final focusing optic relative to the laser (the beam path). Beam expanders and condensers control the focused beam diameter by expanding or condensing the laser beam, thus changing its divergence. Most use multiple optional components which may be positioned relative to one another in order to produce the desired effect. The spacing between the optical components is referred to as the collimation adjustment (Beno B, 2002)

4.1.8. Nd:yag laser

Nd:YAG, The neodymium-doped yttrium–aluminum–garnet ($\text{Y}_3\text{Al}_5\text{O}_{12}$) laser is a solid-state laser. Although very low in efficiency, its compact configuration, ease of maintenance, and ability to deliver light through a fiber-optic cable has helped it to be widely used (app. 25%) in the manufacturing sector. A Nd:YAG laser can provide up to 50 kW of power in pulsed mode and 1 kW in continuous wave mode. (Fabbro,Slimani,2008). Nd-yag laser unit is presented in figure 4.3.

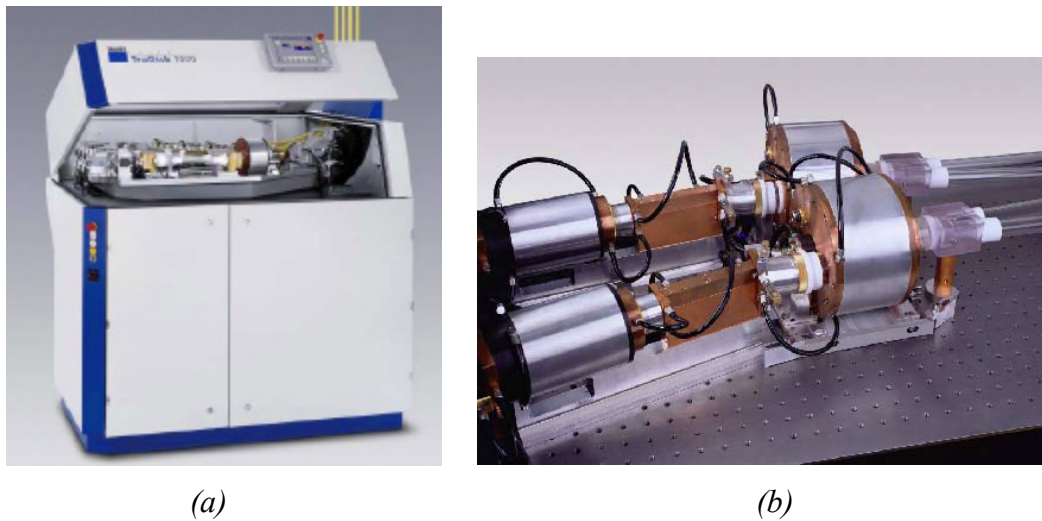


Figure 4.3 : (a) Trudisk 1000 Laser Unit (b) Nd :YAG laser (Trumpfh Technische Buch)

At the station; Trudisk 1000 laser unit is used. This laser unit produces continuous wave laser (CW) with disk .This unit can provide up to 1kW of power in continuous wave mode.

4.2. General Information about Experiment

4.2.1. The process and product information

Mintab 16 was used for the design of our experiments, which includes DOE methods, is an easy-used statistical programme. After running Minitab, DOE methods can be chosen from Stat Menu. Programme can direct you to select general full factorial design and to enter data of inputs.

Experiments have been done in valve group section at HDEV4.1 assembly line. In valve group section, there are 7 laser welding stations and 3 pressing stations. The

station, on which experiments have been done, is one of laser welding stations that holder body and valve body are welded to each other. Firstly, valve body is pressed into holder body at the pressing station. After pressing process, they are welded together at laser welding station. Figure 4.4 shows the working station.



Figure 4.4: Laser welding station where experiments have been done

The station consists of torn table, shielding gas nozzle, optic device and vacuum pipe. The operator places the workpiece on round table, the safety door closes and round table starts to turn with a constant speed. At the mean time, laser beam comes from optic device; shielding gas covers smuts are removed by vacuuming from the welding area during welding process. At the same time, two parts are welded to each other and the process is completed. Before the safety door is opened, shielding gas flow is cut. Operator takes the welded part from the round table. Thus, the operation is completed.

We have two different collimation devices were used, 6 different experiment steps were fulfilled with each and 10 samples of each has been measured in Quality Laboratories. Overall sectioning was applied on all welding areas. Figure 4.5 shows laser welding pool area on the welded parts.

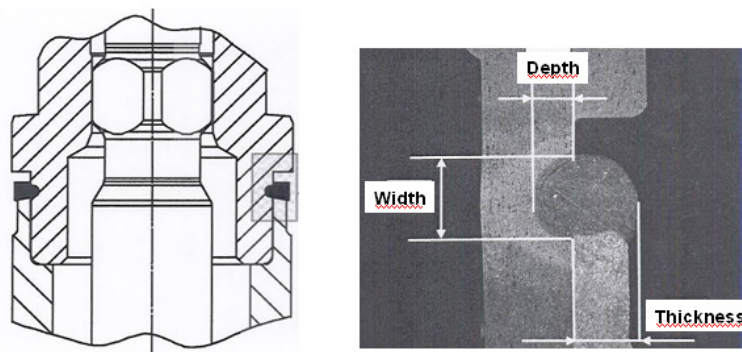


Figure 4.5: Cross-section of welding area and welding pool (RBTR, datasheet of HDEV4.1)

All varieties have 10 sample results for left sides and also for right sides of the welding surfaces. We have taken the average output values of left and right side of every 10 samples were taken separately. There are 60 testing results for depth, width and thickness for every collimation.

4.2.2. The differences between Collimation A and Collimation B

Figure 4.6 indicates the collimation device. Laser beam reflects conically at the end of fiber from laser cable. Laser beam is formed parallel by collimation lens. Focusing lens is used for focusing laser beam onto working piece (welding area).

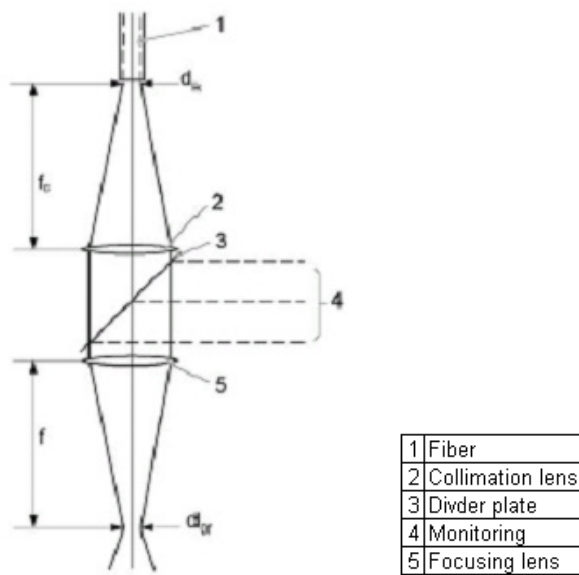


Figure 4.6: Representation of Collimation (Beno B, 2002)

The collimation focal distance f_c is a distance between at the end of fiber to collimation lens. The objective focal distance f is a distance between the focusing lens to the focus. d_{of} is the closest focusing diameter of laser beam to focusing of welding area .

$$d_{of} = \frac{f}{f_c} \cdot d_k \quad (4.1)$$

d_{of} : Focusing diameter [mm]

f : Focal distance of objective [mm]

f_c : Focal distance of collimation [mm]

d_k : Fiber diameter of laser cable [mm]

f_c is 100 mm for collimation A and f_c is 90 mm for collimation B. If f_c is decreased, d_{of} increases. Even f_c is 90 mm, d_{of} gets bigger. Thus, more energy is needed for good welding quality. Therefore, power values are increased. For this reason; nominal power values are dissimilar for both collimations. At this station fiber diameter in laser cable is 0,15 mm.

The below table 4.1 shows parameter values of our experiments for Collimation A and B.

Parameters	Collimation A			Collimation B		
Level	1	2	3	1	2	3
Speed	1	1,5		1	1,5	
Laser Power	300	360	420	380	440	500

Table 4.1: Parameter values of experiments

Laser power values were derived from nominal values of collimation working parameters. For collimation A, nominal laser power value is 360 W, for Collimation B, nominal laser power value is 440 W. Therefore, these 3 laser power values were chosen -60W and +60W of nominal values in range. All experiments were done under the same conditions. Laser power nominal values were defined by several experimental results.

Figure 4.7 shows cross-section photos of 6 experiment steps. The results table of our test belonging to Collimation A is shown at App.1

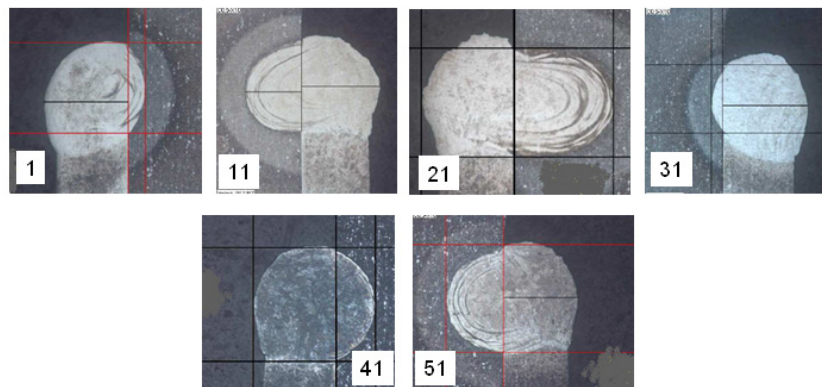


Figure 4.7: Cross-section photos of welding area samples for Collimation A

- 1. welding speed= 1,0 m/min, laser power=300 W
- 11. welding speed= 1,0 m/min, laser power=360 W
- 21. welding speed= 1,0 m/min, laser power=420 W
- 31. welding speed= 1,5 m/min, laser power=300 W
- 41. welding speed= 1,5 m/min, laser power=360 W
- 51. welding speed= 1,5 m/min, laser power=420 W

Figure 4.8 shows cross-section photos of 6 experiment steps. The results table of our test belonging to Collimation B is shown at App.2.

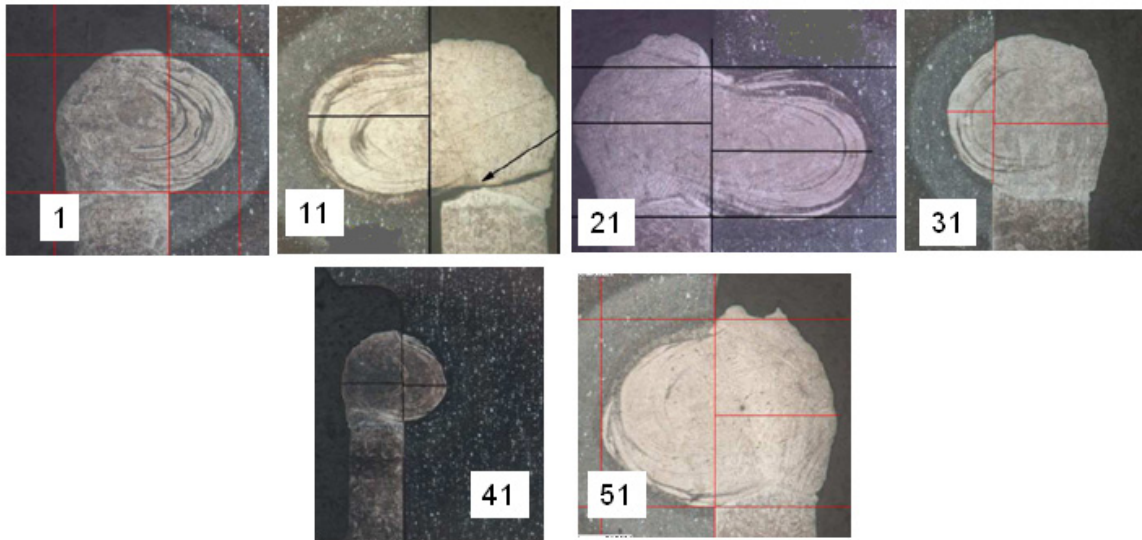


Figure4.8: Cross-section photos of welding area samples for Collimation B

- 2. welding speed= 1,0 m/min, laser power=380 W
- 12. welding speed= 1,0 m/min, laser power=440 W
- 22. welding speed= 1,0 m/min, laser power=500 W
- 32. welding speed= 1,5 m/min, laser power=380 W
- 42. welding speed= 1,5 m/min, laser power=440 W
- 52. welding speed= 1,5 m/min, laser power=500 W

5. EXPERIMENTAL RESULTS

5.1. Main Effects and Interaction Plots Comparison of Collimations

The diagrams versus inputs and outputs one by one indicate the behavior of our experiments and laser welding process (Ezzeddin,2008).

For depth values; Collimation B (Figure 5.1.b) is more effective than Collimation A (Figure 5.1.a). During speed increases from 1,0 m/min to 1,5 m/min, both speed graphs act linearly. Behaviors of Both graphs are nearly same. Those diagrams indicate that depth values increase with increasing power linearly.

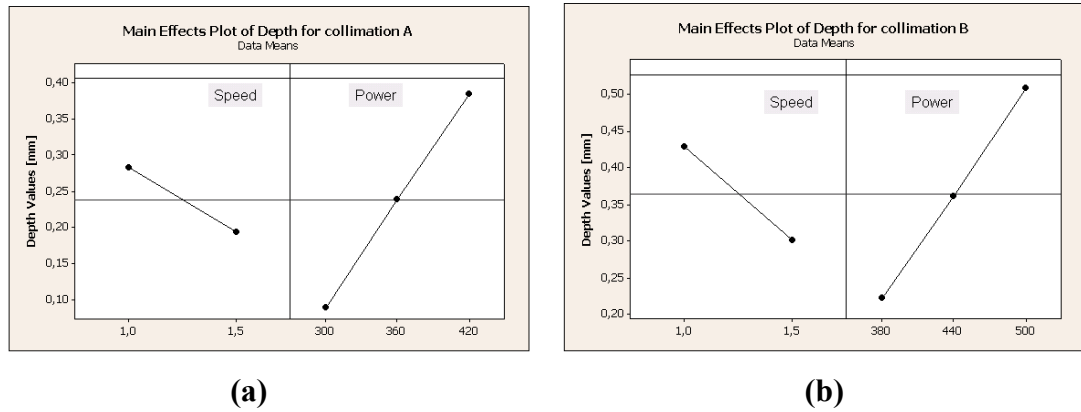
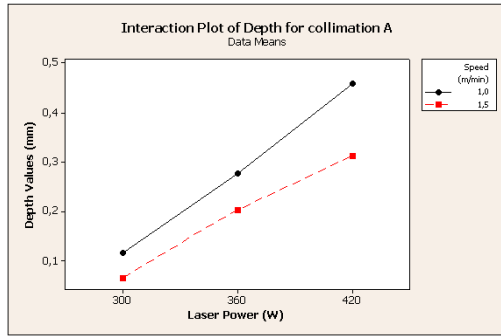
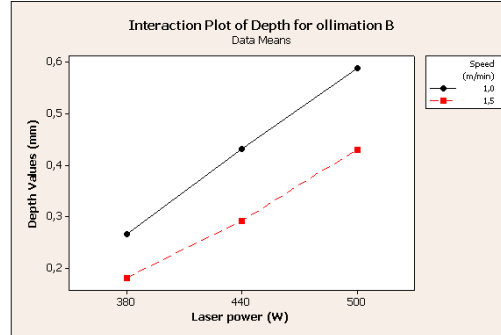


Figure 5.1: Main Effects of Depth for Collimation A and B (a) Collimation A
(b) Collimation B

At the interaction plots for depth; the relation between power and speed is indicated. The red line shows the relationship between all power values and speed 1,5 m/min and the black line shows the relationship between all power values and speed 1,0 m/min. Depth values decrease with increasing speed from 1,0 to 1,5 m/min, whereas depth increases with increasing power. For collimations, power and speed behaviors are practically similar. Thus, the effects of both collimations on the depth are nearly the same. (See Figure 5.2)



(a)

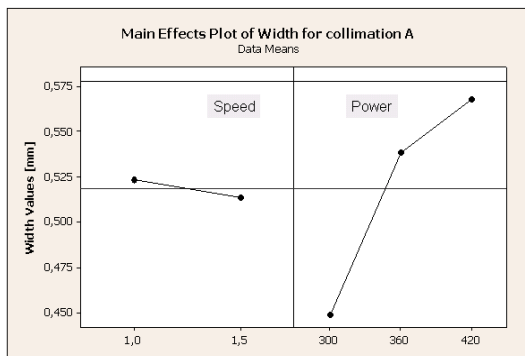


(b)

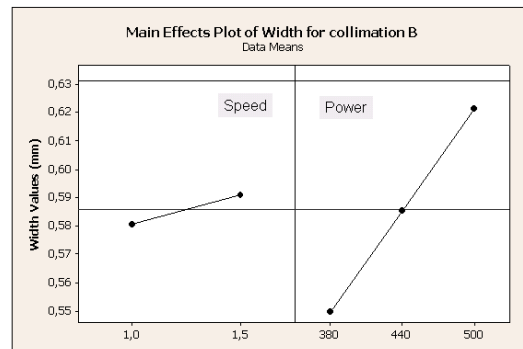
Figure 5.2: Interaction Plots of Depth for Collimation A and B (a) Collimation A

(b) Collimation B

At Collimation A (Figure 5.3), width decreases with increasing speed. On the other hand, at Collimation B width values increase with increasing speed. For both collimations, width values increase with increasing power. For the collimation B, power graph's line is linear, whereas for Collimation A, power graph behavior is different. Between 300 W and 360W, width range is approximately 0.1 mm, but between 360 W to 420 W, width range is only nearly 0.025mm as seen in Figure 5.3.a.



(a)



(b)

Figure 5.3: Main Effects of Width for Collimation A and B (a) Collimation A
(b) Collimation B

The interaction plot for width indicates for collimation A in Figure 5.4.a and the diagram for collimation B in Figure 5.4.b. In figure 5.4.a, at 300W (N-60W), width values at speed 1,0 m /min is much greater than width values at 1,5 m/min. Width on 1,5 m/min is greater than width on 1,0 m/min at nominal power values (360W). Same case is valid for width values in relationship at 420W (N+60W). In figure 5.4.b, width values increase linearly with increasing power on speed 1.5 m/min. On

the other hand, during speed 1,0 m/min, width values increase with increasing power between 380W (N-60W) to 440W (nominal power values), whereas width decreases with increasing power between 440W (N) to 500W (N+60W). At the point of 500W, width on 1,5 m/min is greater than the width on 1,0 m/min. On this output, interaction plots indicate that different collimations affect this output with different behaviors (Ezzeddin,2008)..

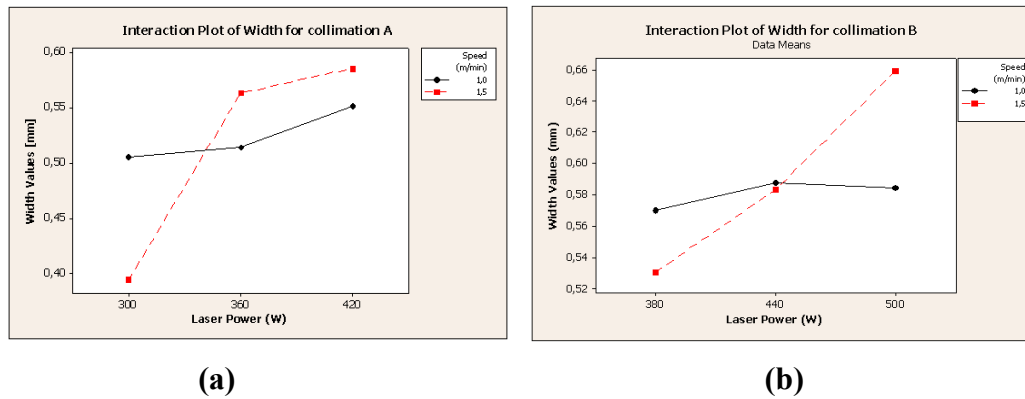


Figure 5.4: Interaction Plots of Width for Collimation A and B (a) Collimation A (b) Collimation B

Look at the main effect plot for thickness; even speed increases from 1,0 m/min to 1,5 m/min, thickness decrease linearly. By the fact of power values, both collimations affect on the thickness of welding pool differently. In figure 5.5.a, meanwhile, thickness values decrease with increasing power between 300W to 360W, width values increase with increasing power between 360W to 420W. In figure 5.5.b; thickness values rise in order of power from 0,435mm to 0,445mm, from 0,445mm to 0,472mm.

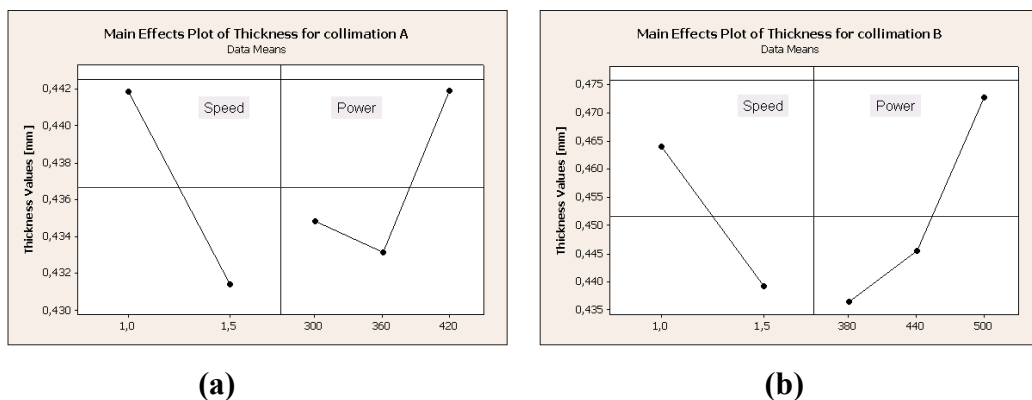


Figure 5.5: Main Effects of Thickness for Collimation A and B (a) Collimation A (b) Collimation B

At the interaction plots; in figure 5.6.a, thickness values increase on speed 1,0 m/min linearly. Providing speed 1,5 m/min, thickness values decrease linearly from 300W to 360 W. After 360W, these increases with small ranges that indicate thickness come stable after 360W. At the point of 360W, thickness on speed 1,0 m/min is much greater than thickness on speed 1,5 m/min. In figure 5.6.b, at 380W, thickness on speed 1,0 m/min and thickness on speed 1,5 m/min have nearly same values. During increasing power from 380W to 440W, thickness on speed 1,5 m/min decreases, but the thickness on speed 1,0 m/min increases linearly (Ezzeddin,2008).

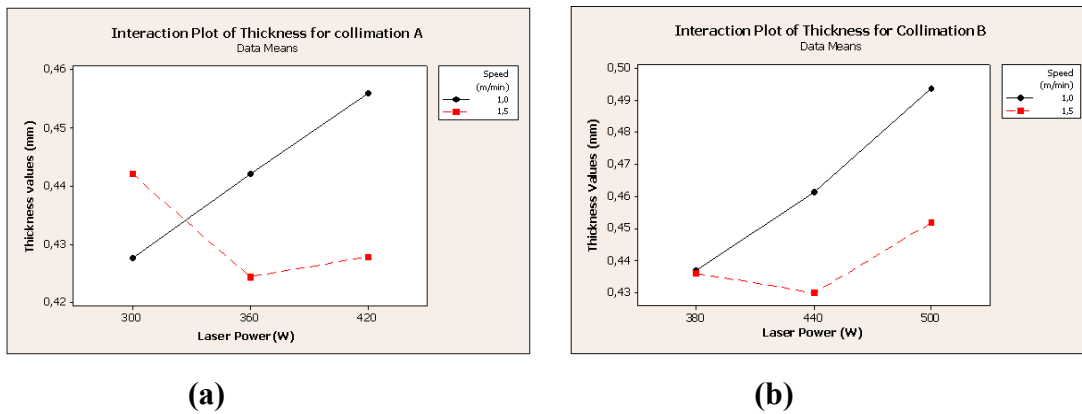


Figure 5.6: Interaction Plots of Thickness for Collimation A and B

(a) Collimation A (b) Collimation B

5.2. Optimization Results For Collimation A Using RSM

5.2.1. RSM results of depth values

The analysis of variance of depth values in table 5.1 shows that the mathematical model is significant for Collimation A. $p=0,000$ demonstrates that the model and also the input parameters, which have this p values, are statically significant at 95% confidence level. Welding speed and laser power, and also the interaction of these inputs are affected this output values strongly. This ANOVA table (see table 5.1) also indicates that the most significant effected parameter is laser power for this output. The same table determines the adequacy measures R^2 , adjusted R^2 and predicted R^2 . The coefficient of determination, R^2 , is found to be 99.43%, so it shows a sufficient agreement between experimental and fitted values which become from regression model. Additionally, the other entire adequacy measures are also close to 100%.(Liang, Chou,2008). In figure 5.7, correlation between actual values and fitted values is very strong. Adequacy of the mathematical model is easily verified by

means of correlation sample outputs and calculated outputs; so the model is derived functions quite properly. The values illustrated in the graph belonging to corresponding experiment sets are grouped well, i.e. scatter behavior is very weak and linearity is apparently present.

Source	DF	Sum of Squares	Mean Square	F	p
Model	3	1,01211	0,33737	3269,05	0,0000
S	1	0,12047	0,120467	1167,3	0,0000
P	1	0,86863	0,868628	8416,83	0,0000
S*P	1	0,02302	0,023016	223,02	0,0000
Residual	56	0,00578	0,000103		
Lack-of-Fit	2	0,00209	0,001044	15,28	0,0000
Pure Error	54	0,00369	0,000068		
Corrected Total	59	1,01789			
$R^2 = 99,43\%$ $R^2 \text{ (pred)} = 99,36\%$ $R^2 \text{ (adj)} = 99,40\%$					

Table 5.1: ANOVA Table of Depth values from Collimation A

The mathematical model is;

$$\text{Depth} = -1,141 + 0.396467*S + 0.004455*P - 0,00159917 S*P \quad (5.1)$$

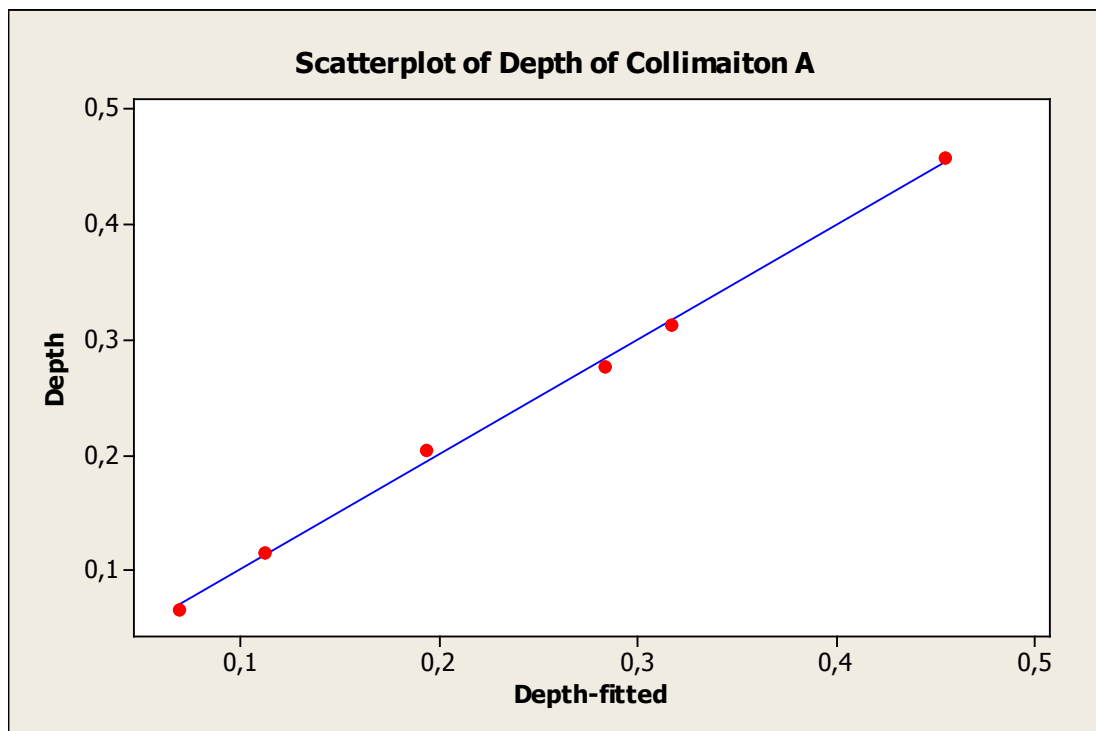


Figure 5.7: The scatter plot of actual and fitted depth values for collimation A

With these facts in hand, residuals have small values and this aspect is valid through the whole line. With a wide range of outputs compared to other graphs illustrated at each value level they are evenly scattered and linearity remains undisturbed (Ezzeddin,2008). Figure 5.8 shows the effect of laser power and welding speed on the depth of collimation A and figure 5.9 is the contour graph of this correlation.

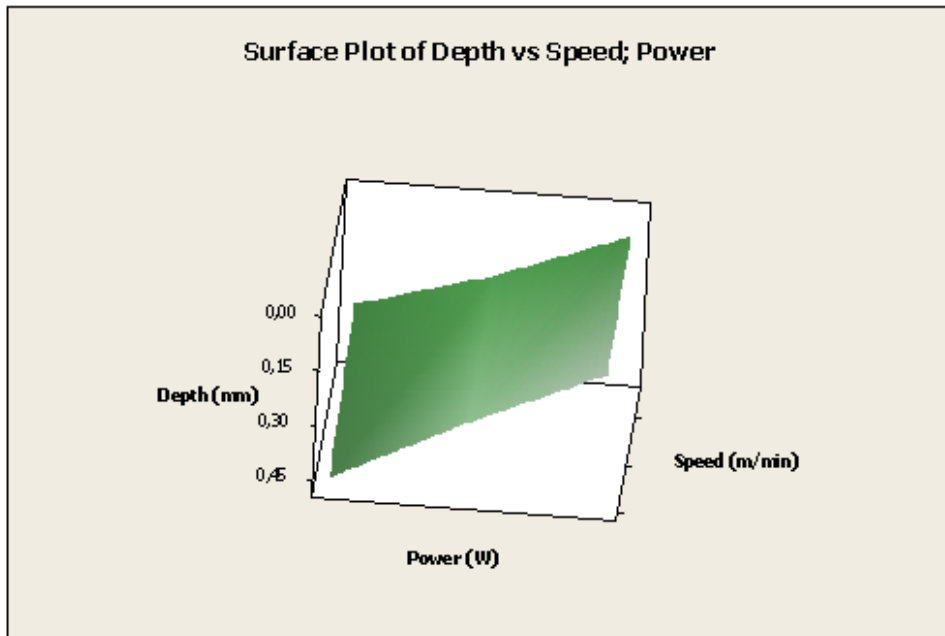


Figure 5.8: 3D graph; the effect of laser power and welding speed on the depth at collimation A

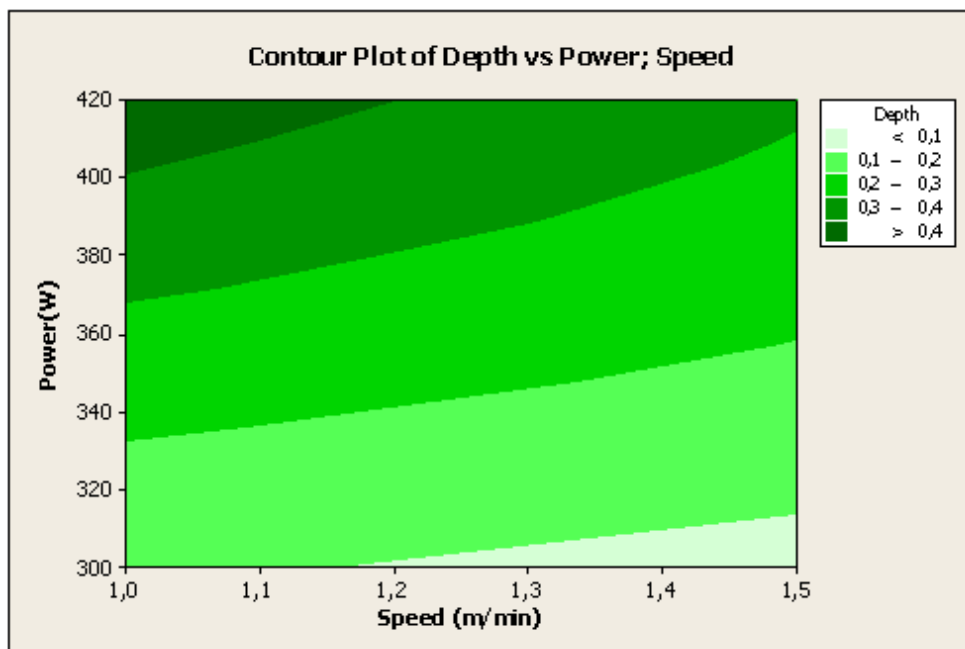


Figure 5.9: Contour graph shows the effect of laser power and welding speed on the depth values at collimation A

5.2.2. RSM results of width values

In table 5.2, the regression model for width can be seen significantly at collimation A. Due to probability value bigger than 0.05, the welding speed effect is very weak, However, welding speed parameter is not negligible, but the interaction of laser power and welding speed are affected strongly. Therefore, welding speed parameter can not be removed from the equation of this model. Laser power, the second order of power and the interaction of laser power and welding speed are significant model terms. However, laser power is the most significant factors associated with the width of welding pool area. R^2 (see table 5.2) defines 80% of agreement between actual and fitted values. This model can estimate the value nearly actual as expected.

Source	DF	Sum of Squares	Mean Square	F	p
Model	4	0,208142	0,052036	55,620	0,0000
S	1	0,001316	0,001316	1,410	0,2410
P	1	0,142206	0,142206	152,010	0,0000
P²	1	0,011841	0,011841	12,660	0,0010
S*P	1	0,05278	0,05278	56,420	0,0000
Residual	55	0,051453	0,000936		
Lack-of-Fit	1	0,025638	0,025638	53,630	0,0000
Pure Error	54	0,025815	0,000478		
Corrected Total	59	0,259595			
		$R^2 = 80,18\%$	$R^2(\text{pred}) = 76,71\%$	$R^2(\text{adj}) = 78,74\%$	

Table 5.2: ANOVA Table of width values from Collimation A

The mathematical model is;

$$\text{Width} = 0,221117 - 0,890533*S + 0,00392667*P - 0,00000827778*P^2 + 0,00242167*S*P \quad (5.2)$$

In figure 5.10, strong linearity can be easily seen. Lightly scattered output groups are mainly affected also by narrow range values. The correlations between actual and fitted values are enabled by low residual values. The mathematical model has been confirmed as adequate. Some sample groups have similar values and they are forming a cloud like set of values (Kinan,Romali,Fiaschi,Dini,Sarri,2009). Figure 5.11 and 5.12 indicate the effect of laser welding and power speed on the width at collimation A.

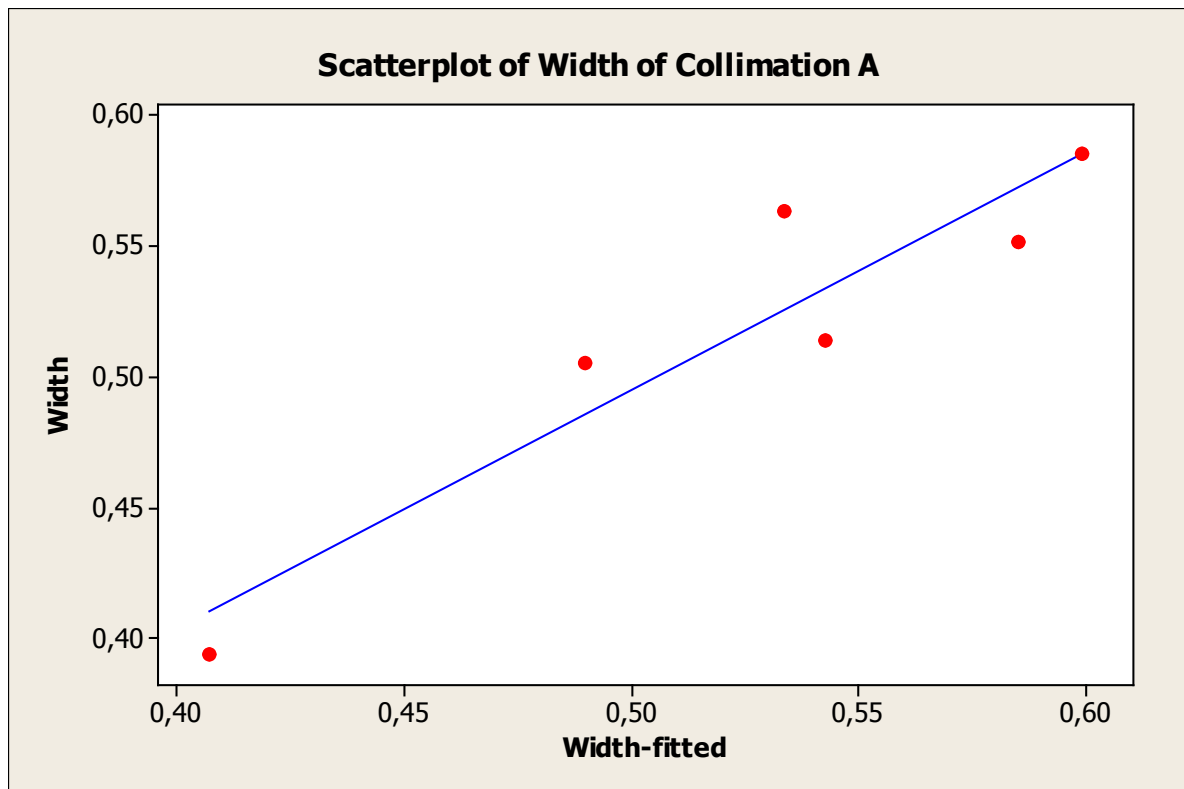


Figure 5.10: The scatter plot of actual and fitted width values for collimation A

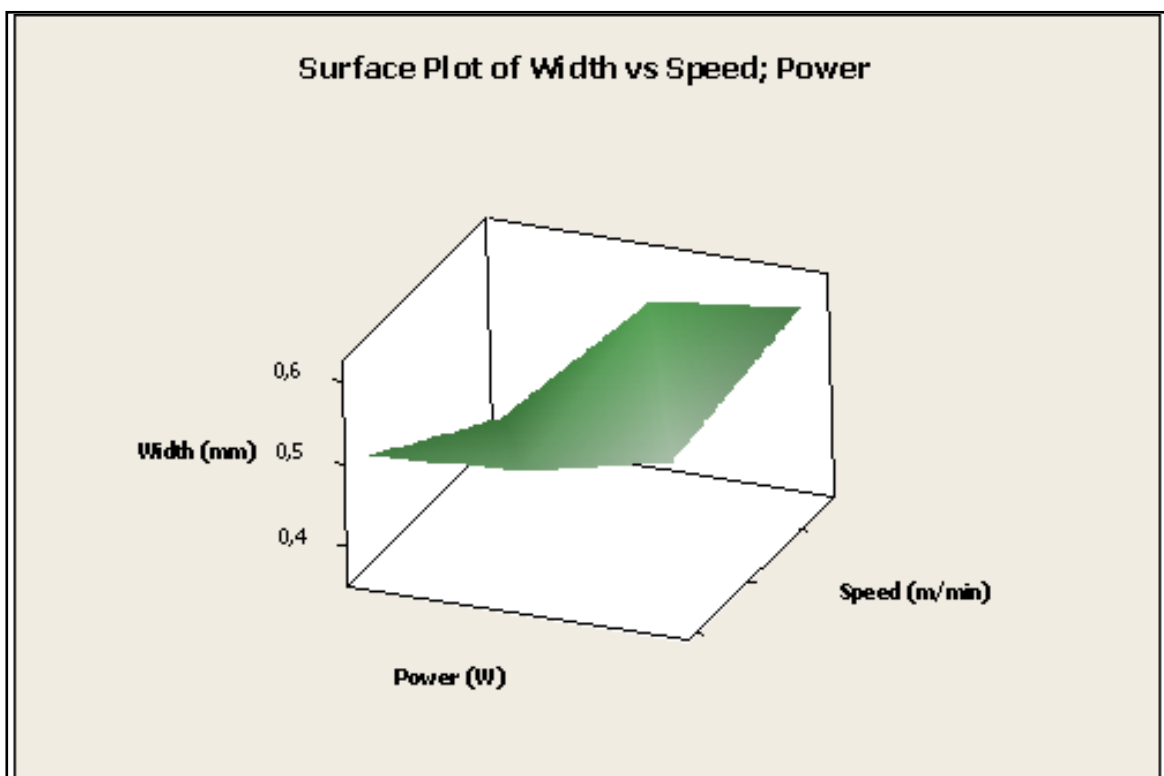


Figure 5.11: 3D graph: the effect of laser power and welding speed on the width at collimation A

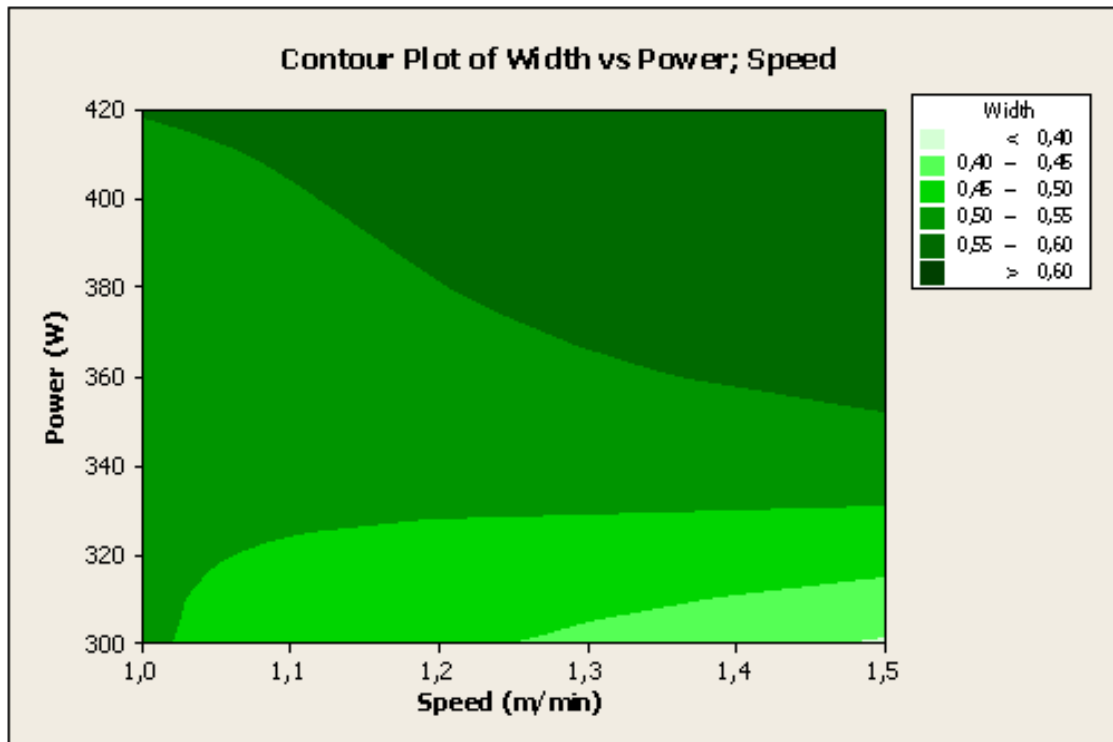


Figure 5.12: Contour graph shows the effect of laser power and welding speed on the width values at collimation A

5.2.3. RSM results of thickness values

The table 5.3 indicates that welding speed is the most significant parameter for thickness of welded pool geometry. Laser power and the second order of laser power have fewer effects on this dimension of welded area. The coefficient of determination R^2 is calculated 58.35%. This means that the model can not present approximate values about actual process behavior %.(Liang, Chou,2008).

Source	DF	Sum of Squares	Mean Square	F	p
Model	4	0,007041	0,00176	19,1800	0,0000
P	1	0,001643	0,001643	17,9100	0,0000
S	1	0,000497	0,000497	5,4200	0,0240
P²	1	0,000364	0,000364	3,9700	0,0510
S*P	1	0,004537	0,004537	49,4400	0,0000
Residual	55	0,005047	0,000092		
Lack-of-Fit	1	0,000382	0,000382	4,4200	0,0400
Pure Error	54	0,004665	0,000086		
Corrected Total	59	0,012088			
$R^2 = 58,25\%$ $R^2(\text{pred}) = 50,38\%$ $R^2(\text{adj}) = 55,21\%$					

Table 5.3: ANOVA Table of thickness values from Collimation A

The mathematical model is;

$$\text{Thickness} = 0,306767 + 0,234667*S - 0,00009875*P + 0,00000145139 *P^2 - 0,00071 S*P \quad (5.3)$$

As at other graphs depicted before above, also Figure 5.13 has a quite linear character. The range is the lowest value of all. Residuals having the lowest range are showing a very narrow band width. The mathematical model is confirmed to be adequate. Due to similar values of sample outputs some groupings have been caused. Although R^2 is 58.35%, the scatter plot proves that the model can fulfill values as expected (Kinan,Romali,Fiaschi,Dini,Sarri,2009). Figure 5.14 and 5.15 indicate the effect of laser welding and power speed on the thickness at collimation A.

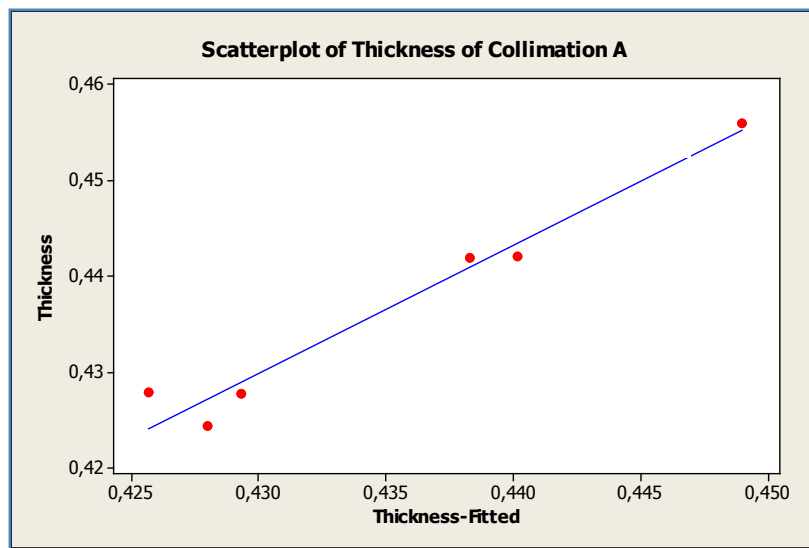


Figure 5.13: The scatter plot of actual and fitted thickness values for collimation A

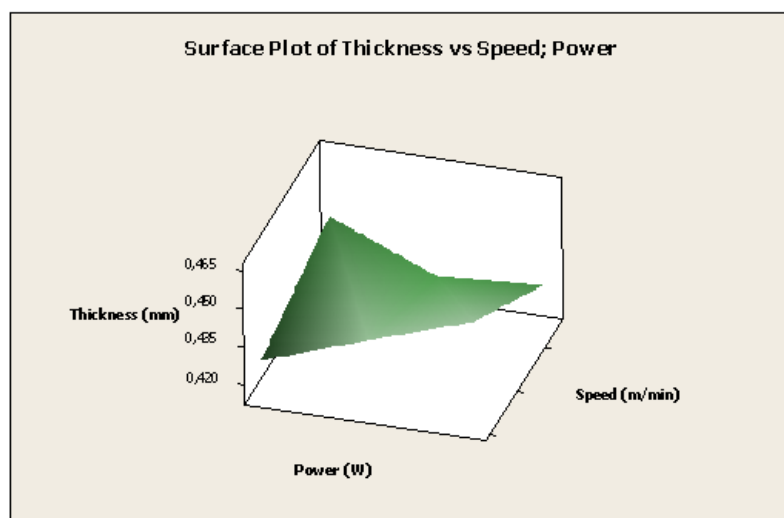


Figure 5.14: 3D graph shows the effect of laser power and welding speed on the thickness at collimation A

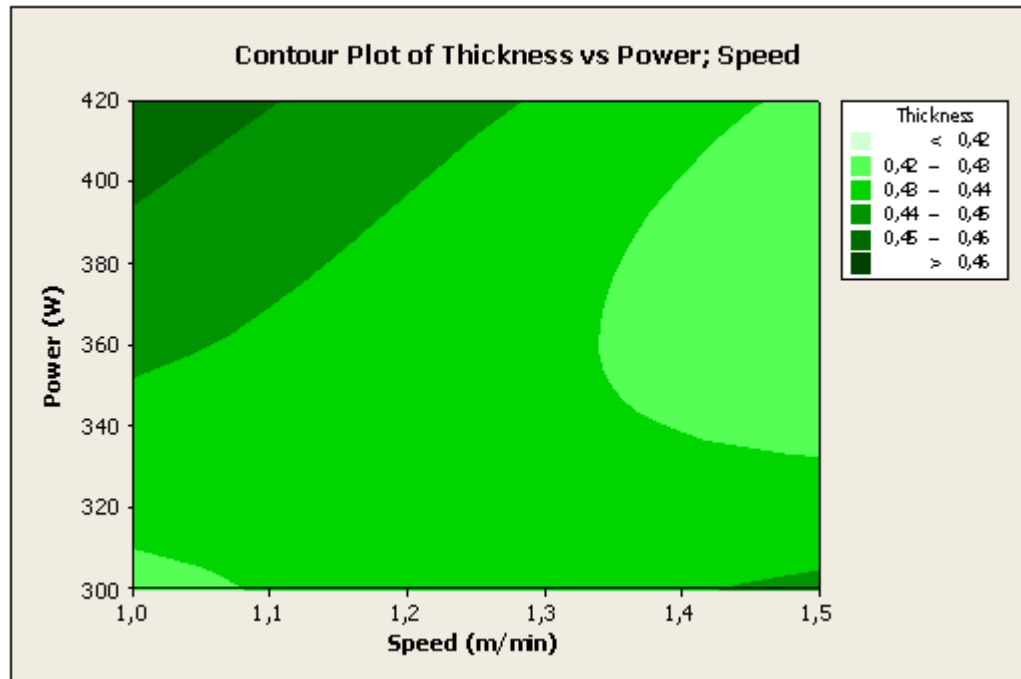


Figure 5.15: Contour graph shows the effect of laser power and welding speed on the thickness values at collimation A

5.3. Optimization Results For Collimation B Using RSM

5.3.1. RSM results of depth values

In table 5.4, laser power and welding speed and also the interaction of power and speed are almost affected the depth of welding pool for collimation B. The main affected of laser power is the most significant. R^2 gives 98.79% of agreement between actual and fitted values. This model approximately estimates the actual process values (Ezzeddin,2008).

Source	DF	Sum of Squares	Mean Square	F	P
Model	3	1,07096	0,356985	1519,58	0,0000
P	1	0,81639	0,816388	3475,12	0,0000
S	1	0,2413	0,2413	1027,15	0,0000
P*S	1	0,01327	0,013268	56,48	0,0000
Residual	56	0,01316	0,000235		
Lack-of-Fit	2	0,00174	0,000871	4,12	0,0220
Pure Error	54	0,01141	0,000211		
Total	59	1,08411			
$R^2 = 98,79\%$ $R^2(\text{pred}) = 98,63\%$ $R^2(\text{adj}) = 98,72\%$					

Table 5.4: ANOVA Table of depth values from Collimation B [originated 17]

The mathematical model is;

$$\text{Depth} = -1,03365 + 0,003899 \cdot P + 0,280567 \cdot S - 0,00121P \cdot S \quad (5.4)$$

These figures have relatively strong correlation between actual (experimental) values and fitted values (predicted by the mathematical model). This indicates that the mathematical model derived has adequacy in correlating physical sample outputs and calculated outputs.

Particularly figure 5.16 illustrates a very strong relation between actual and fitted values; it is lightly scattered and mostly linear form. For this reason, residuals remain confined to limited values and for different test conditions this aspect is valid through the line always having a narrow band width. Though output range is very wide compared to other graphs illustrated at each value level they are evenly scattered and linearity remains undisturbed (Liang, Chou, 2008). Figure 5.17 and 5.18 indicate the effect of laser welding and power speed on the depth at collimation B.

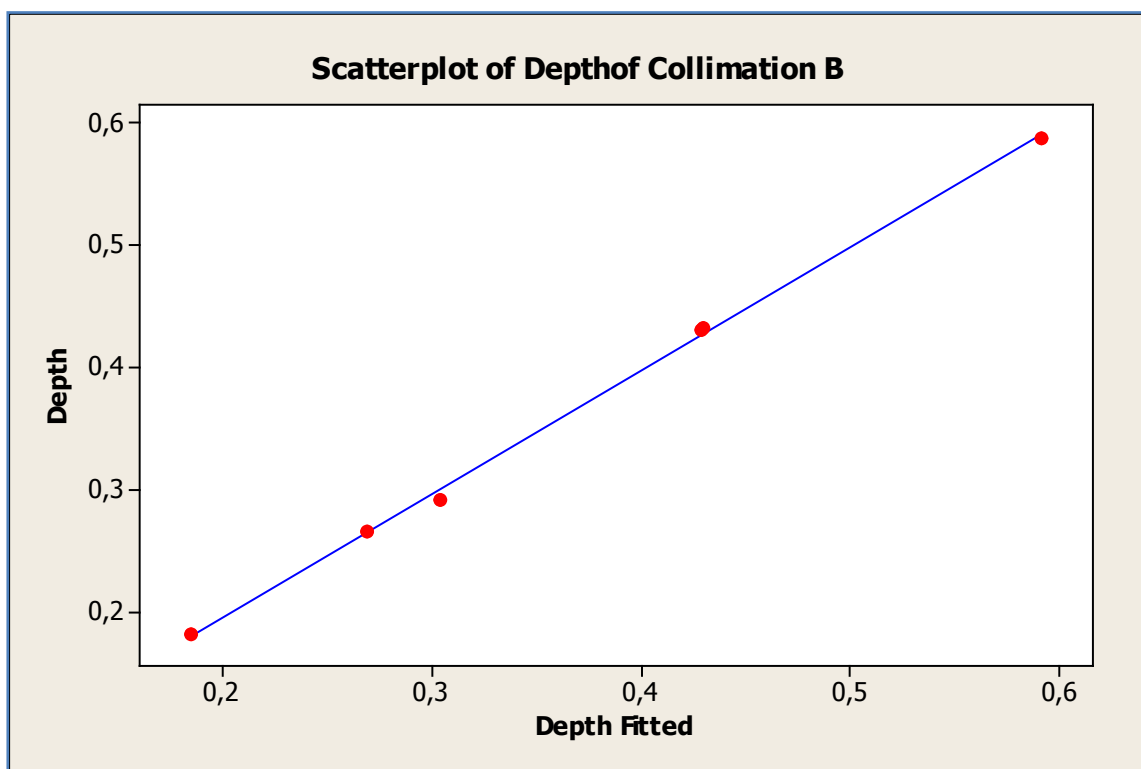


Figure 5.16: The scatter plot of actual and fitted depth values for collimation B

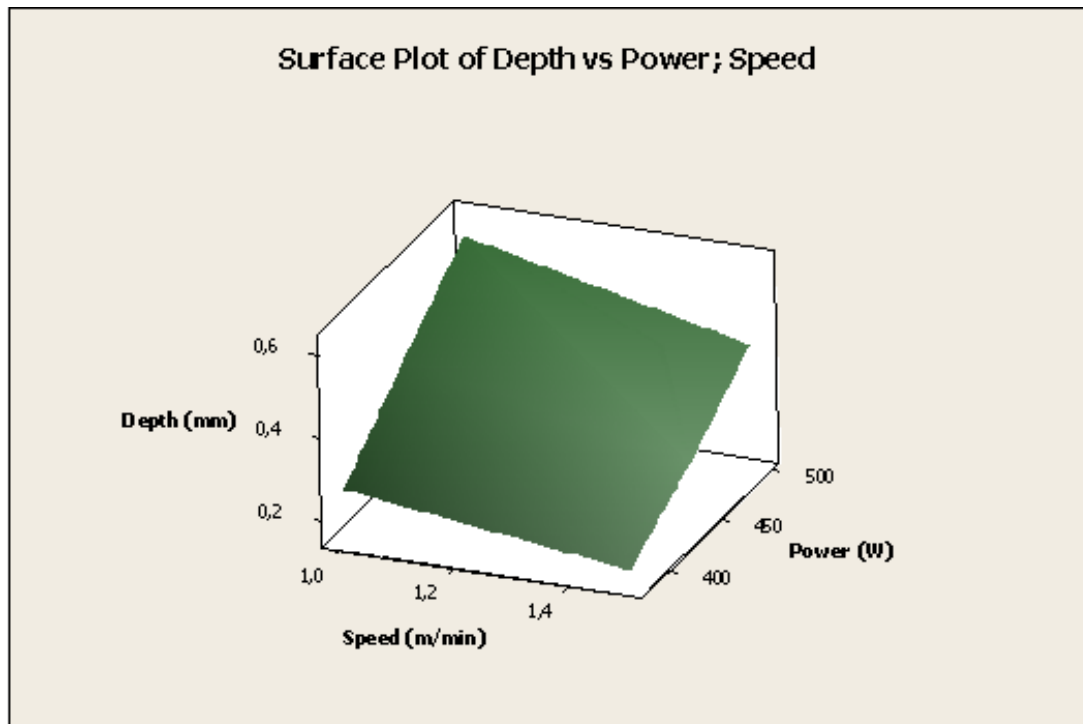


Figure 5.17: 3D graph shows the effect of laser power and welding speed on the depth at collimation B

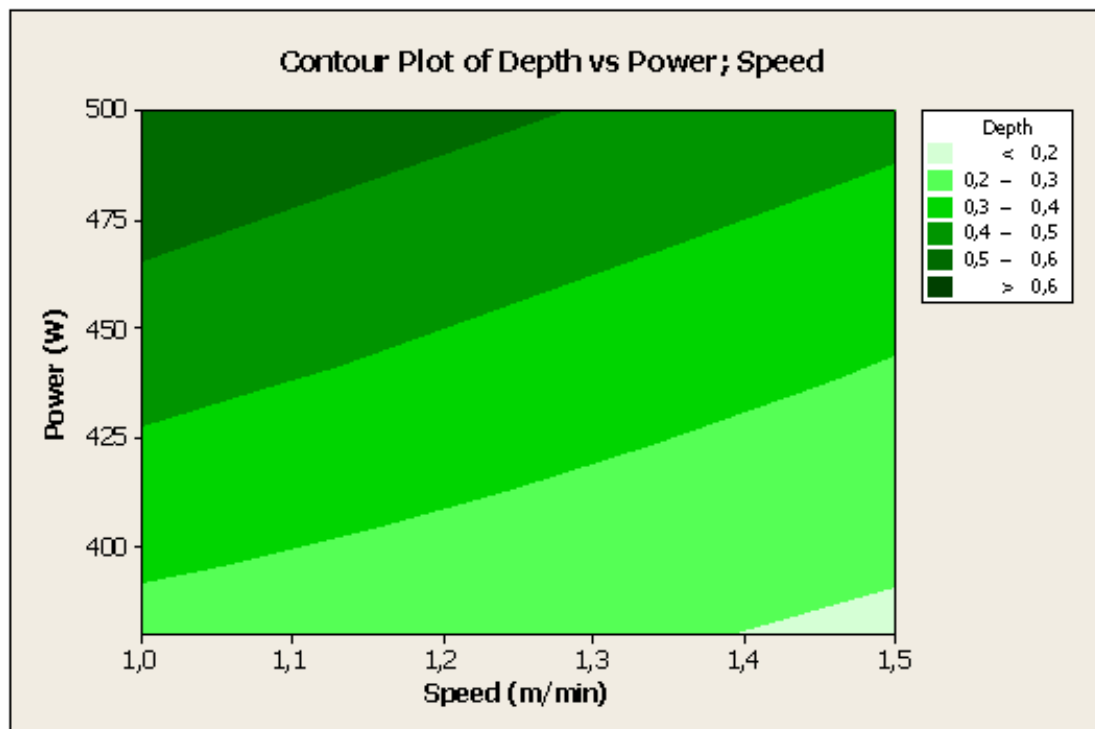


Figure 5.18: Contour graph shows the effect of laser power and welding speed on the depth values at collimation B

5.3.2. RSM results of width values

The table 5.5 shows that laser power and the interaction of laser power and welding speed, and laser power are affected on the width for collimation B significantly. P value of speed is bigger than 0.05, which means the welding speed can not affect the width outputs significantly. On the other hand, p value of the interaction of welding speed and laser power is smaller than 0.05. Therefore, the welding speed coefficient can not removed from equation. R^2 value is 72.03%. This model can present fitted values so close to actual values(Ezzeddin,2008).

Source	DF	Sum of Squares	Mean Square	F	P
Model	3	0,085696	0,028565	48,0700	0,0000
P	1	0,051373	0,051373	86,4600	0,0000
S	1	0,001633	0,001633	2,7500	0,1030
P*S	1	0,03269	0,03269	55,0200	0,0000
Residual	56	0,033275	0,000594		
Lack-of-Fit	2	0,001664	0,000832	1,4200	0,2500
Pure Error	54	0,03161	0,000585		
Total	59	0,11897			
				$R^2(\text{adj}) =$	
				$R^2 = 72,03\% \quad R^2(\text{pred}) = 68,00\% \quad 70,53\%$	

Table 5.5: ANOVA Table of width values from Collimation B

The mathematical model is;

$$\text{Width} = 1,34515 - 0,00179 * P - 0,8177 * S + 0,001906 P * S \quad (5.5)$$

Figure 5.19 shows strong linearity with its narrow output range values. Residuals are relatively scattered though correlation between actual and fitted values kept well. The cloud like group in the middle of the graph is composed of four different experiment parameter combinations; this group is still having the similar set of fitted values. This fact confirms the adequacy of mathematical model, deriving similar values in connection with physical sample outputs (Liang, Chou,2008). Figure 5.21 and 5.21 indicate the effect of laser welding and power speed on the thickness at collimation A.

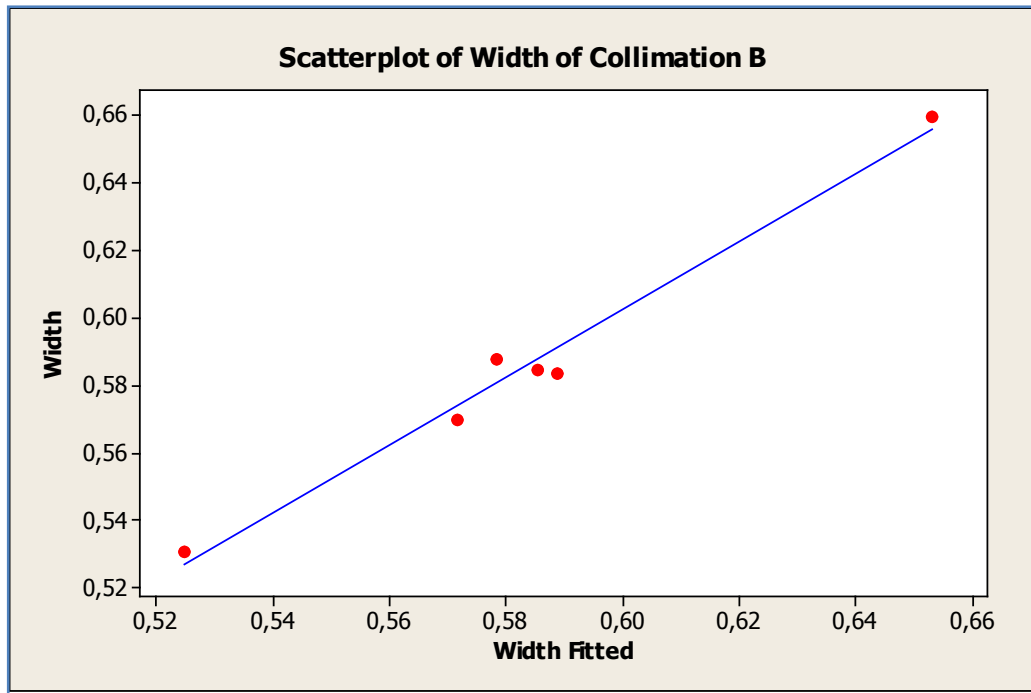


Figure 5.19: The scatter plot of actual and fitted width values for collimation B

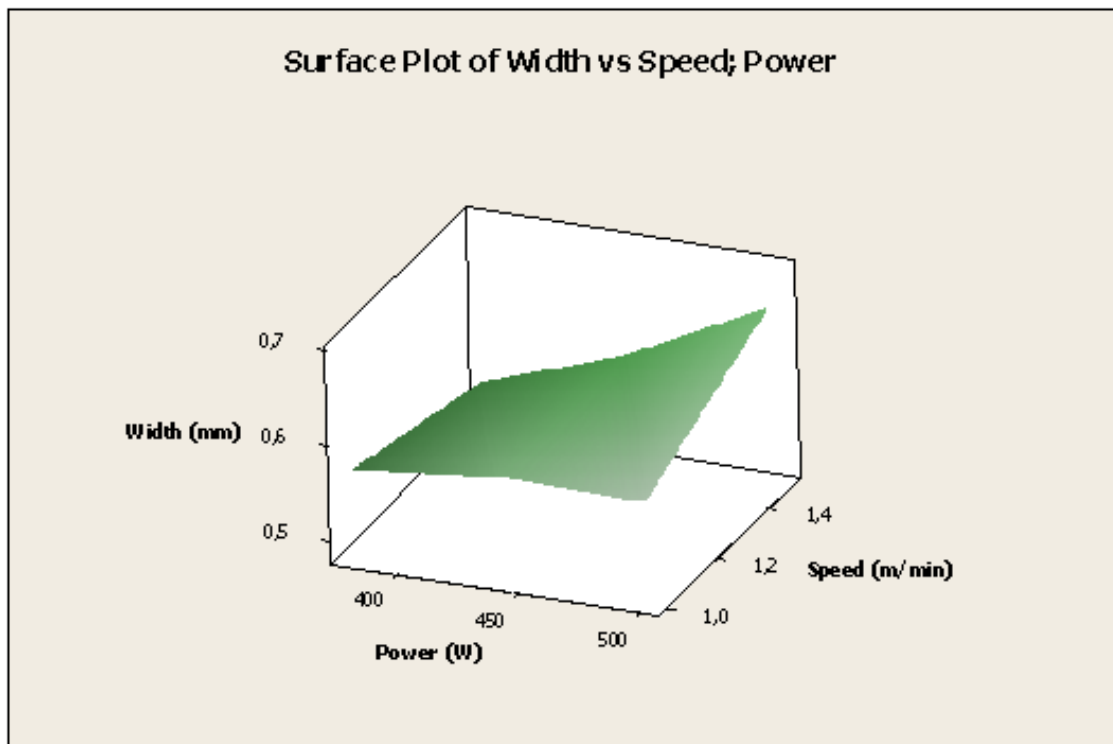


Figure 5.20: 3D graph shows the effect of laser power and welding speed on the width at collimation B

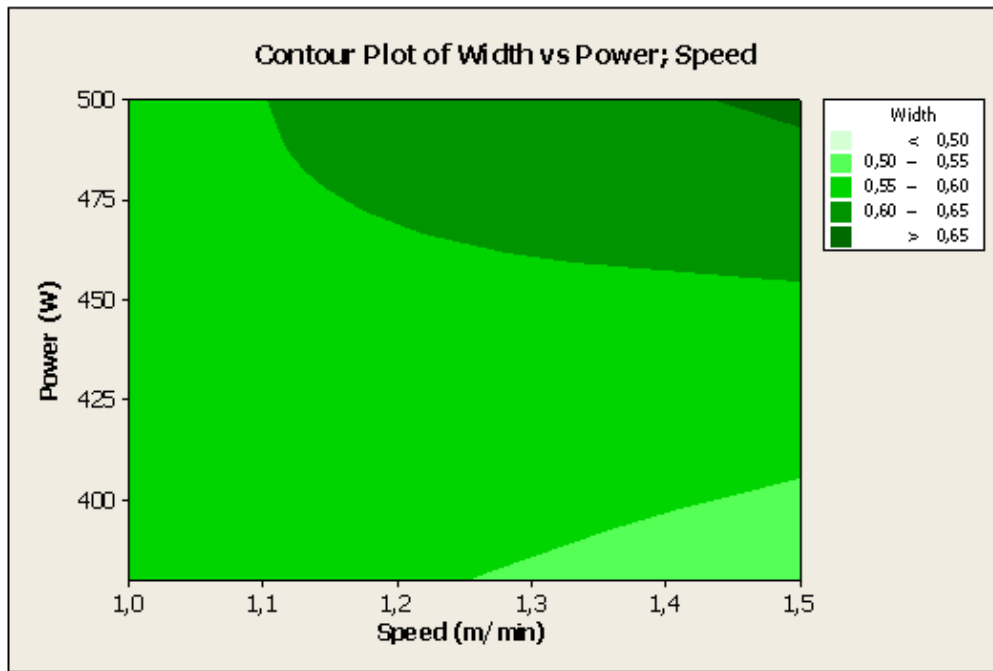


Figure 5.21: Contour graph shows the effect of laser power and welding speed on the width values at collimation B

5.3.3. RSM results of thickness values

The main effect of laser power is not significant for this output model of Collimation B. On the other hand; the second order of laser power and the interaction of laser power and welding speed, and welding speed affect the welding pool thickness diameters. 74.5% of agreement is achieved from the mathematical model. Table 5.6 shows calculated the analysis of variance factors (Ezzeddin,2008).

Source	DF	Sum of Squares	Mean Square	F	P
Model	4	0,208142	0,052036	55,6200	0,0000
S	1	0,001316	0,001316	1,4100	0,2410
P	1	0,142206	0,142206	152,0100	0,0000
P²	1	0,011841	0,011841	12,6600	0,0010
S*P	1	0,05278	0,05278	56,4200	0,0000
Residual	55	0,051453	0,000936		
Lack-of-Fit	1	0,025638	0,025638	53,6300	0,0000
Pure Error	54	0,025815	0,000478		
Total	59	0,259595			
$R^2 = 74,50\%$ $R^2(\text{pred}) = 69,62\%$ $R^2(\text{adj}) = 72,65\%$					

Table 5.6: ANOVA Table of thickness values from Collimation B

The mathematical model is;

$$\text{Thickness} = 0,485814 + 0,2522*S - 0,00106*P + 0,00000252431*P^2 - 0,000685833*S*P \quad (5.6)$$

Figure 5.22 has the narrowest range of all graphs. Though residuals have a relatively wide range, linearity is still kept well. Adequacy of the mathematical model is still available. Due to strong relation between actual and fitted values, correlation between experimental outputs and mathematical model is easily determined. For this reason, the fitted values derived as absolute values are similar to physical sample outputs (Kinan,Romali,Fiaschi,Dini,Sarri,2009). Figure 5.23 and 5.24 indicate the effect of laser welding and power speed on the thickness at collimation A.

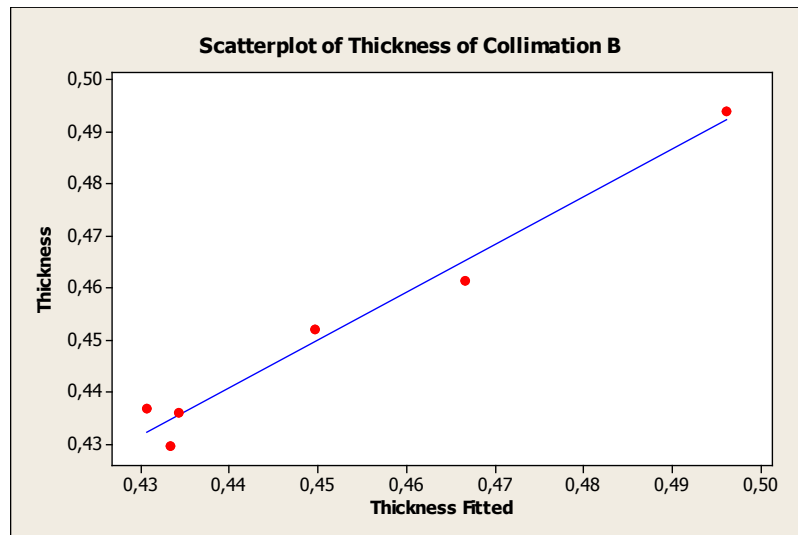


Figure 5.22: The scatter plot of actual and fitted thickness values for collimation B

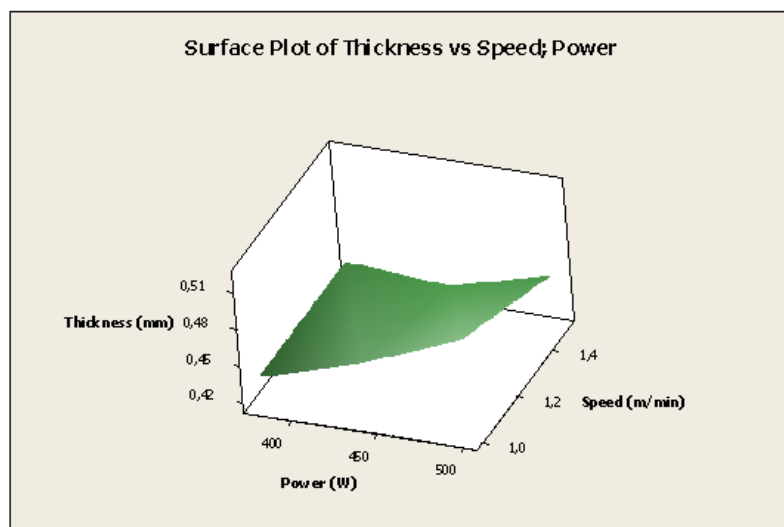


Figure 5.23: 3D graph shows the effect of laser power and welding speed on the thickness at collimation B

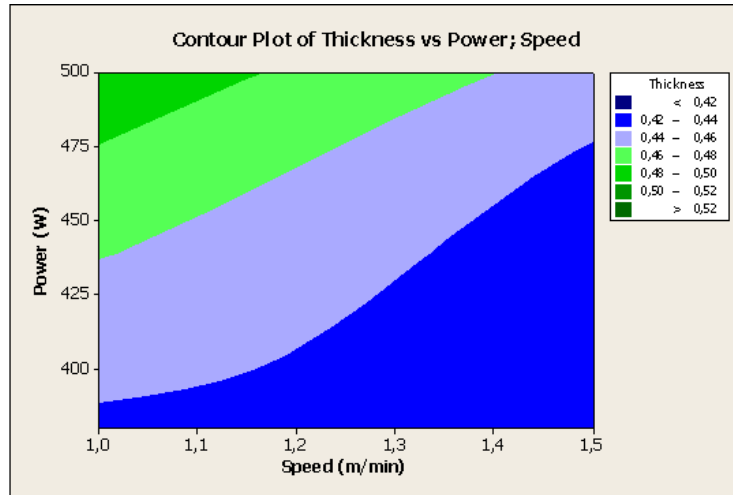


Figure 5.24: : Contour graph shows the effect of laser power and welding speed on the thickness values at collimation B

5.4. Optimization Results Of Experiments Within Different Steps For Collimation A Using RSM

The results of an additional experiment as verification for the mathematical models of collimation A can be seen below Table 5.7. For this experiment 12 samples were used and different combinations of input parameters were tried. Linearity at all three outputs are available and adequacy of the models is present. Residuals are mostly small for all of outputs, where for thickness the lowest values are available. So, in spite of the different input parameters values, the mathematical models functioned well. This trial indicates that the steps of the experiments are increased, the mathematical model of the system is getting to be close to real system behavior.

test no:	Welding Speed	Laser power	Depth	Width	Thickness
1	1,5	330	0,118	0,483	0,432
2	1,5	390	0,237	0,514	0,42
3	1,5	405	0,245	0,602	0,42
4	1,77	300	0,0233	0,361	0,443
5	1,77	330	0,075	0,438	0,44
6	1,77	360	0,132	0,522	0,44
7	1,77	390	0,254	0,558	0,416
8	1,77	405	0,234	0,54	0,418
9	1,77	420	0,254	0,558	0,416
10	2,12	330	0,06	0,299	0,447
11	2,12	390	0,168	0,536	0,422
12	2,12	405	0,212	0,533	0,432

Table 5.7: Additional experiment steps and results

The scatter plot of actual and fitted depth values is linear. (see figure 5.25). At ANOVA table 5.8 presents that R^2 is 96,09%. That means the found system equation for depth is almost the real system.

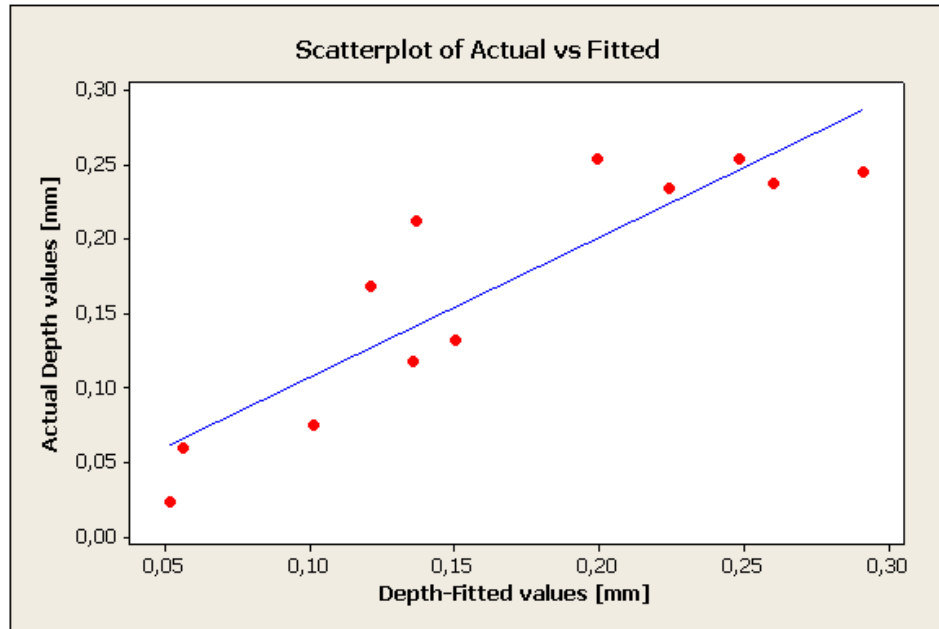


Figure 5.25: The scatter plot of actual and fitted depth values for additional test

Source	DF	Sum of Squares	Mean Square	F	p
Model	5	1,01211	0,33737	3269,05	0,0000
S	1	0,073814	0,014763	29,46	0,0033
P	1	0,069597	0,067491	34,70	0,000
S²	1	0,000	0,000018	0,04	0,855
P²	1	0,000175	0,000178	0,36	0,573
S*P	1	0,000037	0,000037	0,07	0,795
Residual	6	0,003006	0,000511		
Total	11	0,076820			
$R^2 = 96,09\%$ $R^2 \text{ (pred)} = 87,95\%$ $R^2 \text{ (adj)} = 92,83\%$					

Table 5.8: ANOVA Table of depth values

$$\text{Depth} = 0,150171 - 0,027811 * S + 0,122257 * P - 0,002632 * S^2 - 0,013468 * P^2 + 0,004577 * S * P \quad (5.7)$$

The scatter plot of actual and fitted width values is linear. (see figure 5.26). At ANOVA table 5.9 presents that R^2 is 92,02%. That means the found system equation for width is almost the real system.

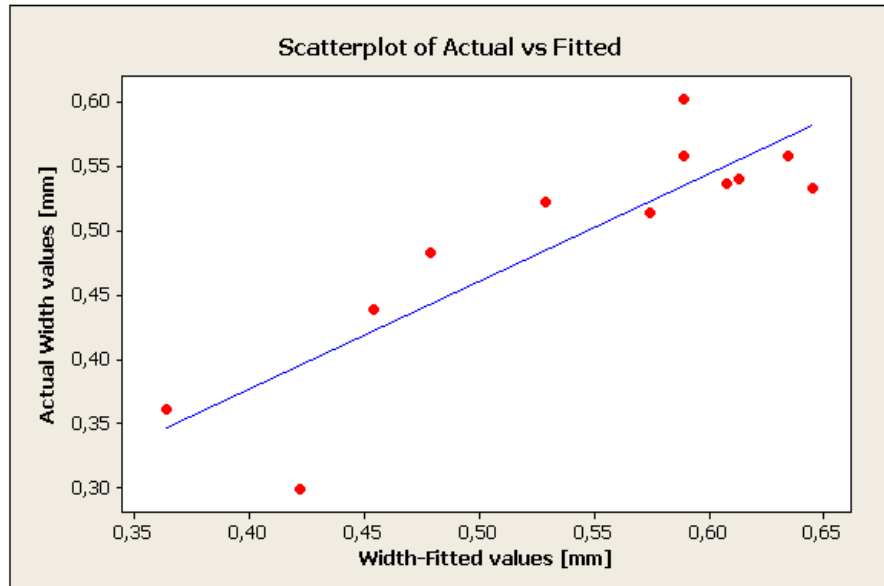


Figure 5.26: The scatter plot of actual and fitted width values for additional test

Source	DF	Sum of Squares	Mean Square	F	p
Model	5	0,078574	0,015715	13,83	0,003
S	1	0,008869	0,014914	13,13	0,011
P	1	0,059976	0,066820	58,82	0,000
S²	1	0,000345	0,000858	0,76	0,418
P²	1	0,001785	0,001918	1,69	0,241
S*P	1	0,007598	0,007598	6,69	0,041
Residual	6	0,006816	0,001136		
Total	11	0,085391			
$R^2 = 92,02\%$ $R^2 \text{ (pred)} = 51,00\%$ $R^2 \text{ (adj)} = 85,37\%$					

Table 5.9: ANOVA Table of width values

$$\text{Width} = 0,49780 - 0,05489 \cdot S + 0,12165 \cdot P - 0,01805 \cdot S^2 - 0,04420 \cdot P^2 + 0,06556 \cdot S \cdot P \quad (5.8)$$

The scatter plot of actual and fitted thickness values is linear. (see figure 5.27).at ANOVA table 5.8 presents that R^2 is 81,98%. That means the found system equation for thickness is almost the real system. Because thickness has narrow tolerance range.

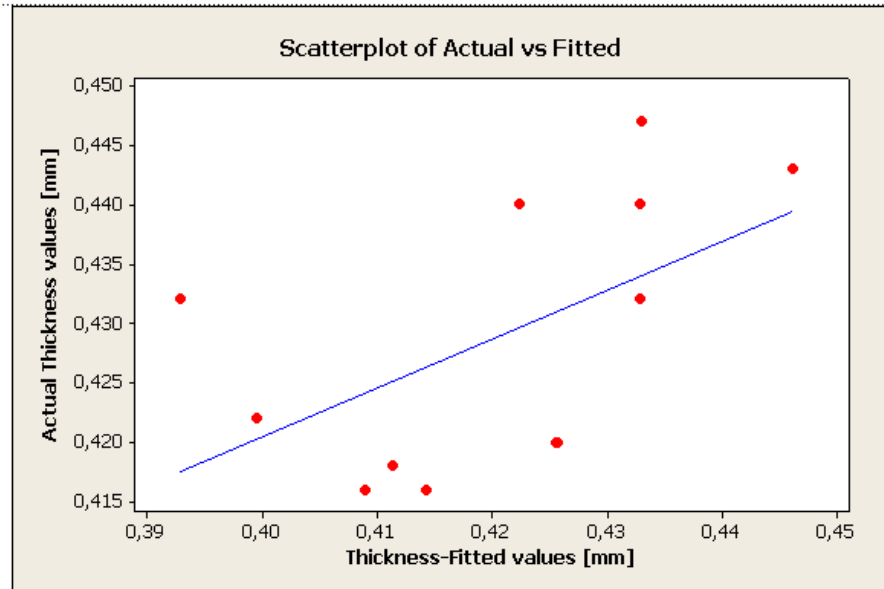


Figure 5.27: The scatter plot of actual and fitted thickness values for additional test

Source	DF	Sum of Squares	Mean Square	F	p
Model	5	0,01188	0,000238	5,46	0,031
S	1	0,000139	0,000147	3,37	0,116
P	1	0,001031	0,000999	22,95	0,003
S²	1	0,000004	0,000002	0,05	0,824
P²	1	0,000003	0,000003	0,07	0,805
S*P	1	0,000010	0,000010	0,24	0,641
Residual	6	0,000261	0,000044		
Total	11	0,001450			
$R^2 = 81,98\%$ $R^2 \text{ (pred)} = 37,00\%$ $R^2 \text{ (adj)} = 66,96\%$					

Table 5.10: ANOVA Table of thickness values

$$\text{Thickness} = 0,432216 + 0,005441 * S - 0,014878 * P + 0,000945 * S^2 - 0,001715 * P^2 - 0,002432 * S * P \quad (5.9)$$

6. CONCLUSIONS

Depth output is highly affected by welding speed and laser power. Independent from collimation A and B, depth value is proportional to laser power and inversely proportional to welding speed. As the power increases energy delivered into the unit surface area (energy density) increases. In figure 5.1, it can be easily seen that graph of collimation B is just like a superposed version of collimation A. it means physical differences between collimation A and B has almost no effect on input parameters behavior. (See at page 51)

In figure 5.3, width is highly affected by welding speed and laser power as well. Characteristic behavior of the graphs is showing different behavior depending on the collimation; in figure 5.3.a, width is inversely proportional to speed and proportional to power. However, effect of speed on width is very low as expected so that curve is almost horizontal. In figure 5.3.b, due to very weak correlation between width and welding speed, the curve is again almost horizontal. As expected power for collimation A is proportional to width although after a certain power level, the change at width becomes negligible which is a natural behavior. For collimation B, since the certain level yet not reached linearity of width-power curve is kept well through the whole graph. (See at page 52)

In figure 5.5, welding speed has high impact on thickness for both collimation A and B; thickness is inversely proportional to welding speed which is a natural result due to dependency on energy intensity. As the speed increases, energy delivered on unit area is decreased. Laser power has an impact on thickness after a certain laser power level; as it is seen from both collimation A and B. (See at page 53)

In figure 5.2, effects of different welding speeds on depth regarding different laser power are depicted. As stated before depth is proportional to laser power; however higher welding speed brings about lower depth values. That's why; at both graphs curves of 1,5 m/min welding speed lying under curves of 1,0 m/min welding speed. (See at page 52)

In figure 5.4, as it is known power is proportional to width. Moreover, welding speed has no direct relation to width as seen from the graphs. Due to the interaction of laser power and welding speed, although lower welding speed values with the increasing laser power reaches the level of width values change at very limited rates. Regarding 1.5 m/min welding speed, the effect of increasing laser power on width can be easily seen. (See at page 53)

In figure 5.6, at low welding speed, laser power is clearly proportional to thickness. Besides, at high welding speed there is no certain behavior with the graphs. It can be decided that at welding speed under 1,5 m/min, thickness can be controlled well through the various laser power level. (See at page 54).

As it was explained above in 1 and 2, adequacy of the mathematical model can be also seen under ANOVA results. The ANOVA table indicates that the most significant input parameter is laser power for all output results. Although there is certain range of R^2 values, it can be seen that the mathematical model yields very similar values to physical sample values. Thickness as output parameter is the different case, as input parameters have very limited impact on that. However, the model still confirms the physical sample values. It should be kept in mind that laser power and welding speed have limited effect on thickness in real life.

Response optimization results; by using RSM (Response Surface Methodology), the optimum input parameter combinations were achieved as listed below. These combinations give optimum output values which are found to be very near to nominal welding geometry values.

For collimation A, response optimization gave optimum welding speed at 1,30 m/min and laser power at 356 W. It means if these optimum values are used as input parameters, the predicted welding geometry outputs are given as predicted responses. The term desirability is the probability of achieving predicted responses. The predicted depth value is 0,22mm with 99,94% of desirability, the predicted width value is 0,53mm with 78,2% of desirability and the predicted thickness value is 0,43mm with 85,06% of desirability.

For collimation B, response optimization yielded optimum welding speed at 1,27 m/min and laser power at 380W. The predicted depth value is 0,22 mm with 100% of

desirability, the predicted width value is 0,55mm with 67,7% of desirability and the predicted thickness value is 0,44mm with 88,6% of desirability.

Verification of response optimum input parameters for collimation A; regarding the optimum input parameters for collimation A, the verification experiment were done with these optimum input parameters and 10 samples were used for this experiment. The other effecting parameters such as mechanical adjustments, shielding gas, vacuum, can change by the time, therefore, small differences between actual and predicted values of outputs were found. As explained in 5, the predicted depth value is 0,22mm with 99,94% of desirability, the predicted width value is 0,53mm with 78,2% of desirability and the predicted thickness value is 0,43mm with 85,06% of desirability, The below tables show the results of this experiment for all output values. All results are in tolerances and almost confirm the desirability. In figure 6.4, the mean value of 10 samples is 0,202 mm. In spite of other changing parameters, this value is a lightly superposed version of predicted result. In figure 6.5, the mean value of 10 samples is 0,55 mm, which lies within the range of desirability. In figure 6.6, the average of 10 sample thickness values is 0,42mm, which is found within the range of desirability of thickness.

Thus, the response optimization results are confirmed by the results of this additional experiment for verification. This confirmation is a very strong proof for the adequacy of mathematical model generated.

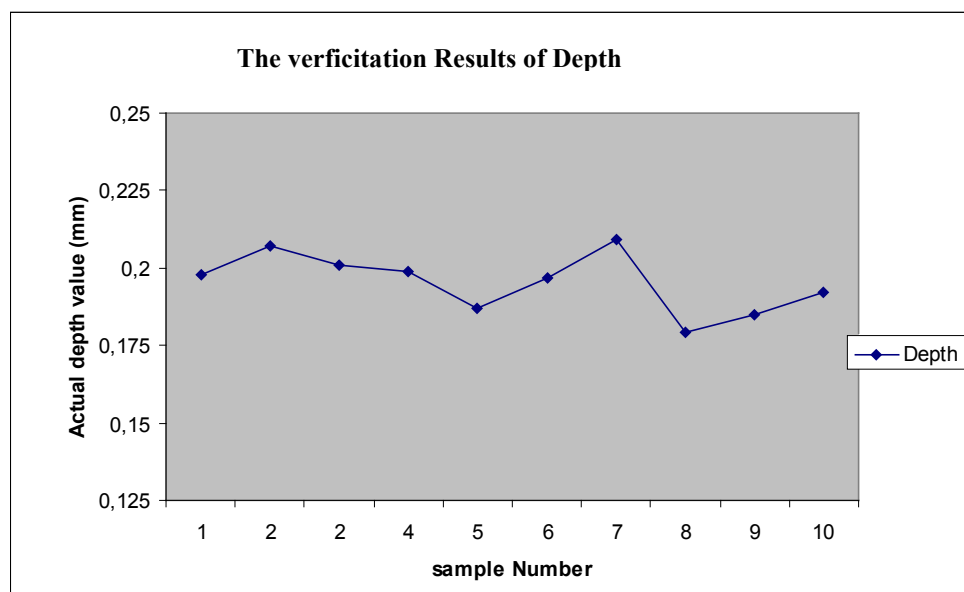


Figure 6.1 The verification Results of Depth

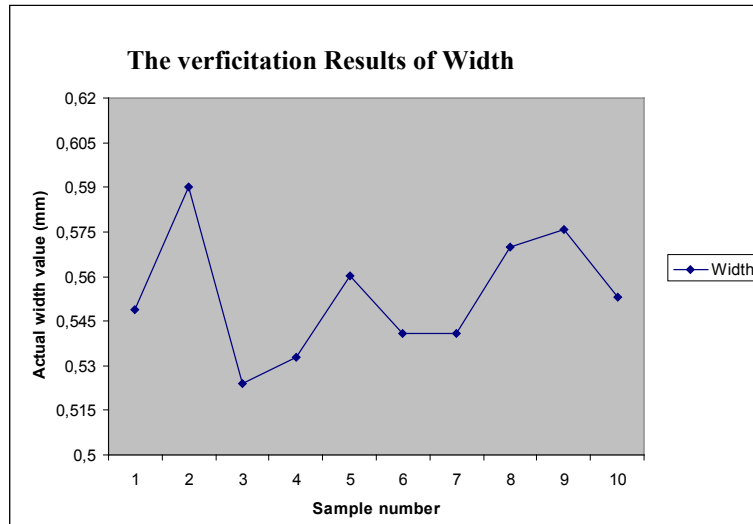


Figure 6.2: The verification Results of Width

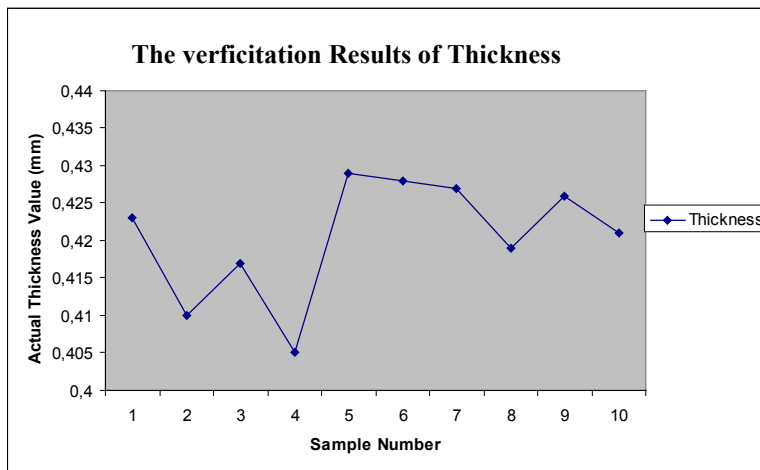


Figure 6.3: The verification Results of Thickness

Interaction contour diagrams from RSM; the below contour plots indicate that the optimum tolerance ranges of all outputs in the white area. Grey areas show that one or more outputs are not within defined optimum tolerances. Upper and lower limits of tolerances can be found on the right side of the plots. In the graph, limits of depth are drawn since the area where depth is feasible is only the white region.

For collimation A, at 1,0 m/min, the maximum laser power value should be approximately 370 W; at 1,5 m/min, the lowest power value should be 320 W through Response surface methodology analysis. (See Figure 6.4)

For collimation B, at 1,0 m/min, the maximum laser power should be almost 400 W, at 1,5 m/min, the highest feasible laser power should be approximately 445 W (See figure 6.5). In the graph, the lower limits of outputs can not be seen, because they are

lying outside of the depicted area. X and Y axis of this graph show the limits of defined input parameters.

The main aim of these graphs is, within the white area any combination of laser power and welding speed give a good welding geometry and the optimum input parameters values, which were defined through response optimization at RSM, are present in feasible white area.

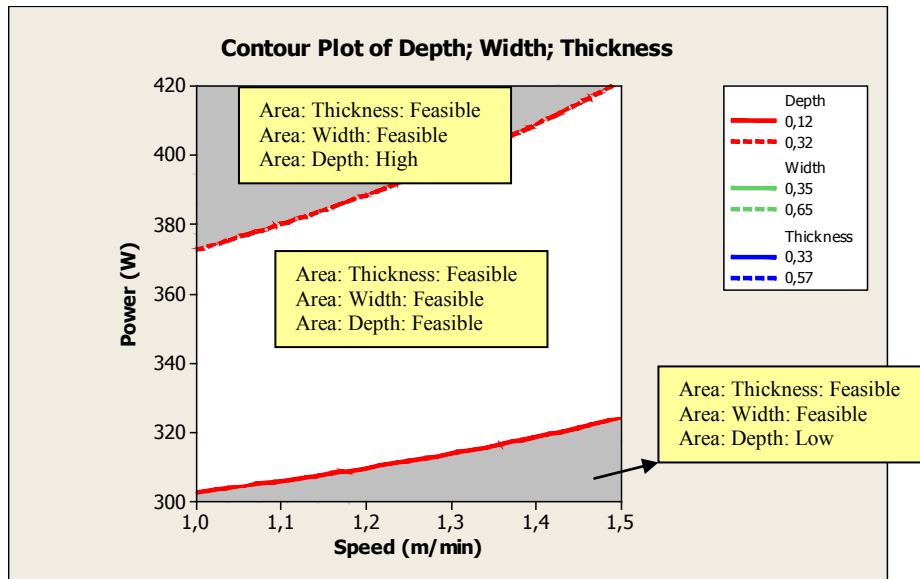


Figure 6.4: Contour graph shows the effect of laser power and welding speed on the depth,width and thickness values and optimum feasible area at collimation A

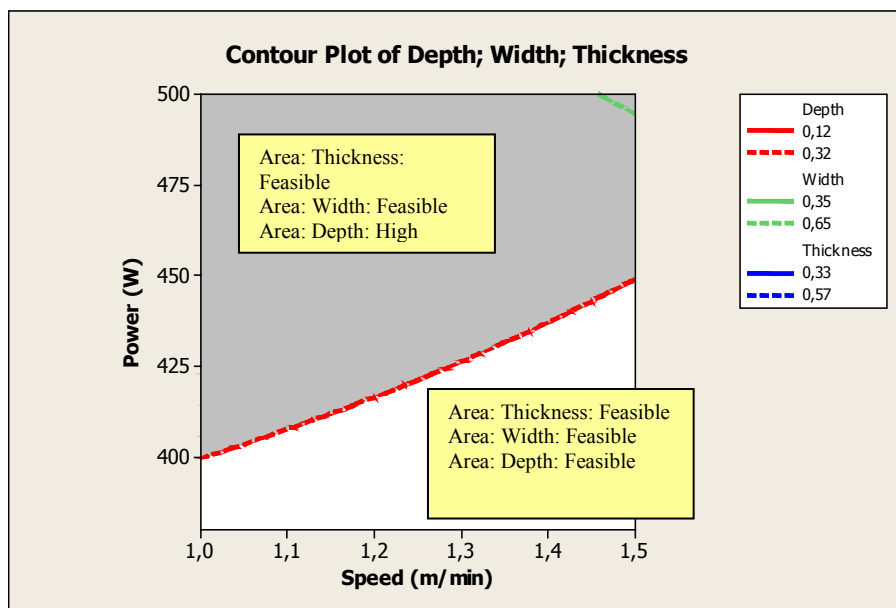


Figure 6.5: Contour graph shows the effect of laser power and welding speed on the depth,width and thickness values and optimum feasible area at collimation B

7. RECOMMENDATION

All these experiments were performed under serial production conditions. If the same experiments were done under laboratory conditions, the mathematical model and verification/validation results could achieve a higher degree of desirability. If further experiments to be performed again under serial product conditions, as a rule of thumb, it is recommended to perform the verification/validation experiments not much later than main experiments.

As it is seen from the conclusions drawn above, the mathematical model generated is quite robust. It means the output value is not very sensitive to little changes at input parameter values. So that under serial production conditions, the desired welding geometry can be clearly estimated by means of running this kind of mathematical model with the input of optimum welding parameters.

RSM (Response Surface Methodology) is a quite useful statistical method to define optimum values for other kinds of processes and is also used to estimate the other effecting parameters and to evaluate the behavior of the process (system). Especially, the result graph is very user friendly with its visualization; it enables faster analysis of effects coming from input parameters.

This study is helpful for a clear understanding of the behavior of laser welding process at the industrial use.

REFERENCES

- Anawa E.M., Olabi A.G., 2007:** Usings Taguchi method to optimize welding pool of dissimilar laser-welded components: School of Mechanical&Manufacturing Engineering, Dublin City University,Ireland
- Baş Deniz, Boyaci Ismail H.,2006 :** Modelling and Optimization I: Usability of response surface methodology: Department of Food Engineering. Faculty of Engineering, Hacettepe University, Turkey
- Beno Benhabib, 2002 :**Manufacturing design, Production, Automation and Integration, University of Toronto,2002
- Benypounis K.Y., . Olabi A.G., . Hashmi M.S.J 2005:** Optimizing the laser-welded butt joints of medium carbon steel using RSM: School of Mechanical and Manufacturing Engineering, Dublin City University, Ireland
- Benypounis K.Y., Olabi A.G., Hashmi M.S.J., 2005:**Effect of laser welding parameters on the heat input and weld-bead profile: School of Mechanical and Manufacturing Engineering, Dublin City University
- Bradley Nuran, 2007:** The Response Surface Methodology: Master of Science, Department of Mathematical and Computer Science, Indiana University of South Bend
- Çelen Serap, 2006:** Paslanmaz Çeliklerin Lazer Kaynağında Kaynak Parametrelerinin Bağlantının Dayanım ve Korozyon Özelliklerine Etkisinin İncelenmesi, Dokuz Eylül Üniversitesi Fen Bilimleri Enstitüsü
- Devor Richard E., Tsong-how Chang John W. Sutherland, 1992:** Statical Quality Design and Control,1992
- Durman Burçin M., Yrd. Doc. Dr. PAKDİL Fatma,2009:** İstatistiki Proses Kontrol Uygulamaları için Bir Sistem Tasarımı: Başkent Üniversitesi, Mühendislik Fakültesi, Endüstri Mühendisliği Bölümü, Türkiye
- Ezzeddin Mohamed Hassan, 2008:** Feasibility and Optimisation of Dissimilar Laser Welding Components :PhD.Thesis,2008, School of Mechanical &Manufacturing Engineering, Dublin City University, Ireland
- Fabbro R'emy, Slimani Sonia, Coste Fr'ederic and Briand Francis, 2008:** Study of keyhole behaviour for full penetration Nd–Yag CW laser welding
- John C.ION, 1991:** Laser Processing of Engineering Materials

- Khurilandre A. I. and Mukhopadhyay Siuli, 2006:** Response surface methodology
- Kinan M.M.A, Romali L., Fiaschi M., Dini G., Sarri F. 2009:** Experimental design approach to the process parameter optimization for laser welding of martensitic stainless steel in a constrained: Department of Mechanical, Nuclear and Production Engineering, University of Pisa, Italy
- Liang Lin Hsuan, Chou Chang Pin, 2008:** Modelling and optimization of Nd:YAG laser micro-welded process using Taguchi method and a neural network
- Mathews Paul G., 2004 :** Design of Experiments With MINITAB: Classroom Exercises and Labs
- Menasce Daniel A.Prof, Dept. of Computer Science George Mason University,2001:** Design of Experiments: Factorial Designs,2001
- Minitab 16 Helpdesk**
- Norenda B. Dahotre, Sondip P. Harimkar, 2008:** Laser Fabrication and Machining of Materials: Springer,2008
- Pana Lung Kwang, Wang Che Chung, Hsiao Ying Ching, Ho Kye Chyn, 2006:** Optimization of Nd:YAG laser welding onto magnesium alloy via Taguchi analysis; ChungTai Institute of Health Science and Technology,Taiwan
- Ramsayer Reiner M.Dr, 2010:** Laserschweißen-Grundlagen, Systemtechnik und Anwendungen in der Bosch : Collodium 2010, BOSCH Group, Germany
- RBTR** Prüfvorschrift (Datasheet) HDEV4.1 Ventilkörper-Haltekörper
- Shukor Sivarao, T.J.S. Anand&Ammar :** DOE Based Statistical Approaches in Modelling of Laser Processing –Review & Suggestion: International Journal of Engineering & Technology
- Tabak Derya, 2010:** The Effects of Cleaning Chemicals on Spatter Phenomena at laser welding Process of the Stainless Steel: M.Sc.Thesis, Istanbul Technical University, Advanced Technologies
- Trumpfh Technische Buch/Handbook**
- Wonnacott T. H. and . Wonnacott R. J,1981:** Regression: A second course in Statistics, John Wiley & Sons, 1981

APPENDICES

APPENDIX A.1 : The experimental data for collimation A

COLLIMASION_A											
No:	Speed	Power	Depth	Width	Thickness	No:	Speed	Power	Depth	Width	Thickness
1	1	300	0,108	0,499	0,415	31	1,5	300	0,0665	0,365	0,4475
2	1	300	0,112	0,5045	0,438	32	1,5	300	0,067	0,4145	0,42
3	1	300	0,118	0,5165	0,4205	33	1,5	300	0,0705	0,394	0,45
4	1	300	0,1275	0,5215	0,422	34	1,5	300	0,072	0,393	0,4415
5	1	300	0,11	0,4905	0,4295	35	1,5	300	0,0645	0,3855	0,4435
6	1	300	0,1195	0,489	0,4275	36	1,5	300	0,06	0,368	0,4515
7	1	300	0,1155	0,5285	0,429	37	1,5	300	0,066	0,388	0,456
8	1	300	0,118	0,521	0,4195	38	1,5	300	0,0625	0,376	0,445
9	1	300	0,113	0,4925	0,4395	39	1,5	300	0,0685	0,4455	0,432
10	1	300	0,116	0,484	0,436	40	1,5	300	0,061	0,405	0,4335
11	1	360	0,294	0,484	0,4535	41	1,5	360	0,2085	0,565	0,4215
12	1	360	0,2815	0,49	0,453	42	1,5	360	0,2195	0,572	0,419
13	1	360	0,2725	0,5495	0,4365	43	1,5	360	0,203	0,55	0,4195
14	1	360	0,286	0,5215	0,437	44	1,5	360	0,199	0,5545	0,4285
15	1	360	0,2705	0,4845	0,4625	45	1,5	360	0,197	0,559	0,418
16	1	360	0,2535	0,5885	0,4175	46	1,5	360	0,21	0,566	0,4315
17	1	360	0,263	0,5285	0,437	47	1,5	360	0,201	0,585	0,425
18	1	360	0,28	0,49	0,4415	48	1,5	360	0,19	0,553	0,4255
19	1	360	0,2805	0,498	0,4445	49	1,5	360	0,211	0,5885	0,424
20	1	360	0,2835	0,505	0,4365	50	1,5	360	0,195	0,5375	0,431
21	1	420	0,47	0,5285	0,4655	51	1,5	420	0,302	0,6025	0,4265
22	1	420	0,4635	0,5435	0,455	52	1,5	420	0,321	0,586	0,425
23	1	420	0,4515	0,5625	0,4625	53	1,5	420	0,314	0,6075	0,429
24	1	420	0,463	0,578	0,4335	54	1,5	420	0,31	0,6075	0,425
25	1	420	0,4555	0,5595	0,453	55	1,5	420	0,3155	0,567	0,4175
26	1	420	0,4615	0,532	0,4635	56	1,5	420	0,322	0,5505	0,4225
27	1	420	0,461	0,5685	0,4655	57	1,5	420	0,3075	0,594	0,4195
28	1	420	0,454	0,548	0,456	58	1,5	420	0,3015	0,5985	0,44
29	1	420	0,468	0,5425	0,457	59	1,5	420	0,3165	0,57	0,438
30	1	420	0,4365	0,55	0,4485	60	1,5	420	0,316	0,57	0,435

APPENDIX A.2: The experimental data for collimation B

COLLIMASION_B											
No:	Speed	Power	Depth	Width	Thickness	No:	Speed	Power	Depth	Width	Thickness
1	1	380	0,2715	0,5975	0,4295	31	1,5	380	0,1635	0,549	0,4815
2	1	380	0,271	0,561	0,43	32	1,5	380	0,172	0,5475	0,4395
3	1	380	0,265	0,576	0,432	33	1,5	380	0,1835	0,547	0,432
4	1	380	0,2535	0,551	0,462	34	1,5	380	0,19	0,5005	0,427
5	1	380	0,2665	0,579	0,4385	35	1,5	380	0,189	0,544	0,4285
6	1	380	0,247	0,5835	0,4335	36	1,5	380	0,181	0,532	0,422
7	1	380	0,2475	0,58	0,44	37	1,5	380	0,1765	0,543	0,428
8	1	380	0,2685	0,574	0,428	38	1,5	380	0,18	0,53	0,431
9	1	380	0,2745	0,53	0,4505	39	1,5	380	0,2045	0,488	0,4335
10	1	380	0,2855	0,566	0,4245	40	1,5	380	0,1765	0,524	0,438
11	1	440	0,422	0,6145	0,4535	41	1,5	440	0,2935	0,6045	0,429
12	1	440	0,427	0,606	0,4685	42	1,5	440	0,282	0,62	0,4355
13	1	440	0,429	0,561	0,496	43	1,5	440	0,282	0,572	0,433
14	1	440	0,4565	0,5545	0,4705	44	1,5	440	0,2695	0,598	0,433
15	1	440	0,431	0,5935	0,4535	45	1,5	440	0,318	0,563	0,426
16	1	440	0,4205	0,5995	0,462	46	1,5	440	0,2955	0,585	0,433
17	1	440	0,4245	0,614	0,4455	47	1,5	440	0,294	0,5865	0,4175
18	1	440	0,3985	0,6295	0,437	48	1,5	440	0,2925	0,56	0,441
19	1	440	0,4405	0,5575	0,4625	49	1,5	440	0,2965	0,56	0,418
20	1	440	0,472	0,5475	0,465	50	1,5	440	0,2895	0,584	0,431
21	1	500	0,5935	0,5625	0,488	51	1,5	500	0,4265	0,6185	0,451
22	1	500	0,549	0,6265	0,4885	52	1,5	500	0,4385	0,6745	0,4475
23	1	500	0,599	0,569	0,481	53	1,5	500	0,439	0,6425	0,451
24	1	500	0,5645	0,6345	0,497	54	1,5	500	0,4265	0,6525	0,452
25	1	500	0,5905	0,5895	0,489	55	1,5	500	0,438	0,6655	0,443
26	1	500	0,5905	0,578	0,4865	56	1,5	500	0,4345	0,681	0,47
27	1	500	0,6195	0,5325	0,521	57	1,5	500	0,43	0,652	0,456
28	1	500	0,596	0,5695	0,5215	58	1,5	500	0,4195	0,6925	0,452
29	1	500	0,578	0,5755	0,48	59	1,5	500	0,426	0,67	0,452
30	1	500	0,5915	0,6055	0,485	60	1,5	500	0,431	0,6445	0,444

CURRICULUM VITAE



Name Surname: Asli BOZAN

Place and Date of Birth: BURSA, 01.05.1985

Address: Ataevler Mah. 1. Akpelin Sok. İlkbahar sitesi B blok No:14/5

Nilüfer/BURSA

E-Mail: a.bozan6@gmail.com

B.Sc.: Mechanical Engineering, Balıkesir Üniversitesi 2007

List of Publications and Patents: The optimization of laser welding seam geometry by using response surface methodology

PUBLICATIONS/PRESENTATIONS ON THE THESIS

- Bozan Asli, Kural Ayhan, Cangar Haluk, The optimization of the laser welding seam geometry by using response surface methodology. **International Congress on Advances in Welding Science and Technology for Construction, Energy and Transportation Systems (AWST - 2011). 24-25 October 2011, Antalya, Turkey**

